Role of RECQ5 Helicase in MUS81-mediated Resolution of Aberrant Replication Intermediates

---

Dissertation zur

Erlangung der naturwissenschaftlichen Doktorwürde

(Dr. sc. nat.)

vorgelegt der

Mathematisch-naturwissenschaftlichen Fakultät der

Universität Zürich von

Stefano Di Marco

aus

Italien

Promotionskomitee

Prof. Dr. Massimo Lopes (Vorsitz)

Dr. PD Pavel Janscak (Leitung der Dissertation)

Prof. Dr. Petr Cejka

Dr. Pietro Pichierri

Zürich, 2016

1. Summary

RECQ5 is a member of the RecQ DNA helicase family, a group of highly conserved proteins that are essential for the maintenance of genomic stability. It has been shown that RECQ5 interacts with RAD51 recombinase and disrupts RAD51-ssDNA filaments to suppress aberrant homologous recombination events. The aim of this thesis was to explore the functional significance of the physical interaction of RECQ5 with the MUS81-EME1 endonuclease, which is known to process late replication intermediates at common fragile sites (CFSs) during early mitosis to facilitate chromosome segregation. We have found that RECQ5 associates with CFS loci in a manner dependent on MUS81 and is required for the appearance of MUS81-dependent chromatid breaks/gaps at CFSs following replication stress, a phenomenon termed "expression of CFSs", which is required for proper sister chromatid disjunction. Accordingly, RECQ5-depleted cells showed increased frequency of anaphase bridges and micronuclei, and accumulation of CFS-associated 53BP1 nuclear bodies in G1 cells, phenotypes related to defective chromosome segregation. Moreover, we found that mutational inactivation of the helicase or RAD51-binding domains of RECQ5 increased binding of RAD51 to CFSs, impaired their expression and led to aberrant sister chromatid separation. Consistent with these findings, RECQ5 was found to counteract the inhibitory effect of RAD51 on 3'-flap cleavage by MUS81-EME1 *in vitro*. Lastly, we have found that expression of CFSs is dependent on phosphorylation of RECQ5 by CDK1 at Ser727. These results suggest that RECQ5 disrupts RAD51 filaments formed on stalled replication forks at CFS and hence facilitates their processing by the MUS81-EME1 endonuclease for proper sister chromatid disjunction during mitosis.

2. Zusammenfassung

RECQ5 ist ein Mitglied der Familie der RecQ DNA Helikasen, einer Gruppe von stark konservierten Proteinen, welche essentiell sind für die Aufrechterhaltung genomischer Stabilität. Es wurde gezeigt, dass RECQ5 mit der RAD51 Rekombinase interagiert und RAD51-ssDNA-Filamente zerstört, um anomale homologe Rekombinationsereignisse zu unterdrücken. Das Ziel dieser Arbeit war es, die funktionelle Bedeutung der physikalischen Interaktion von RECQ5 mit der MUS81-EME1 Endonuklease zu untersuchen. Letztere ist bekannt dafür, während der frühen Mitose späte Replikationszwischenprodukte bei Common Fragile Sites (CFSs) zu prozessieren, um die Verteilung der Chromosomen zu erleichtern. Wir haben festgestellt, dass RECQ5 in Abhängigkeit von MUS81 mit CFS Loci assoziiert ist und für das Erscheinungsbild von MUS81-abhängigen Chromatidbrüchen/-lücken bei CFS infolge Replikationsstress verantwortlich ist. Dieses Phänomen wird „CFS Expression“ genannt und ist erforderlich, um die einwandfreie Trennung von Schwesterchromatiden zu gewährleisten. Dementsprechend zeigen RECQ5-depletierte Zellen eine erhöhte Anzahl an Anaphasen-Brücken und Micronuclei und eine Anhäufung von CFS-assoziierten 53BP1 nuclear bodies in G1 Zellen auf - allesamt Phänotypen, welche mit fehlerhafter Chromosomenverteilung zusammenhängen. Ausserdem haben wir festgestellt, dass die mutationelle Inaktivierung der Helikase- oder RAD51-Bindungsdomäne von RECQ5 zur verstärkten Bindung von RAD51 zu CFS führt, die CFS Expression behindert und fehlerhafte Chromosomenverteilung hervorruft. In Übereinstimmung mit diesen Ergebnissen hat sich herausgestellt, dass RECQ5 dem inhibitorischen Effekt von RAD51 auf die MUS81-EME1-abhängige Abspaltung von 3’-Flaps *in vitro* entgegenwirkt. Schliesslich, konnten wir zeigen, dass die Expression von CFS

abhängig ist von der Phosphorylierung von RECQ5 auf Ser727 durch CDK1. Diese Resultate lassen vermuten, dass RECQ5 RAD51-Filamente zerstört, welche an angehaltenen Replikationsgabeln bei CFS entstehen, und dadurch deren Prozessierung durch die MUS81-EME1 Endonuklease erleichtert, um eine fehlerfreie Verteilung der Schwesterchromatiden während der Mitose zu gewährleisten.

3. Introduction

3.1 - Genomic instability and cancer

Genomic instability is a distinctive marker of many cancers. In hereditary cancers, genomic instability arises from mutations in DNA repair genes that drive tumorigenesis (mutator phenotype hypothesis) [1]. In sporadic (non-hereditary) cancers, the molecular basis of tumorigenesis remains elusive, but new evidences are in disagreement with the mutator phenotype hypothesis. Instead, recent observations support the oncogene-induced DNA replication stress model, where mutations in tumor suppressor genes, such as TP53, ATM and CDKN2A arising as a consequence of oncogene-induced DNA damage drive genomic instability and tumorigenesis [2]. The increasing importance of the involvement of genomic instability in cancer development, prompted D. Hanahan and R. A. Weinberg to include genome instability as an enabling characteristic in the hallmarks of cancer [3].

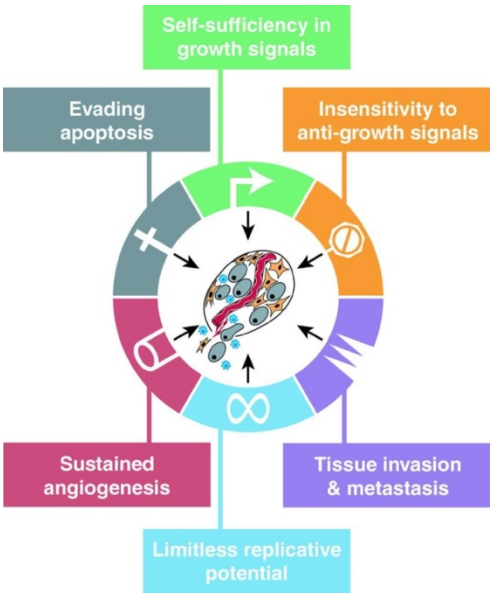

Figure 1. The six hallmarks of cancer proposed by Hanahan and Weinberg in 2000. [4]

The hallmarks of cancer, first proposed in 2000 [4], include six biological principles that reflect the capabilities for tumor growth and metastatic dissemination (Figure 1). Apart from sustaining proliferative signaling, evading growth suppressor, resisting cell death, enabling replicative immortality, inducing angiogenesis, and activating invasion and metastasis, the authors included two other emerging hallmarks: reprogramming of energy metabolism and evading immune destruction, and two enabling characteristics: genome instability and mutation, and tumor-promoting inflammation [3] (Figure 2).

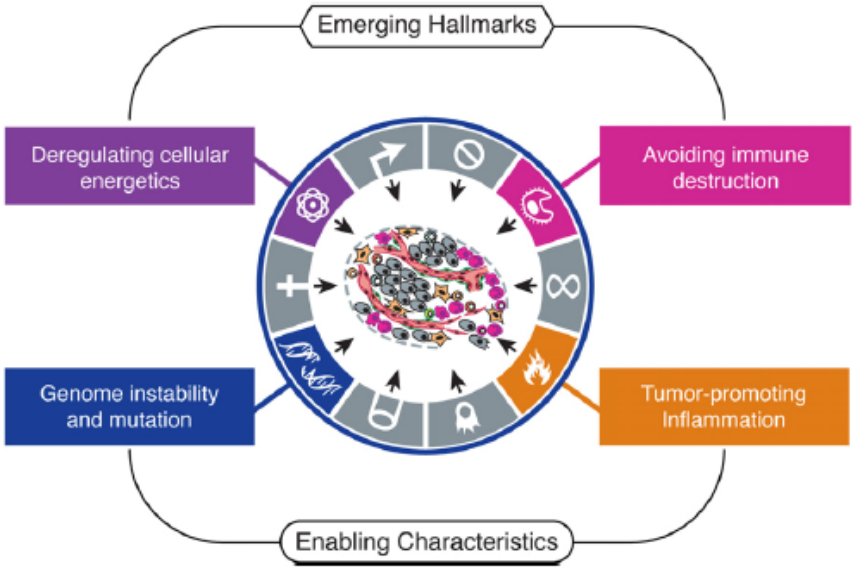

Figure 2. Schematic of the next generation hallmarks of cancer in addition to the six one proposed in 2011. [3]

3.2 – DNA repair pathways

The human genome is constantly threatened by endogenous reactive metabolites and environmental mutagens (i.e. UV light, ionizing radiations, chemicals) [5]. Spontaneous DNA damage can also affect the stability of the genome, and several base mutations have been described, including base substitutions, deletions and insertions of one or more base pairs [6]. The sequencing of the human genome [7] brought to light many proteins involved in different DNA-repair pathways. Mutations in DNA-repair genes drive the oncogenesis process and are associated with hereditary diseases [8]. Accumulation of DNA damage above a certain threshold alters physiological metabolic processes (e.g. DNA synthesis, mRNA production, etc.), arrests cell proliferation and triggers apoptosis [5]. In order to protect the integrity of the genome, the cell has developed a repertoire of efficient repair mechanisms. The *base-excision repair* (BER) removes non-helix-distorting base lesions, such as those derived from oxidation, deamination and alkylation processes. The *nucleotide-excision repair* (NER), in contrast to BER, can repair DNA adducts generated by UV light (e.g. pyrimidine dimers, 6,4-photoproducts) or chemicals (benzo[a]pyren). Mismatch repair (MMR) eliminates mis-incorporated nucleotides, deletion/insertion loops generated by polymerase slippage during replication and mismatches generated by spontaneous deamination of 5-methylcytosine or by strand exchange during DNA recombination. *Homologous recombination* (HR) and *non-homologous end-joining* (NHEJ) constitute mechanisms for repair of DNA double-stranded breaks (DSBs, Figure 3).

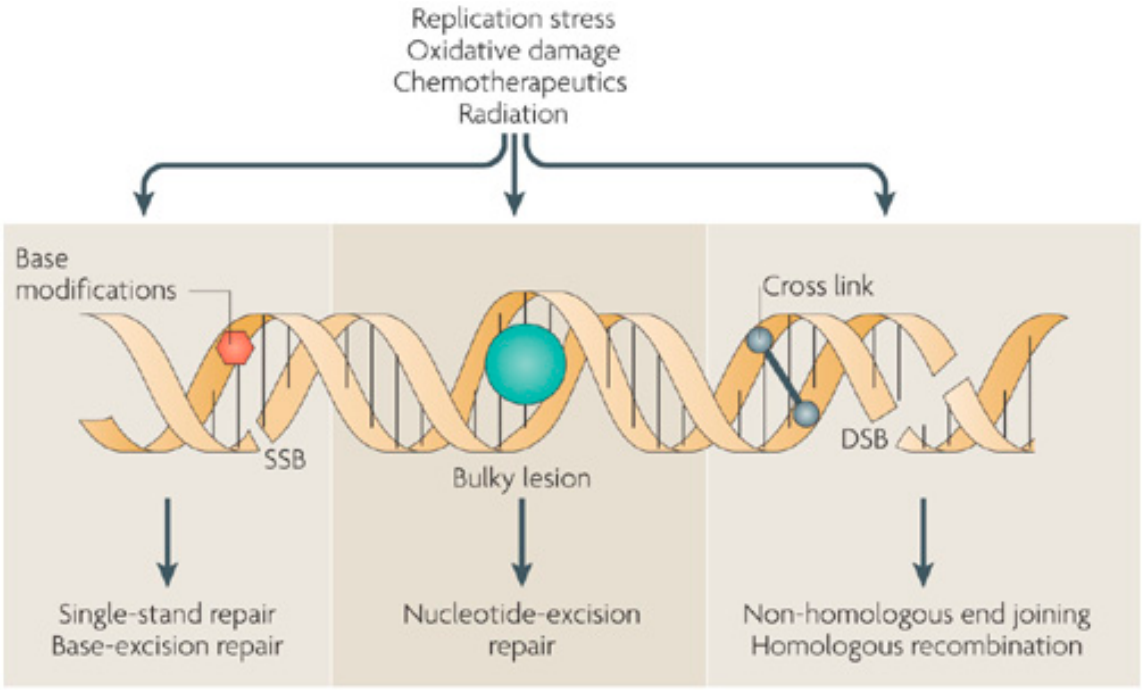

Figure 3. Endogenous and exogenous agents can threaten the genome. The lesions generated by toxic agents are repaired by different and specialized DNA repair mechanisms. SSB: Single-stranded break; DSB: Double-stranded break. [9]

HR, considered to be error-free, takes advantage of the intact homologous region on undamaged sister chromatid to copy the information lost by DNA breakage. NHEJ, does not require a template to restore the continuity of damaged DNA strands, but it can lead to loss of genetic information. DNA damage triggers an ordered action of numerous proteins, a process often called the DNA damage response (DDR). After DNA damage occurs, sensor proteins recognize the damage and activate the DDR pathway. Transducer proteins amplify the damage-induced signal and, in turn, activate effector proteins. The latter promote cell cycle arrest, allowing the repair enzymes to correct the damage [10]. It is clear that the study of the molecular mechanisms of these processes is essential to understand the biogenesis of tumor formation and to develop efficient cancer therapies.

3.3 – DNA replication

The first evidence that complementary base pairing provides the basis for DNA replication comes from Watson and Crick studies revealing that the nucleotides in the template strand guide the complementary bases in the new strand [11]. Given the antiparallel nature of the DNA molecule, *DNA polymerases* move in a 3' -> 5' direction on the template strand, and therefore they add nucleotides only in the 5' -> 3' direction. The *leading strand* is synthesized continuously, while the *lagging strand* has to be synthesized in short, discontinuous segments, known as *Okazaki fragments*. The result of this mechanism is that the new strand grows in the opposite direction of the movement of the *replication fork* (Figure 4). DNA polymerases are accurate enzymes, with an error rate of less than one mistake for every 10^7 nucleotides added. Moreover, some DNA polymerases have an intrinsic proofreading activity. In addition, the post-replicative mismatch repair system is able to distinguish mismatches in the newly synthesized DNA strand [12]. The replication process can be subdivided into three different steps: initiation, elongation and termination. The major enzymatic functions carried out at the replication fork are well conserved from prokaryotes to eukaryotes.

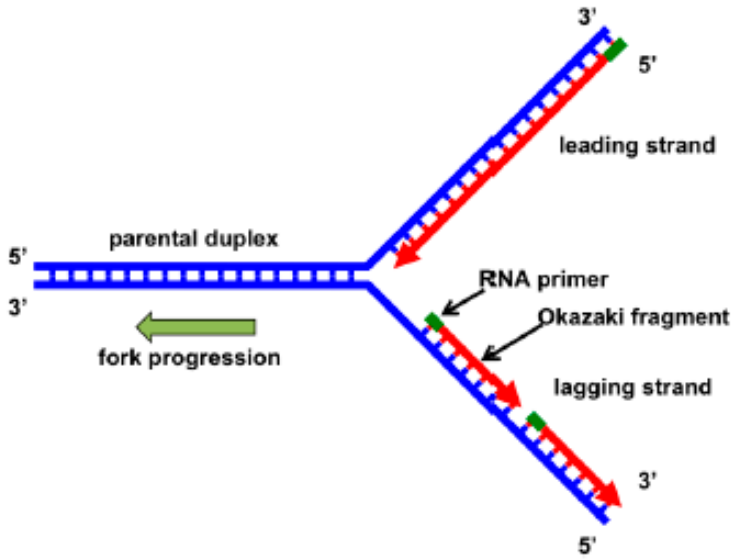

Figure 4. Schematic of the replication fork. DNA replication on the leading strand proceeds continuously (5' -> 3'), meanwhile on the lagging strand DNA synthesis occurs in a discontinuous manner (3' -> 5'). In green, RNA primers initiate synthesis on the leading strand, and every Okazaki fragments on the lagging strand. [13]

The replication machinery is a massive complex coordinating many proteins that all work at the site of replication, forming the *replisome* responsible for copying the genome in the cell. DNA replication is an energetically costly process. In G1 phase of the cell cycle, many DNA replication regulatory processes are initiated. Polymerase ε, synthesizes DNA in a continuous fashion in the direction of DNA unwinding. Polymerase δ replicates DNA on the template, lagging strand [14]. The Okazaki fragments produced by Pol δ are between 100 and 200 bases in lengths. The lagging strand contains longer stretches of ssDNA, coated by single-stranded binding proteins, which stabilizes the ssDNA regions by preventing secondary structure formation or other recombinogenic events. In eukaryotes, ssDNA stabilization is carried out by the heterotrimeric complex named replication protein A (RPA) [15]. Each Okazaki fragment is preceded by an RNA primer, which is displaced by the next Okazaki fragment. In eukaryotes, few DNA bases upstream of the DNA primer is

displaced, leading to the creation of flap structures that, eventually, are processed by endonucleases, such as FEN1. The gap formed is then sealed by DNA ligase I [16, 17]. Besides polymerases, helicase enzymes have an essential role during the replication process. The replicative helicase unwinds the parental DNA duplex, exposing the two ssDNA templates, which become the substrates of DNA polymerases. In eukaryotes, three different polymerases are required for DNA replication: α, δ, ε [18, 19]. Since polymerases cannot start the nucleotide polymerization on their own, but they require a primer to initiate the process, polymerase α creates a short nucleotide RNA molecule followed by 10-20 DNA bases at the origins [20, 21]. Although, Pol α is required for replication, it cannot continue the process. Instead, following the RNA primer synthesis, clamp loaders perform the switching required to exchange Pol α with Pol ε to the leading strand, and Pol δ to each of the Okazaki fragments on the lagging strand.

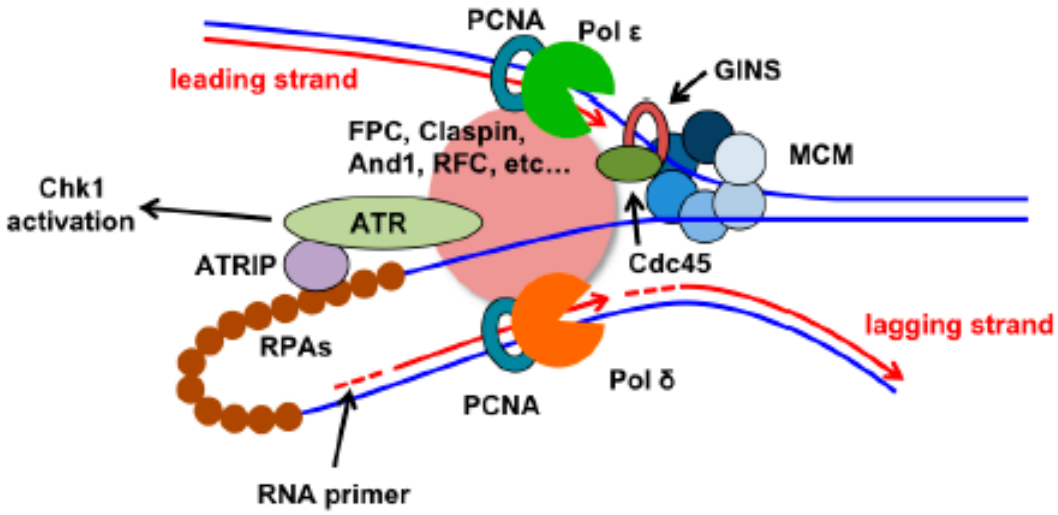

Figure 5. Replication on the leading and lagging strand is performed by Pol ε and Pol δ, respectively. Replisome factors (FPC, Claspin, And1, RFC) regulate polymerase function and coordinate DNA synthesis with unwinding of the template strand by Cdc25-MCM-GINS. The replisome is also linked with checkpoint proteins in order to promote genomic stability during the replication process. [13]

The replicative helicase is a hexameric complex comprised of the mini-chromosome maintenance proteins, MCM2-7 [22]. The MCM helicase is an ATPase, and it is required during the whole S phase for DNA replication [23, 24]. MCM proteins are recruited to replication origins in G1 phase and redistributed on DNA during S phase to the replication forks [25]. Although prokaryotic replication initiates at a single locus, in eukaryotes, DNA replication fires from multiple origin sites. Origins are recognized by the *origin recognition complex* (ORC) [26]. During late mitosis and G1 phase, Cdt1 and Cdc6 proteins associate with origin sites and recruit MCM2-6 helicases [25, 27]. When double hexamers of the MCM2-7 complex are loaded, the *pre-replication complex* (pre-RC) is formed [28], replication origins are considered to be licensed to initiate DNA synthesis. Origin firing is orchestrated by kinases, the cyclin E-CDK2 at the onset of S phase and Cdc7 kinase before origin firing [29]. At this point, origin melting occurs and DNA unwinding exposes the two strands of the duplex as template for DNA polymerases (Figure 5).

3.3.1 – S-phase DNA damage checkpoint

The genetic information must be preserved during every cell division, thus DNA replication needs to be completed with high fidelity [13]. For this reason, the cell cycle includes checkpoints in order to ensure that a certain process is started only after the previous one has been successfully completed [30]. Moreover, since many checkpoint factors are involved in the DNA damage response [31], checkpoints contribute to the avoidance of genomic instability [32].

Excessive or premature initiation of replication can cause replication stress [33]. Cells with perturbed G1/S control, such as oncogene-transformed cells, are

particularly sensitive to replication stress. In response to excessive DNA damage, normal cells block the cell cycle in G1 phase, before DNA replication starts, or in G2 phase, before entering into mitosis. Typically, replication fork-associated damage provokes a response that slows down the replication progress throughout the S phase, by controlling forks and initiation events. In mammals, DNA damage response is mediated by three kinases, the Ataxia Telangiectasia Mutated (ATM) kinase, the ATM- and RAD3-related (ATR) kinase, and the DNA-dependent protein kinase (DNA-PK) [34]. All of these three protein kinases belong to the phosphoinositide 3-kinase (PI3K)-related kinases (PIKKs) that share sequence homology and phosphorylate an overlapping set of substrates. Based on their function and sequence homology, the PIKK family can be grouped into six subfamilies [34]. Their targets often have a SQ/TQ cluster domains (SCDs). ATR is hyperactivated in response to a variety of DNA damages and is essential for cell viability. On the contrary, ATM is activated following DSB formation and its loss in budding yeast is not lethal. However, in mammals, mutations of ATM or ATR lead to enhanced cancer susceptibility. Once ATM or ATR are localized to the site of DNA damage and activated by DNA sensing proteins, both kinases initiate a signaling cascade that transduces the signal through the mediator proteins Claspin, BRCA1, MDC1 and 53BP1 to the effector kinases CHK1 and CHK2. Effector kinases are transiently recruited to DNA damage sites and are released after their activation, allowing transmission of the checkpoint response to a range of effector proteins.

The G1/S and G2/M checkpoints represent a global cellular response, in which checkpoint kinases regulate cell-cycle events distant from the lesions that initiated the signaling [35]. On the contrary, the intra-S phase checkpoint does not prevent cell-cycle transition but it slows down DNA replication in the presence of DNA damage during S-phase by inhibiting origin firing or reducing the rate of replication fork progression. Origin regulation is a global response in which factors act *in trans*

to DNA lesions that can be far from the origins being regulated [36]. Checkpoint-dependent replication fork slowing may, if the checkpoint does not affect all forks, be regulated *in cis* to DNA damage and only the forks encountering DNA damage would be slowed. The drugs used in checkpoint response studies are described in the next chapter.

Stalled replication forks can be stabilized during the S-phase checkpoint, allowing the completion of replication in the presence of DNA damage [37]. Moreover, the S-phase checkpoint prevents excessive nuclease activity and ssDNA formation at stalled forks [38]. Lastly, checkpoint-mediated stabilization of stalled replication forks prevents fork breakage, a source of gross chromosomal rearrangements and cell death [39].

Sometimes, it is advantageous for the cell to circumvent replicative arrests and postpone the repair of the lesions. This process, known as DNA damage tolerance (DDT) or lesion bypass, can be accomplished in two different pathways that are well evolutionary conserved from yeast to human. In translesion DNA synthesis (TLS), the replicative polymerase is replaced with a specialized TLS polymerase that binds to the PCNA, and replicates past the damage, but this mechanism has high risk of mutagenesis [40]. In template switching, considered accurate, the stalled polymerase makes use of an alternative, undamaged template, that is the newly synthesized daughter strand on the sister chromatid [41].

3.4 – Replication stress and cancer

Amongst the hallmarks of cancer, one can find the oncogene-induced replication stress and DNA damage. Interestingly, enhanced replication stress has been shown to confer a weakness to cancer cells (Table 1) [42, 43]. Targeting excessive replication stress in cancer cells with activated oncogenes seems to be promising

approach for specific killing of these cells [43-45]. Oncogene-induced replication stress is characterized by a rapid activation of ATR and Chk1 in response to abnormal DNA replication intermediates, excessive origin firing and DNA breakage at fragile sites, regions that replicate late with difficulties (described later). Studies have underlined a gene-dosage mechanism of ATR and Chk1, since mice heterozygous for these kinases are tumor prone, while low level of ATR contrasts tumor formation, due to a sufficiently strong replication stress in cells expressing oncogenes, leading to senescence or cell death [46].

Human disease	Aetiology		Characteristics
	Affected pathway	Defective protein(s)	
Aicardi-Goutieres syndrome (OMIM 610333, 610181, 610329, 225750, 612952)	Removal of ribonucleotides, RNA–DNA hybrids	RNase H2, TREX1, SAMHD1	Neurological dysfunction, appearance of chilblains
Amyotrophic lateral sclerosis 4 (OMIM 602433)	Resolution of RNA–DNA hybrids, transcription termination	Senataxin	Childhood- or adolescent-onset degeneration of motor control
Ataxia-ocular apraxia 2 (OMIM 606002)			Adolescent-onset cerebellar ataxia
Ataxia-telangiectasia-like disease (OMIM 604391)	MRN complex; ATR/ATM activation	Mre11	Neurodegeneration, ataxia
Bloom syndrome (OMIM 210900)	DNA remodelling, replication fork structure resolution	BLM	Premature ageing, growth retardation, cancer predisposition
Cancer[137]	Many	Many	Uncontrolled cell growth, leading to organ failure
Ciliopathies[138]	Centrosome, primary cilia formation	CEP164, Nek8, Mre11, Znf423, Fan1	Dysfunction or degeneration of organs, particularly kidney, retina, and brain
Congenital dyserythropoetic anemia, type 1 (OMIM 224120)[127]	Histone deposition	CDAN1	Anaemia, skeletal abnormalities
Fanconi anaemia[44]	DNA inter-strand crosslink repair	FANC family of proteins	Heterogenous — bone marrow failure, skeletal defects, hypopigmentation, cancer predisposition
	Replication fork protection	FANCD2, BRCA2	
Friedreich's ataxia (OMIM 229300)	Trinucleotide repeat expansion	FXN	Neurodegeneration (ataxia, loss of coordination, loss of sensation)
Laminopathies[139]	Nuclear envelope structure	Lamins	Premature ageing
Meier-Gorlin syndrome (OMIM 224690)	Origin licensing, centrosome maintenance	ORC1, ORC4, ORC6, CDT1, CDC6	Growth retardation, microcephaly
Nijmegen breakage syndrome (OMIM 251260)	MRN complex; ATR/ATM activation	Nbs1	Microcephaly, growth retardation, cancer predisposition
Nijmegen breakage syndrome-like disorder (OMIM 613078)	MRN complex; ATR/ATM activation	Rad50	Microcephaly, growth retardation, mental retardation
Rothmund-Thomson syndrome (OMIM 268400)	DNA remodelling, replication fork structure resolution	RecQL4	Premature ageing, growth retardation, cancer predisposition
Schimke immuno-osseous dysplasia (OMIM 242900)	Replication fork stabilization and reversal; DNA re-annealing	SMARCAL1 / HARP	Dwarfism, skeletal abnormalities, renal failure, and immunodeficiency
Seckel syndrome (OMIM 210600)	ATR signalling	ATR, ATRIP, CENPJ, CEP152, PCNT	Growth retardation, dwarfism, microcephaly, mental retardation
Spinocerebellar ataxia type 10 (OMIM 603516)	Trinucleotide repeat expansion	ATXN10	Ataxia, seizures
Werner syndrome (OMIM 277700)	DNA remodelling, replication fork structure resolution	WRN	Premature ageing, growth retardation, cancer predisposition
Wolf-Hirschhorn syndrome (OMIM 194190)[125]	DNA damage response, nucleosome deposition	NELF-A (WHS2), SLBP, MMSET (WHS1)	Growth retardation, mental retardation, seizures
Xeroderma pigmentosum — variant (OMIM 278750)	Translesion synthesis	Polymerase η	Cancer predisposition (especially skin cancer)

OMIM numbers refer to the Online Mendelian Inheritance in Man database.

Table 1. Human diseases associated with defects in the replication stress response. [33]

Taken together, these observations elucidate a still unknown multistep process of tumor development involving the DNA damage response (DDR) and the replication stress response (RSR). ATR/Chk1 (replication stress response) and ATM/Chk2 (DSB response) checkpoint kinases can prevent oncogene-driven tumorigenesis [44, 45]. ATR/Chk1 haploinsufficiency, which limits RSR and DDR signaling can, under these conditions, promote cancer. However, in advanced stage tumors with enhanced replication stress that already trespassed the DDR barrier, ATR/Chk1-mediated RSR can facilitate the tumor to deal with the persistent replication stress (Figure 6).

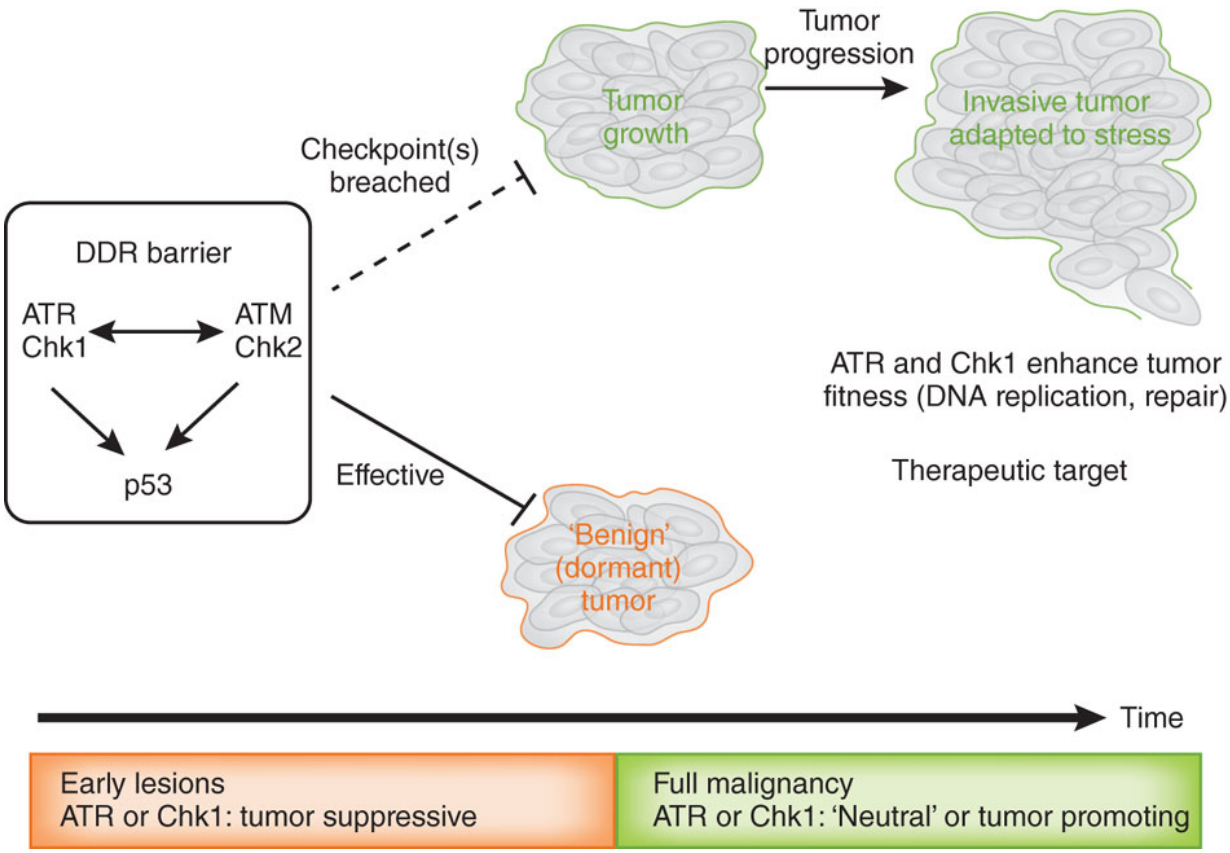

Figure 6. The ATR/Chk1 pathway during tumorigenesis. Oncogene-activated early lesions experience replication stress and DNA damage, which in turn triggers the repair response and checkpoint activation, towards senescence or death of tumor cells. Tumor cells that defeat the DDR barrier, can continue their proliferation. Tumors in an advanced stage, where oncogene expression promote a constant replication stress and genetic instability, can take advantage of the ATR-Chk1 signaling pathway to ensure their survival. [47]

3.4.1 – Drugs used to study checkpoint responses

Although natural impediments, such as secondary DNA structures (e.g. G-quadruplexes), RNA-DNA hybrids or tightly bound transcription complexes (e.g. at rDNA or tRNA genes) can create an obstacle for the replication fork [48], DNA-damaging and fork stalling agents are extensively used to provoke a checkpoint response that, usually, does not occur during natural or endogenous replication fork impediment formation (Table 2). The checkpoint response is more prone to be activated in cells deficient for DNA repair. Other lesions that expose primed ssDNA and activate the replication checkpoint arise when replicative helicase and polymerase functions are uncoupled [49]. To trigger the replication checkpoint, one can treat cells with hydroxyurea (HU) or aphidicolin (APH).

Treatment/Impediments	Mode of action	Result	Responders (*S.cerevisiae*)
hydroxyurea (HU)	inhibits ribonucleotide reductase—dNTP pools become depleted	uncoupling of helicase and polymerase function; ssDNA is exposed	Mec1, Mrc1, Sgs1
aphidicolin	inhibits DNA polymerases	uncoupling of helicase and polymerase function; ssDNA is exposed	Mec1, Mrc1
methylmethanesulfonate (MMS)	alkylates DNA	uncoupling of helicase and polymerase function; ssDNA is exposed; in addition DNA repair takes place, that also leads to ssDNA; requires replication forks to induce checkpoint response	Mec1, Rad9 (Mrc1, Sgs1)
ultraviolet light/4-NQO	induces Thymidine dimerization	induces DNA repair, that leads to ssDNA	Mec1, Rad9 Mrc1
crosslinking agents (cisplatin/nitrogen mustard)	causes DNA inter-strand crosslinks	both helicase and polymerase are blocked; in addition DNA repair takes place, that also leads to ssDNA	Mec1/Tel1, Rad9
ionizing irradiation (IR)/bleomycin	causes single and double strand breaks	breaks are directly recognized by MRX-Tel1; resection leads to ssDNA	Mec1/Tel1; Rad9
camptothecin (CPT)	inhibits Topoisomerase I, keeps it in a DNA-bound confirmation	both helicase and polymerase are blocked; double strand breaks are actively induced by DNA repair machinery	Mec1/Tel1, Rad9
natural fork barriers (rDNA, t-RNA genes, transcription	slow down replisome progression	both helicase and polymerase are slowed down	-

Table 2. The table summarizes S. cerevisiae checkpoint responses, depending on the treatment. [50]

HU inhibits ribonucleotide reductase (RNR) by reducing the reactive tyrosyl radical in the active center of the enzyme [51]. If RNR is inhibited, when replication is initiated, dNTP pools are depleted, and this leads to a stalling of DNA polymerases [52]. Aphidicolin directly inhibits DNA polymerases [53] without affecting the replicative helicase [24]. Thus, polymerases are blocked, but MCM helicases continue to move generating long stretches of ssDNA that trigger the replication

checkpoint [54]. It is worth to mention that low doses of aphidicolin enhance replication stress by slowing down the progression of replication forks, while high dose of this drug provokes a complete arrest of polymerase movement.

On the other hand, interstrand crosslinks (ICLs; e.g. caused by cisplatin) block the MCM helicase in front of the replication fork. In this case, there is no immediate activation of the replication checkpoint, and no uncoupling of helicase and polymerase. Usually, the replication fork pauses 20-40 base pairs from the lesion, and structure-specific nucleases will process the template or nascent strands generating ssDNA, and this will lead to checkpoint activation [55, 56].

Alkylation of DNA can be formed by methyl methanesulfonate (MMS) treatment. Alkylation creates bulky lesions that do not activate checkpoint response *per se*, but require a collision with a replication fork to trigger checkpoint activation [37].

Ionizing radiation (IR) or radiomimetic drugs (e.g. bleomycin) cause DSBs which, in turn, activate the DNA damage response through the ATM kinase, and after processing, through ATR [57]. On the other hand, UV treatment induces ATR-mediated response, because of pyrimidine dimer formation and this adduct is recognized by the NER machinery, which creates a ssDNA patch during the repair process [58].

Replication forks can also be arrested after camptothecin (CPT) treatment, which inhibits DNA topoisomerase I (Top1) by blocking DNA relegation after Top1 created a ssDNA nick and becomes covalently linked to the DNA end [59]. The replication run-off model [60] shows that replication forks running into these ssDNA nicks are converted into DSBs. The torsional stress generated by Top1 inhibition may lead to fork slowing, and this mechanism is actively mediated by Mus81 endonuclease that generates DSBs [61].

3.5 – RecQ helicase family

Helicases are motor proteins that utilize chemical energy derived from nucleotide triphosphate (NTP) hydrolysis for unwinding nucleic acid duplexes [62]. The RecQ helicase family is conserved in many species: *S. cerevisiae*, *S. pombe*, *Arabidopsis*, *Drosophila*, *C. elegans* and mammals [63, 64]. In humans and mice, there are five RecQ helicase family members: RECQ1, WRN, RECQ4, RECQ5 and BLM (Figure 7). These motor proteins are required for genomic stability and therefore are classified as genome caretakers (Table 4).

Helicase proteins are subdivided into six superfamilies (SF1 to SF6), and RecQ helicases belong to the SF2 helicase superfamily. They have in common a helicase domain (350-400 a.a.), containing seven conserved motifs that include the Walker A and B boxes involved in ATP binding and hydrolysis, respectively. In addition, RecQ helicases contain the RQC (RecQ C-terminal) domain that features a zinc-binding motif, a helix-hairpin-helix, winged-helix (WH) domain, and a β-hairpin motif [65, 66]. This domain mediates binding of these helicases to G-quadruplex DNA and stabilizes helicase binding to other structures. The RQC domain of RECQ1 organizes the binding to ssDNA-dsDNA junctions, and the β-hairpin couples ATP hydrolysis to DNA unwinding [67, 68]. Moreover, WRN's RQC domain can enter in contact with the phosphate backbone on 5'-ssDNA overhangs [66].

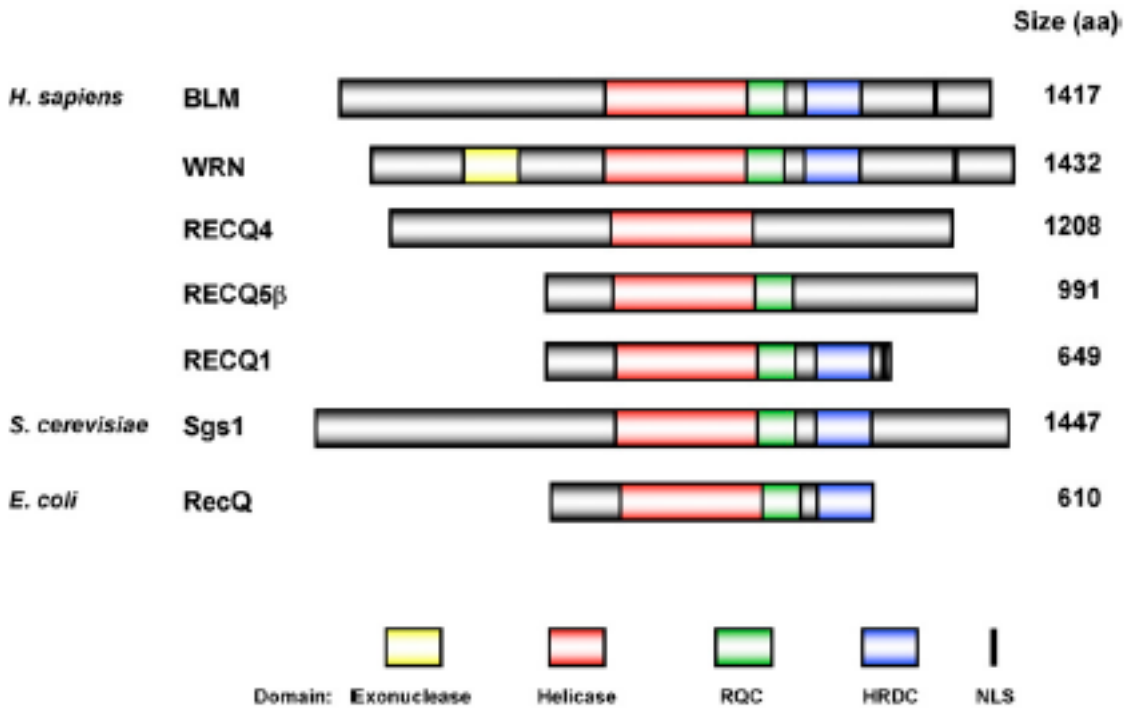

Figure 7. Domain structure of the RecQ helicase family in human and the homologs found in *S. cerevisiae* and *E. coli*. [69]

WRN and BLM helicases also contain the HRDC (Helicase and RNaseD C-terminal) domain [65], which mediates their recruitment to laser-induced DSBs [70] and sites of MMS- and mitomycin C-induced DNA damage [71]. RecQ helicases possess a DNA-dependent ATPase and an ATP-dependent 3'->5' DNA helicase activity, and also a DNA strand annealing activity. RecQ enzymes are involved in processes such as DNA replication, disruption of recombination intermediates, joint molecules and G4-DNA structures [72].

Helicase	Growth or proliferation	Radiation or chemotherapy sensitivity
RECQL1	RECQL1-targeted siRNA decreased proliferation, induced DNA damage and elevated SCE of endocervical carcinoma HeLa cells[21], and induced mitotic cell death in lung, prostate, bladder, colon and liver cancer cells[26] and HCC cells[3] *in vitro*. RECQL1-targeted siRNA also suppressed tumour growth in mouse xenograft lung, liver, pancreatic and colorectal cancer models[27], liver cancer with transplanted human HCC[3], and nude mice carrying FaDu or D-562 hypopharyngeal carcinoma xenografts[25]. RECQL1-targeted siRNA decreased proliferation of human hypopharyngeal carcinoma[25] and glioblastoma cells *in vitro*[28].	RECQL1-targeted siRNA decreased proliferation of HeLa cells exposed to camptothecin or ionizing radiation[21], and caused a camptothecin-induced replication restart defect in U2OS osteosarcoma cells *in vitro*[129]. RECQL1-targeted siRNA enhanced an antitumour effect of cisplatin in nude mice carrying FaDu hypopharyngeal carcinoma xenografts, and co-treatment with cisplatin increased DNA damage, apoptosis and mitotic catastrophe[25]. RECQL1-targeted siRNA and RECQL1-targeted shRNA sensitized glioblastoma[28] and HeLa and U2OS cells[24], respectively, to hydroxyurea *in vitro*. RECQL1-targeted siRNA sensitized glioblastoma cells to TMZ *in vitro*[28]. RECQL1-targeted shRNA sensitized HeLa and U2OS cells to 8-MOPS *in vitro*[24].
WRN	WRN-targeted siRNA decreased proliferation of human hypopharyngeal carcinoma cells *in vitro* and suppressed tumour growth in nude mice carrying FaDu or D-562 hypopharyngeal carcinoma xenografts[25]. WRN-targeted shRNA decreased tumour establishment and tumour growth in MYC overexpressing non-small-cell lung cancer mouse xenografts[184].	WRN-targeted siRNA enhanced the antitumour effect of cisplatin in nude mice carrying FaDu hypopharyngeal carcinoma xenografts; this combination increased DNA damage and induced apoptosis and mitotic catastrophe[25].
BLM	BLM-targeted siRNA caused a 2.5-fold increase in SCE in HeLa cells [223].	NR
WRN and BLM	WRN-targeted shRNA or BLM-targeted shRNA decreased proliferation of U2OS cells *in vitro* with BLM depletion having a greater effect[224]. Cells co-depleted for WRN and BLM showed reduced proliferation that was comparable to BLM-depleted cells.	BLM-targeted or WRN-targeted shRNA sensitized U2OS cells to camptothecin, cisplatin or 5-FU. BLM-targeted shRNA sensitized U2OS cells to hydroxyurea. Co-depletion did not further sensitize cells to any tested chemotherapies[224].
RECQL4	RECQL4-targeted siRNA inhibited proliferation and increased DNA damage and apoptosis of prostate cancer cells *in vitro*. RECQL4-targeted shRNA caused metastatic cancer cells to display reduced cell invasiveness and suppressed tumour growth in nude mice[7].	NR
RECQL5	RECQL5-targeted shRNA decreased proliferation of HeLa cells *in vitro*[29].	RECQL5-targeted shRNA increased 53BP1 foci in HeLa cells[225].

Table 4. Effect of human RecQ helicase family depletion on cell proliferation, tumor growth and sensitivity to chemotherapy/radiation. Adapted from [73].

RECQ1 helicase is the shortest of the human RecQ family members, and it is involved in branch migration and restart of reversed forks during S phase upon topoisomerase I inhibition [74]. Mutation in RECQ1 gene is not linked to any human disease [75].

WRN is the only RecQ helicase that contains a 3'->5' exonuclease activity, and it binds onto overhanging 5' ends of the guide strand of duplex DNA and cleaves the target strand, degrading substrates found during DNA repair and intermediates in DNA replication [76]. Inherited loss-of-function mutations in human WRN gene result in Werner's syndrome that is characterized by premature aging and shortened

cellular lifespan (median age of death 47 years). WS patients suffer from osteoporosis, athero- and arteriosclerosis and a high cancer incidence [77].

Mutations in RECQ4 gene lead to autosomal recessive disorders, known as Rothmund-Thomson syndrome, RAPADILINO syndrome and Baller-Gerold syndrome. Cells carrying defects in RECQ4 genes show chromosomal abnormalities and genomic instability. RECQ4 interacts with the replication machinery, and it is involved in replication progression and stress response [78].

The BLM and RECQ5 helicases will be described in more details in the next chapters.

3.5.1 - BLM helicase

Genetic defects in the BLM gene are responsible for the autosomal, recessive disease called Bloom syndrome (BS). This disorder is characterized by retarded growth, head development defects and cancer predisposition. The skin of BS patients presents erythema that become chronic to sun exposition [79].

BS cells show elevated frequency of sister chromatid exchanges (SCEs) [80] due to aberrant processing of recombination intermediates [81]. BLM acts in complex with replication protein A and TOPOIIIα, and it suppresses the formation of crossover products generated by resolution of homologous recombination intermediates containing Holliday junctions [82]. As already mentioned in chapter 3.5.1, the BTR-containing BLM complex can catalyze double Holliday junction dissolution, a reaction that produces only non-crossover products.

BLM has been linked to interstrand crosslink (ICL) DNA repair pathway. The FA pathway is implicated in cellular resistance to DNA ICLs and other forms of replication stress [83]. The FA pathway leads DSBs towards HR, thus preventing inappropriate NHEJ repair [84]. BLM is located in a multi-protein nuclear complex

with FA core complex proteins to recognize DNA lesions [85]. BLM interacts with FANCJ to maintain chromosomal stability [86]. Therefore, BLM has a role in the recognition of the ICL and strand resection of a DSB, together with FANCJ and MRN complex, that arises from an unhooked ICL (Figure 8) [87]. Moreover, BLM has

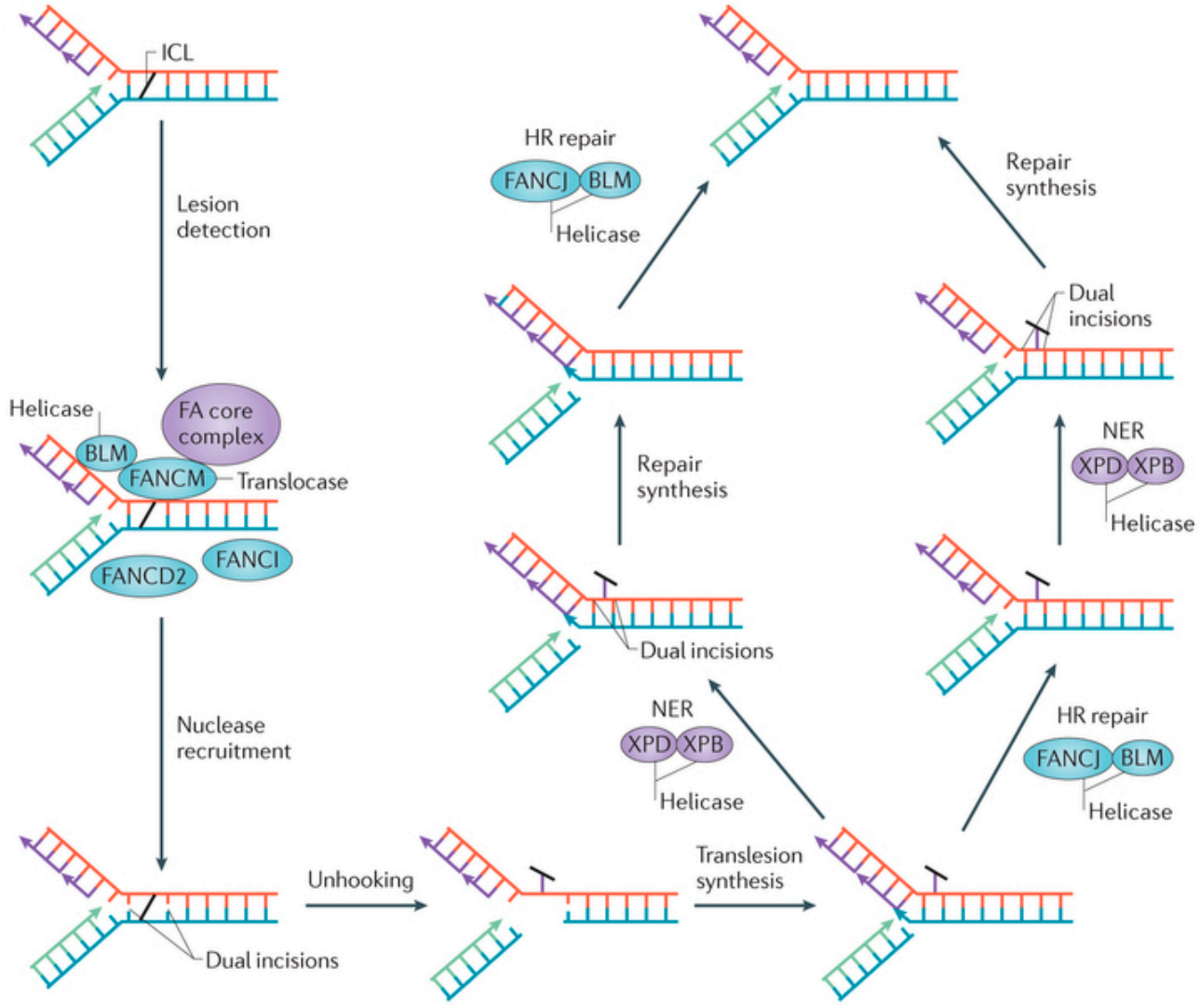

Figure 8. Involvement of BLM helicase in the interstrand crosslink DNA repair mechanism. Following lesion detection, nucleases incises on each side of the crosslink and remove the aberration, leaving a gap that generate a DSB from the fork. Other parallel pathway can resolve the lesion as well. Adapted from [73].

an important role in mitosis to resolve DNA bridging between sister chromatids during anaphase, promoting correct chromosome segregation and preventing aneuploidy [88, 89].

3.5.2 – RECQ5 helicase

Mutations in RECQ5 gene have not been linked to any human disease, but Recq5 knockout mice show elevated levels of sister chromatid exchange and predisposition to various types of cancer (Table 5) [90], suggesting that RECQ5 plays an important role in genome stability maintenance.

Tumors found in Recql5 deficient mice[1]

Tumor type	Number	Percentage (%)	Age (days)
Lymphomas	14	28%	
Thymic lymphoma	1	2%	193
Follicular lymphoma	5	10%	647[3]
Plasmacytoid lymphoma	8	16%	606[3]
Solid tumors	12	24%	
Squamous cell carcinoma	1	2%	480
Lung adenocarcinoma	6	12%	613[3]
Heptocellular carcinoma	1	2%	660
Breast carcinoma	1	2%	647
Liver hemangioma	3	6%	588[3]
Total	26[2]	52%	

[1] 50 *Recql5*$^{-/-}$ and 32 *Recql5*$^{+/+}$ mice were aged up to 22 months (660 days) and monitored daily for tumor development. 2 wild type mice (6%) developed mild lymphomas at the end of the study.
[2] 26 tumors found in 23 *Recql5*$^{-/-}$ mice (46%). 3 mice (6%) had multiple tumors.
[3] Average ages of all cases.

Table 5. Summary of cancers found in Recql5$^{-/-}$ mice. [90]

Although RECQ5 deficiency in DT40 cells does not compromise genome stability, it has been observed that absence of both RECQ5 and BLM in these cells result in higher levels of SCEs, compared to the level of SCEs in $BLM^{-/-}$ mutant [91]. Moreover, in C. elegans, absence of RECQ5 reduced its lifespan and increased the sensitivity to ionizing radiation [92].

RECQ5 helicase is present in human cells in three different isoforms, RECQ5α, RECQ5β and RECQ5γ, produced by alternative splicing. The first 410 amino acids of these isoforms are identical and form the helicase domain of the enzyme. RECQ5α is the shortest isoform, and it only contains the helicase domain. RECQ5β contains the helicase domain, a RQC domain, and a unique C-terminal domain that is not present in the other isoforms (Figure 9). RECQ5γ is comprised of the helicase domain followed by a short region of 25 amino acids [93]. RECQ5β (from now on mentioned as "RECQ5") possesses an ATP-dependent 3'->5' helicase activity and a DNA strand-

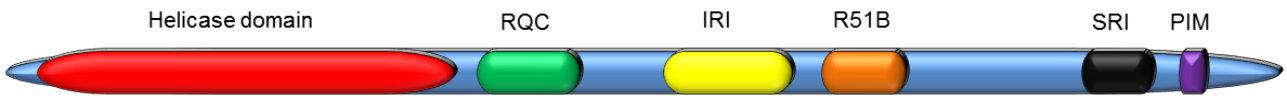

Figure 9. Schematic representation of RECQ5 domain for its enzymatic activity and for some of the main interacting partners. IRI domain: Internal RNAPII-interacting. R51B: RAD51 binding domain. SRI: Set2-Rpb1-interacting. PIM: PCNA-interacting motif.

annealing activity residing in the C-terminal domain. The DNA strand-annealing activity is inhibited by the replication protein A (RPA) and ATP [94].

RECQ5 interacts with RAD51 recombinase that mediates DNA homology search and strand exchange during HR [90]. In this context, RECQ5 can disrupt RAD51 presynaptic filaments, in a reaction that depends on ATP. The removal of RAD51 is followed by RPA binding in order to prevent reloading of RAD51 and unscheduled recombination (Figure 10).

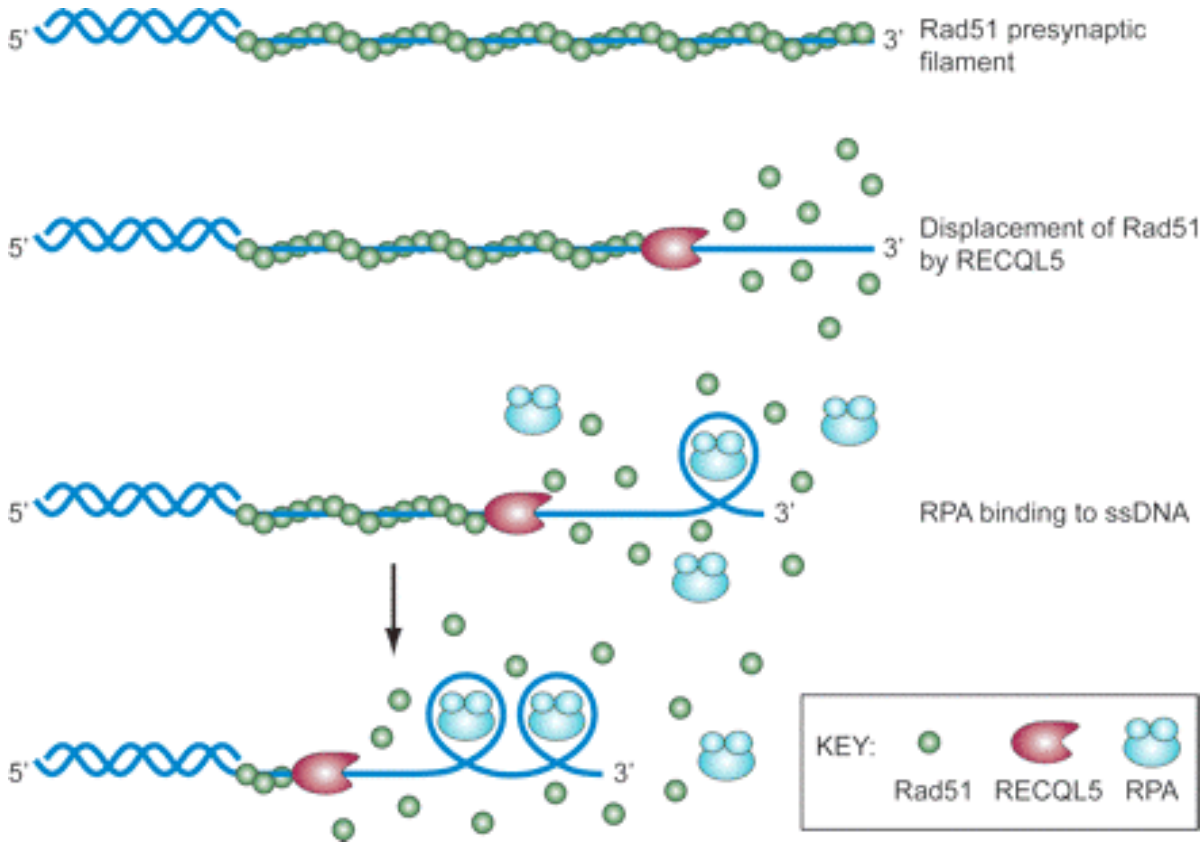

Figure 10. Model for RECQ5-mediated disruption of RAD51 presynaptic filament during HR proposed in [90].

Interestingly, RECQ5 directly interacts with RNA polymerase II (RNAPII), and is the sole member of the RecQ helicase family to have this property [95]. RECQ5 binds to the Ser2,5-phosphorylated C-terminal repeat domain (CTD) of the largest subunit of RNAPII (Rpb1) through the Set2-Rpb1-interacting (SRI) domain located at RECQ5 C-terminus. Moreover, RECQ5 is enriched on transcribed genes during the elongation phase of transcription [96]. In the context of active transcription, RECQ5 was shown to act as an elongation factor to maintain genomic stability during the transcription process. RECQ5 depletion promotes a general transcription stress, characterized by RNAPII stalling, pausing, arrest or backtracking [97].

3.6 – Structure-specific endonucleases

As already mentioned in the previous chapters, faithful DNA duplication of the genome is fundamental process and yet very challenging. The replication fork can encounter numerous obstacles during DNA replication, which impede its natural progression. Collisions between the replication machinery and lesions in the DNA template can occur, due to hydrolytic-oxidative processes, cellular metabolites and DNA damaging agents [5]. Replication forks have also to deal with obstacles arising from tightly bound proteins to DNA, secondary structures, transcription machineries and torsional stress [98]. Last but not least, low supplies of dNTPs during compromised replication dynamics can retard replication forks progression [99].

Stalled replication forks are recognized by the S phase checkpoint, inhibiting cell cycle progression and late origin firing [101]. The stalled replication forks are protected by the checkpoint itself, permitting to resume DNA synthesis once the obstacle on DNA is removed. Replication fork restart is facilitated by HR, which creates branched intermediates between sister chromatids. These structures must be resolved by generating intact chromosomes before cells enter into mitosis. Delays in replication fork restart can lead to DSB formation (Figure 11) [102]. In *Escherichia coli*, the RuvC structure-specific nuclease processes HR intermediates and replication fork cleavage, in order to allow another fork to assemble and complete DNA duplication. In eukaryotes, three conserved nucleases have been identified, sharing similar properties with RuvC, but not biochemically equivalent: MUS81-Mms4/MUS81-EME1 (budding yeast/human), Yen1/GEN1 and Slx1-Slx4/SLX1-SLX4 (Table 6).

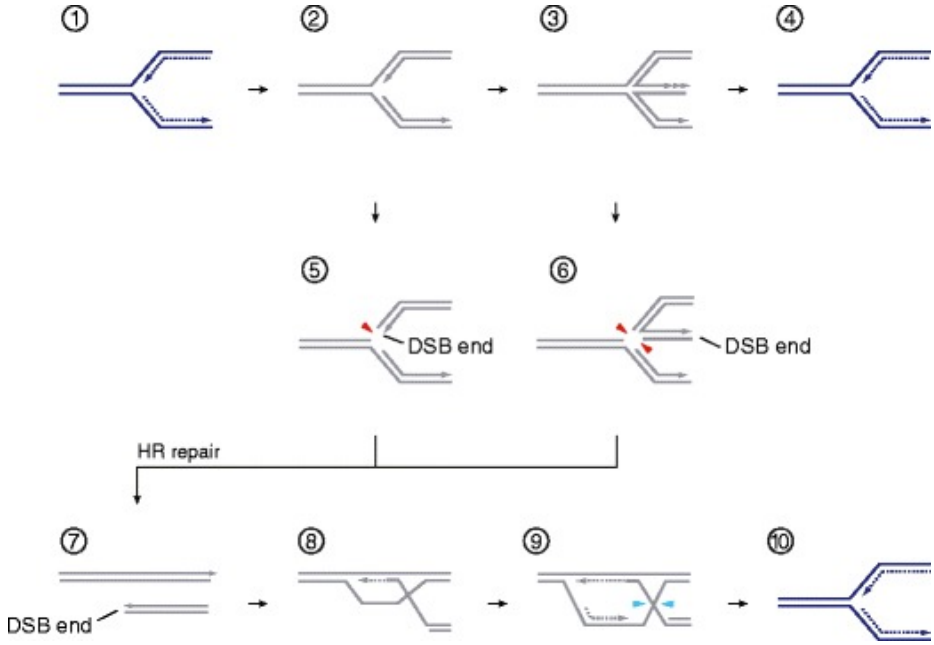

Figure 11. Replication fork recovery. 1) Replication fork movement can be perturbed by different obstacles, and 2) potentially arresting the replication fork (inactive fork in grey); 3) replication fork regresses, by annealing of the nascent leading and lagging strands with one another, leading to the formation of a HJ-like structure. Template switching allows leading strand extension (triple arrowhead) if the lagging strand had been extended further than the leading strand prior to regression; 4) if the obstacle is removed (or if template switch bypass), HJ branch migration may reset an active fork (in blue). Alternatively, deliberate fork cleavage can occur 5), and MUS81-EME1 may act directly on the replication forks (red arrowhead); 6) replication fork cleavage may occur after conversion of the three-way junction into a four-way HJ intermediate. 7-10) Recombination-dependent replication/break- induced replication (BIR) pathways can reactivate a processive replication fork from a DSB after breakage or spontaneous replication fork collapse. [100]

Indentifying subunit	Protein complex	Endonuclease family	Known in vivo function(s)	References
Rad1	*Sc*Rad1–Rad10	XPF	NER, ICL, SSA	(Cox and Parry 1968; Fishman Lobell et al. 1992)
	*Sp*Rad16–Swi10	XPF	NER, MTS	(Carr et al. 1994; Schmidt et al. 1989)
	*At*RAD1–RAD10	XPF	NER, ICL, SSA	(Gallego et al. 2000; Dubest et al. 2002)
	*Dm*MEI-9–ERCCI	XPF	NER, ICL, Meiosis	(Radford et al. 2005)
	*Hs*XPF(ERCC4)–ERCC1	XPF	NER, ICL	(Biggerstaff et al. 1993; van Vuuren et al. 1993)
Mus81	*Sc*Mus81–Mms4	XPF	HR, RF, Meiosis, ICL	(Interthal and Heyer 2000)
	*Sp*Mus81–Eme1	XPF	HR, RF, Meiosis	(Boddy et al. 2000)
	*At*MUS-EMEA/EMEB	XPF	HR, RF	(Berchowitz et al. 2007)
	*Dm*MUS81–EME1	XPF	HR	(Johnson-Schlitz and Engels 2006; Trowbridge et al. 2007)
	Hs/MmMUS81–EME1	XPF	HR, ICL	(Abraham et al. 2003; Dendouga et al. 2005; Svendsen et al. 2009)
Yen1	*Sc*Yen1	Rad2/XPG	N/D	
	*Dm*GEN	Rad2/XPG	N/D	
	*Ce*GEN-1	Rad2/XPG	DSBR	(Bailly et al. 2010)
	*Hs*GEN1	Rad2/XPG	N/D	
Slx4				
	*Sc*Slx4 complexes			
	Rad1–Rad10–Slx4	XPF	SSA	(Flott et al. 2007)
	Slx1–Slx4	UIY–YIG	rDNA	(Kaliraman and Brill 2002)
	*Sp*Slx4 complexes			
	Slx1–Slx4	UIY–YIG	rDNA	(Coulon et al. 2004)
	*Dm*MUS312 complexes			
	MEI-9–ERCC1?–MUS312	XPF	NER, ICL, Meioses	(Yildiz et al. 2002)
	SLX1–MUS312	UIY–YIG	N/D	
	*Ce*HIM-18 complexes		HR, RF, DSBR, meioses	(Saito et al. 2009)
	XPF–ERCC1?–HIM-18	XPF	N/D	
	SLX1–HIM-18	UIY-YIG	N/D	
	*Hs*BTBD12 complexes			
	XPF–ERCC1?–BTBD12	XPF	N/D	
	MUS81–EME1?–BTBD12	XPF	N/D	
	SLX1–BTBD12	UIY–YIG	HR, ICL, DSBR	(Andersen et al. 2009; Fekairi et al. 2009; Svendsen et al. 2009; Munoz et al. 2009)

N/D not determined, *NER* nucleotide excision repair, *SSA* single-strand annealing, *MTS* mating-type switching, *HR* homologous recombination, *RF* replication fork support, *ICL* interstrand crosslink repair, *rDNA* ribosomal DNA maintenance, *DSBR* double-strand break repair

Table 6. Summary of the species-specific structure-selective endonucleases, organized by their binding partners, endonuclease superfamily, and the pathway in which they are involved. [103]

3.6.1 – Mus81-Mms4/MUS81-EME1

Mus81 was identified in a two-hybrid screens using Rad54 as bait in *S. cerevisiae* [104] and the DNA damage response kinase Cds1 (ScRad53, hCHK2) as bait in fission yeast [18]. Mus81 forms a heterodimer with a non-nucleolytic subunit: Mms4 in budding yeast or EME1 in fission yeast and humans [18, 105]. Mus81 and

Mms4/EME1 are required for the recombination-mediated DNA repair during replication fork restart, and for yeast meiotic recombination. Mus81 is essential in the absence of the dHJ dissolution complex, Sgs1-Top3-Rmi1 [18, 105] in *S. cerevisiae*, *S. pombe*, *A. thaliana*, and *D. melanogaster*. Loss of MUS81/EME1 increases the number of gross rearrangements [106], and in somatic cells, MUS81 is required for HR at stalled or broken replication forks [107, 108]. Eukaryotic cells with defects in these genes show hypersensitivity to a variety of replication fork stalling agents, including MMS, HU and CPT [104, 109, 110].

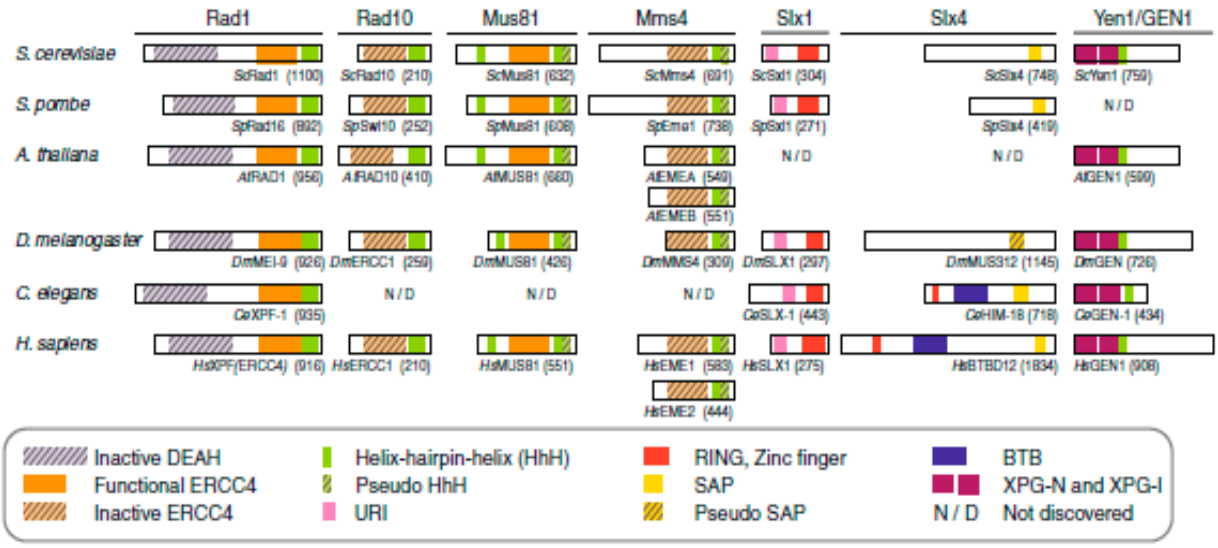

Figure 12. Domain structure and architecture of eukaryotic structure-selective junction endonucleases. Protein names and amino acids length are noted below each protein. N/D, not discovered. [103]

The substrates of Mus81-Mms4/MUS81-EME1 consist of duplex DNA with a 3'-single-stranded flap (3'-flap), double-stranded three-way junctions that resemble replication forks, HJ precursors, and ligated HJs [111, 112] (Figure 12). Although the activity of the Mus81 complex on fully-fledged HJs is weak, nicked HJs are efficiently resolved [113, 114]. MUS81 and EME1 belong to the XPF endonuclease family and contain an ERCC4 nuclease domain and a tandem helix-hairpin-helix $(HhH)_2$ domain (Figure YYX) [115]. The ERCC4 nuclease domain in MUS81 is catalytically active, but

the equivalent domain in EME1 evolutionary diverged and is inactive. Despite that, EME1 is essential for the stability and activity of MUS81, acting as a regulatory subunit. MUS81 can also interact with EME2 [116], but the precise role of MUS81-EME2 complex in mammals is still under investigation [117].

3.6.2 – Yen1/GEN1

GEN1 (Yen1 in yeast) was first identified in rice as OsSEND-1 [118] in a search for novel Rad2 family endonucleases. GEN1 (XPG-like endonuclease) contains both N-terminal and internal conserved Rad2/XPG family endonuclease domains. Rad2 (human XPG) creates the 3' incision to free the damaged nucleotide during NER.
GEN1 is monomeric but dimerizes on HJ DNA in order to introduce symmetric incisions, resolving HJs in a RuvC-like manner. Other GEN1 substrates include 5'-flaps and replication forks [119] (Figure 13).

Deletion of Yen1 in *S. cerevisiae* enhances the sensitivity to replication fork-RAD52-dependent damage in mus81Δ cells, indicating that Mus81 and Yen1 can work in overlapping pathways during processing of replication intermediates in budding yeast [120].

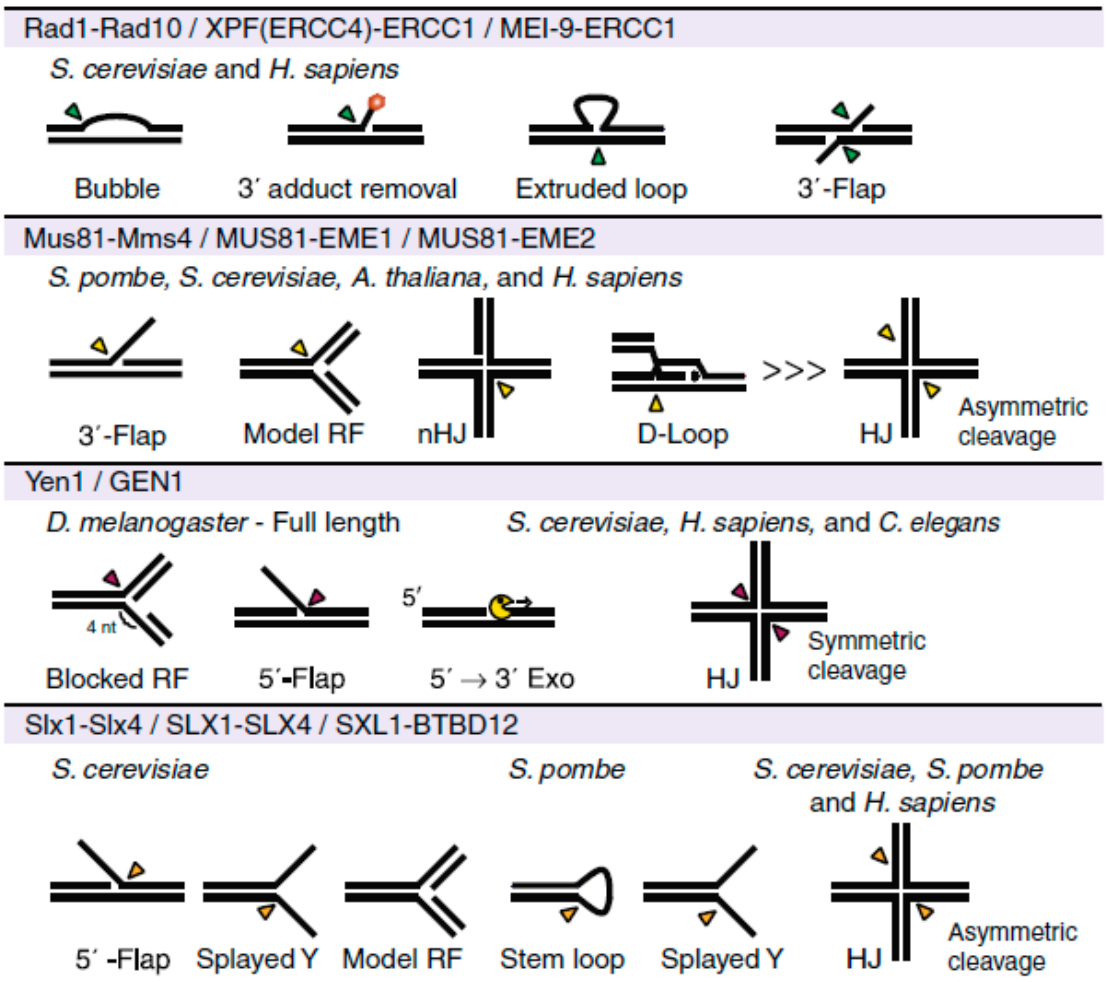

Figure 13. Substrate specificity of eukaryotic structure-selective junction endonucleases. Incision sites legend: Rad1 (green triangles), Mus81 (yellow triangles), Yen1/GEN1 (purple triangles), Slx1-Slx4 (orange triangles).

3.6.3 – Slx1-Slx4

Slx1 and Slx4 were identified in *S. cerevisiae* by a genetic screen for synthetic lethal mutations with a defect in the Sgs1 helicase [105]. Sequence alignment revels Slx1 to have a conserved UvrC-intron (URI)-endonuclease domain and a C-terminal RING/PHD-type zinc finger domain (Figure 12), placing Slx1 into the URI-YIG family of endonucleases including *E. coli* UvrC [121]. A genetic analysis of *S. cerevisiae* slx1

and slx4 deletion phenotypes identifies these genes to function in the recombination-mediated repair of stalled replication forks [122].

Slx1-Slx4 complex cleaves a variety of DNA junctions *in vitro* showing preference for Y-shaped structure, 5'-flaps, and replication forks. Slx1-Slx4 has an activity towards mobile HJs and very low activity with fixed HJs [122]. In addition, Slx4 serves as a scaffolding platform that binds to Mus81-Eme1, XPF-ERCC1, and SLX1 [123], forming a high molecular weight complex. Moreover, the endonuclease activity of both Mus81-Eme1 and Slx1 is stimulated by Slx4 [123], suggesting that the increase in cleavage activity reflects a formation of a proper heteromeric protein structure.

3.7 – Homologous recombination and Holliday Junction intermediates

Homologous recombination (HR) is a fundamental process in both mitotic and meiotic cells. In meiosis, HR is responsible for genetic diversity during the production of haploid gametes. In somatic cells, HR pathway leads to an error-free repair of DSBs, and thus it maintains genomic stability.

HR, in mitotic cells, requires an intact sister chromatid that it uses for the homologous pairing and strand exchange with the damaged chromatid. These early interactions are destabilized to promote non-crossover (NCO) structures through the synthesis-dependent strand-annealing (SDSA) pathway [124]. In few cases, strand exchange is followed by second-end capture, DNA synthesis, and nick ligation to generate a joint DNA molecule called double Holliday Junctions (dHJs, Figure 14) [125].

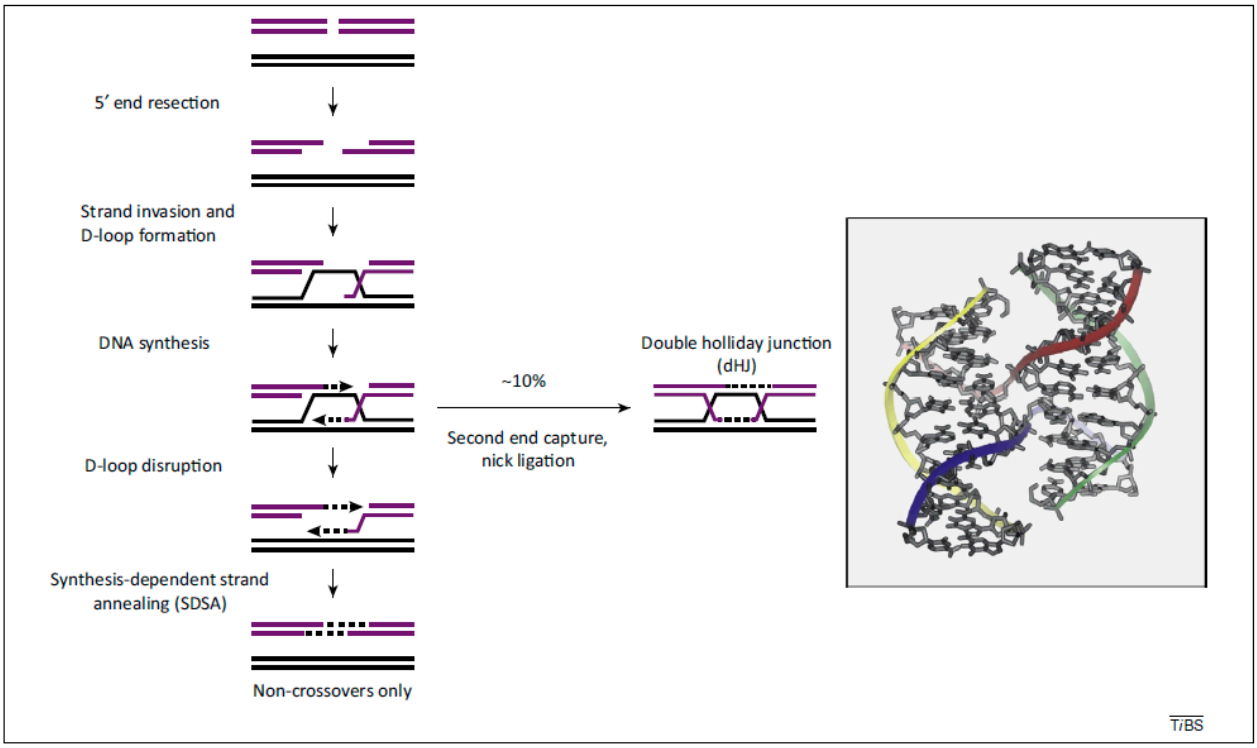

Figure 14. Schematic of the homologous recombination DNA repair pathway. HR takes place in S and G2 phases of the cell cycle and repairs DSBs taking advantage of the intact sister chromatid (black) as a template. The first step of the pathway is the 5'->3' resection, which generates ssDNA tails. The resected DNA ends are recombinogenic and invade the homologous template to form a displacement loop (D-loop) structure. After this process, DNA synthesis occurs. At this stage, the resulting D-loop can be disrupted and the displaced DNA can reanneal to the second DSB end, in a pathway known as synthesis-dependent strand annealing (SDSA), that yields non-cross over products (NCOs). Sometimes, DNA synthesis is followed by second-end capture and nick ligation, generating double Holliday Junctions (dHJs). DHJs can be processed to yield non-crossover (NC) or crossover (CO) products, depending on the enzymes involved. [126]

dHJs form a covalent linkage between two recombining DNA molecules, and their removal is an essential step for a correct chromosome segregation. The enzymes involved in processing these structures are highly specialized, and already described in the previous chapter (3.5).

3.7.1 – Holliday Junction dissolution

BLM has been shown to interact with Topoisomerase IIIα (TopoIIIα) and, along with RMI1 and RMI2, recruits and stimulates TopoIIIα activity on DNA [127]. The BLM-TopoIIIα-RMI1-RMI2 (BTRR) complex promotes the convergent branch migration of a dHJ to form a hemicatenane that is a junction between two double-stranded DNA molecules, where a strand from one molecule winds around the complementary strand from the other DNA molecule (Figure 15). Hemicatenanes are afterwards dissociated by the topoisomerase activity [128]. The dissolution pathway yields only NCO products (Figure 16). COs are detrimental for somatic cells and the dissolution pathway is required for avoidance of loss of heterozygosity (LOH) and tumorigenesis. The BTRR complex is also responsible for DNA topology regulation and resolves aberrant mitotic structures at centromeres [129].

3.7.2 – Holliday Junction resolution

The HJ resolution pathway requires structure-specific endonucleases, namely MUS81-EME1, SLX1-SLX4 and GEN1. GEN1 cleaves HJs by generating symmetrical nicks across the junction to produce nicked duplex intermediates. On the other hand, MUS81-EME1 can cleave intact HJs with low efficiency, but it has high affinity with 3'-flaps and replication forks (see chapter 3.5). SLX1-SLX4 and MUS81-EME1 cooperatively cleave HJs by a nick and counter-nick mechanism. SLX4 coordinates the recruitment on the active sites in a manner that SLX1-SLX4 introduces the first nick, producing an HJ-intermediate that is further processed by the MUS81-EME1 endonuclease [130]. Unlike GEN1, the SLX-MUS complex cleaves HJs asymmetrically, in order to create two cuts at different positions relative to the junction. Thus, the

resulting product contains short single-stranded gaps and flaps that require further processing before ligation [126].

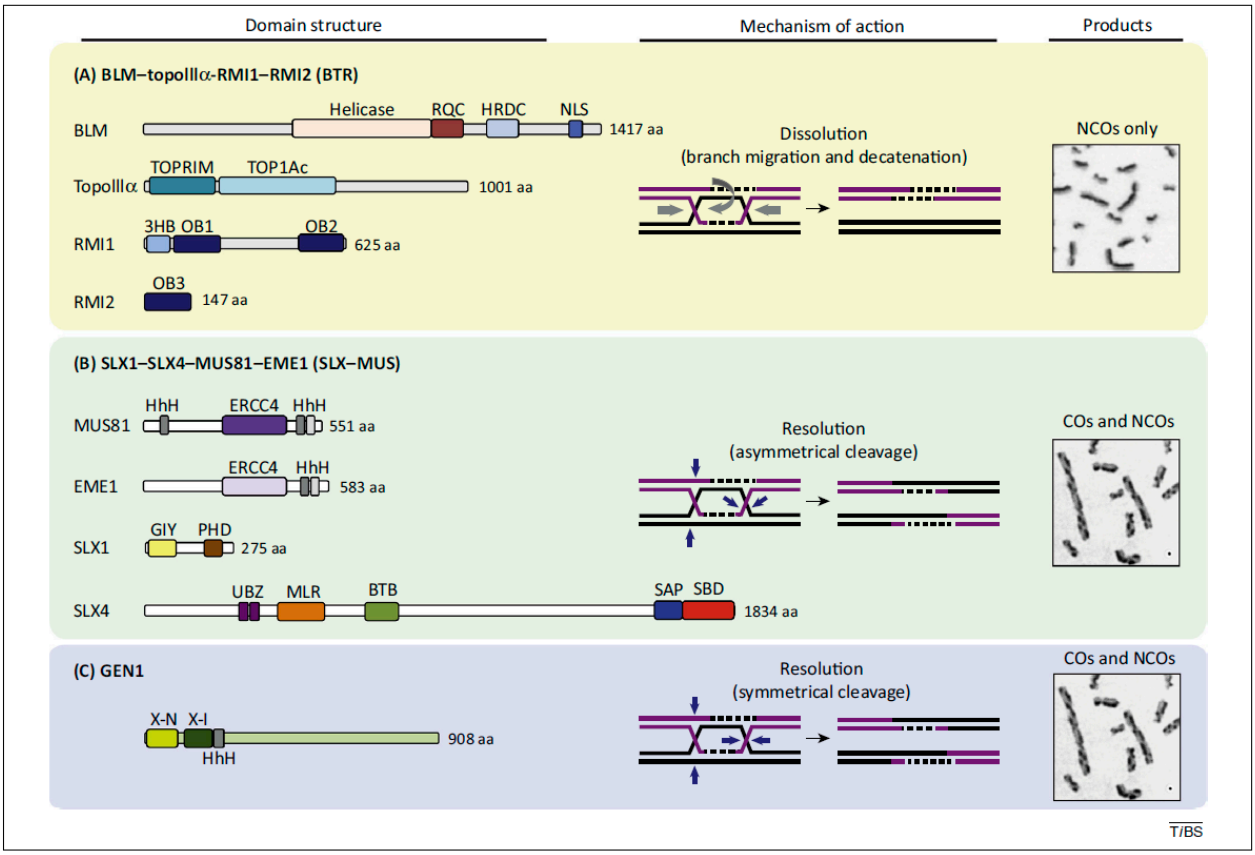

Figure 15. Illustration of the enzymes involved in HJ dissolution or resolution pathways. A) Dissolution by the BTR complex. Left: domain structures of BLM, TopoIIIα, RMI1 and RMI2. BTR-proficient cells show low level of sister chromatid exchanges (SCEs, right picture). 3HB: 3 helix bundle; HRDC: helicase and RNase D C-terminal; NLS: nuclear localization signal; OB: oligonucleotide/oligosaccharide binding. B) Resolution by SLX-MUS complex. Left: domain structures of MUS81, EME1, SLX1 and SLX4. HhH: helix-hairpin-helix; dark and light grey indicate active and inactive motifs, respectively. Resolution pathway leads to NCO and CO products, and SCEs (left picture). BTB: Bric-a-brac tramtrack broad complex; GIY: GIY-YIG nuclease domain; MLR: MUS312-MEI9 interaction-like region; SAP: SAF-A/B, Acinus, and PIAS; SBD, SLX1-binding domain; UBZ: ubiquitin-binding zinc finger. C) Resolution by GEN1 resolvase. Left) Domain structure of GEN1. X-N, X-I: xeroderma pigmentosum complementation group G N-terminal and internal nuclease domains. GEN1 generates both NCO and CO products. [126]

3.8 – Unresolved replication intermediates

Faithful DNA replication is an essential step in order to maintain genome integrity and to generate intact daughter cells. Although replication is a tightly regulated process, it can be threaten by various kinds of impediments [131]. Unresolved problems arising from the S phase can affect chromosome segregation during mitosis. Incompletely replicated loci and incompletely resolved intermediates produced in S phase processes, such as DNA repair or recombination, can pass the G2/M barrier and be directly carried into the M phase with under-replicated, or unresolved, chromosomes [132]. Replication forks can stall especially in genome regions where natural obstacles present on its way [133]. Natural impediments, such as unusual secondary structures, transcription machinery and late replicated genome regions, generate additional challenges for the cell to maintain genomic stability.

Despite the presence of checkpoint signaling that is activated following DNA replication stress, there are genomic regions that escape this surveillance. This is particular true for those regions that are late replicated, such as common fragile sites, and intrinsically difficult to replicate regions, such as centromeres and telomeres. Under-replicated and/or unresolved DNA structures that are not processed in S phase are inevitably carried over into mitosis. Although still unclear, it seems that the cell has evolved a survival mechanism that allow it to minimize the formation of aberrations and genomic instability during chromosome segregation. Defects dragged from S phase are eventually taken care in G1 phase of the next cell cycle [134].

3.8.1 – Chromosomal fragility

Replication stress can induce gaps and breaks, known as fragile sites, that are cytogenetically visible on metaphase chromosomes [135]. Fragile sites are inherited by Mendelian genetics, and they can be mapped to specific chromosome arm regions [136]. Fragile sites are classified as common (present in all individuals) and rare (present in less than 5% of the population). Fragile sites are "expressed" when they are visible on metaphase chromosomes and their frequency can be calculated. Expression of fragile sites can be induced by different classes of replication inhibitors (i.e. aphidicolin, folate, thymidylate) [133]. Occurrence of fragile sites has been linked with human diseases such as fragile X syndrome, a common heritable form of mental retardation [137].

Rare fragile sites are caused by expansions of repetitive nucleotides (di- and trinucleotide microsatellites) and AT-rich minisatellites extended at an abnormal length, that are responsible for various diseases. At least 80 common fragile sites have been described in the human genome and the most studied include 3p14.2 (FRA3B), 16q23 (FRA16D), 6q26 (FRA6E), 7q32.3 (FRA7H) and Xp22.3 (FRAXB) [133]. As already mentioned, common fragile sites are normal part of the DNA architecture and characterized by long AT-rich sequences and prone to formation of secondary structures (i.e. hairpins). Interestingly, CFSs such as FRA3B and FRA16D overlap with putative tumor-suppressor genes, FHIT and WWOX, respectively.

Numerous aberrant DNA structures have been shown to be present within CFSs, including stalled replication forks, persistent R-loops and unresolved replication intermediates. Recently, different labs revealed that CFS expression involves an active mechanism rather than mechanical chromosome breakage following chromatin condensation in mitosis [138, 139]. In these publications, it has been shown that structure-specific endonucleases, MUS81-EME1 and ERCC1, cleave

unresolved replication intermediates at CFSs coming from S phase in early mitosis (Figure 16). Absence of MUS81 or ERCC1 significantly increased frequency of anaphase bridges, micronuclei formation and eventually caused 53BP1 nuclear body accumulation in G1 of the next cell cycle.

Taken together, these findings suggest that CFSs can represent a physiological signal for replication termination, thus regulating the S-M phase transition. In turn, CFS expression is a required step to promote a correct chromosome segregation and it explains the activation of specialized enzyme complexes for this processes at the onset of mitosis.

3.8.2 – Centromeres

Fragile sites are not the only genome hot spots where the replication machinery fails to complete DNA synthesis due to formation of particular DNA structures. Centromeres hold sister chromatids together and allow correct alignment on mitotic spindles [140]. Centromeric heterochromatin consists of repetitive elements, such as α-satellite DNA, and recombinatorial events can produce looped structures in these regions [141]. These structures can generate replication problems and in yeast, centromeres are sites where the replication fork pauses [142], and they are hot spots for chromosome breakage and rearrangements in mammals [143].

Among the unprocessed DNA structures that can persist at centromeres, the double-stranded DNA catenanes are the most common. Catenanes are fully replicated and intertwined molecules generated as a consequence of the topological stress during DNA replication, and they must be resolved before chromosome segregation in anaphase [144]. Since DNA topoisomerase IIα (TOPOIIα) performs decatenation activity in humans [145], it can disentangle intertwined duplex DNA molecules. It has been proposed that TOPOIIα decatenation activity is restrained

from resolving catenanes on centromeres because cohesion proteins shield those region, and only at the metaphase-anaphase transition (when cohesins are cleaved) can resolve these structures [146].

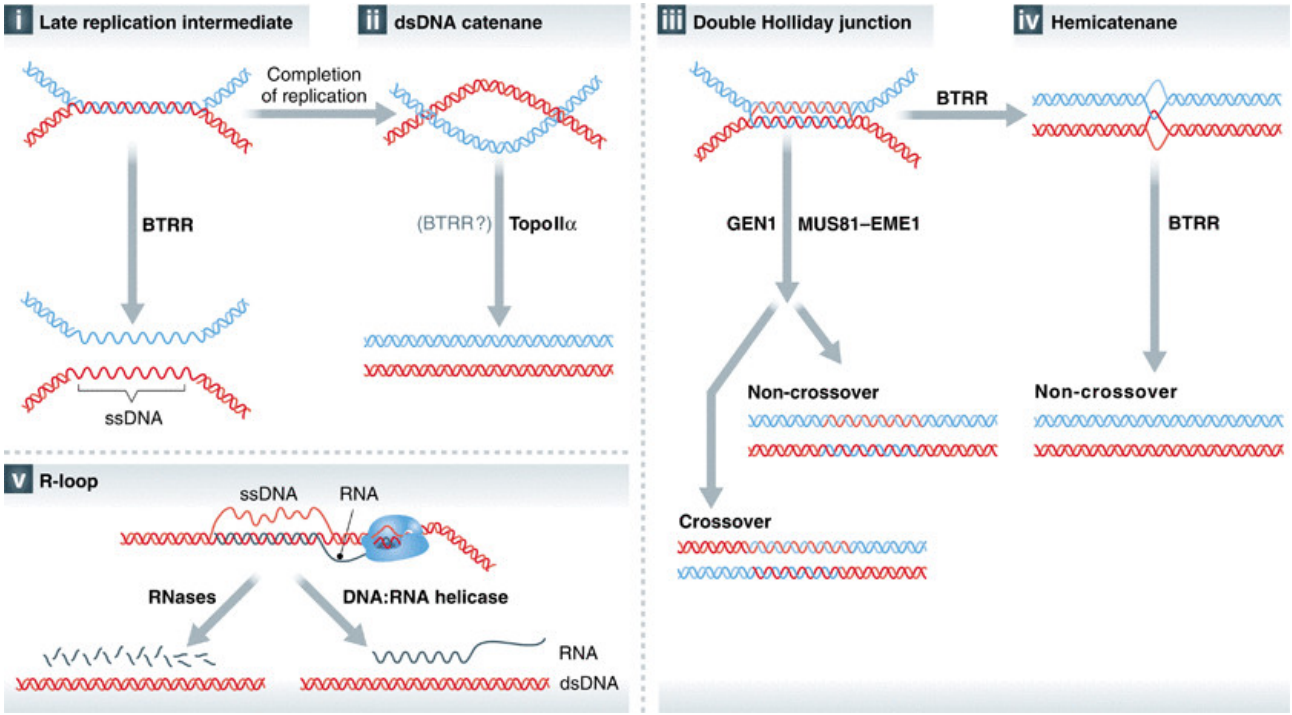

Figure 16. Schematic of S phase structures persisting in mitosis. i) Late replication intermediates that escape MUS81-EME1-mediated cleavage are processed by the BTRR complex. The result of the dissolution can generate ssDNA stretches that enter the mitotic phase. ii) dsDNA catenanes are resolved by the TOPOIIα enzyme that decatenates the entanglement, forming two fully replicated double-stranded duplexes. iii and iv) MUS81-EME1-mediated resolution pathway is covered in the chapter 3.5. v) RNA-DNA hybrids (R-loops) are formed during the transcription process. Helicases can unwind R-loops and the RNA transcript is released and dissociated, followed by DNA complementary strand reannealing. [132]

3.8.3 – Telomeres

Telomere regions are another category of hot spots where replication forks frequently stall due to the presence of telomere-binding proteins and G-quadruplex secondary structures forming in the G-rich telomeric strand [147]. Telomeres are specialized structures, consisting of tandem repeats of TTAGGG nucleotides. They cap the chromosome ends, and prevent chromosome end-to-end fusions and limit the erosion caused by the end-replication problem of DNA replication [148, 149]. The frequent replication fork stalling at telomeres can lead to fork regression, cleavage and collapse, and these regions are sensitive to replication stress, as much as fragile sites are [150]. Moreover, like common fragile sites, telomeres can behave as sensors for genomic stress, since they can trigger the senescence pathway once they reach a critical short length. Replication stress can induce an abnormal DNA damage at telomeres that leads to telomere dysfunction-induced senescence that is independent from the telomere length [151].

4. Aim of the study

Chromosome segregation during mitosis is essential for correct distribution of the genetic material to daughter cells. Common fragile sites (CFSs) are evolutionary conserved loci that are replicated during late S-phase and, recurrently, give rise to gaps or breaks on metaphase chromosome spreads upon partial inhibition of DNA synthesis, a phenomenon termed expression of CFSs. MUS81-EME1 endonuclease has been shown to have an active role in CFS expression, promoting a correct sister chromatid disjunction in anaphase. Previous studies in Janscak's and Krejci's laboratories have shown that MUS81 forms a stable complex with RECQ5 DNA helicase and that RECQ5 stimulates cleavage of forked DNA structures by MUS81-EME1 *in vitro*. The aim of this study was to explore the role for RECQ5 in MUS81-mediated processing of late replication intermediates at CFSs during early mitosis. By chromatin immunoprecipitation, we tested whether RECQ5 associates with CFSs in response to replication stress. By cytogenetic analysis, we tested the effect of RECQ5 depletion on CFS expression and the frequency of mitotic phenotypes that arise due to chromosome segregation defects (e.g. anaphase bridges, micronuclei). We also explored the possibility that RECQ5 disrupts RAD51 filaments formed on stalled replication forks at CFSs, and hence facilitates MUS81-EME1-mediated cleavage of these structures in mitosis. Finally, we have explored the functional significance of mitosis-specific phosphorylation of RECQ5 at Ser727, which was discovered in Janscak's laboratory.

5. Results

5.1 – Discovery of physical and functional interactions between MUS81-EME1 endonuclease and RECQ5 DNA helicase

By coimmunoprecipitation, a former PhD student in our laboratory, Daniela Hühn [152], discovered that MUS81 exist in a complex with RECQ5 in human osteosarcoma U2OS cells (Figure 17). Work conducted by Zdenka Hasanova in the laboratory of Prof. Lumir Krejci have revealed that RECQ5 binds to the MUS81-EME1 complex *in vitro*. Specifically, using GST pull-down assay, Zdenka Hasanova found that RECQ5 formed a tight complex with GST-MUS81-EME1 *in vitro* [153]. Moreover, she observed a strong interaction between RECQ5 and GST-MUS81 alone, suggesting that on the MUS81-EME1 heterodimer, RECQ5 binds to the MUS81 subunit [153].

Next, Zdenka Hasanova investigated whether RECQ5 affects the nuclease activity of MUS81-EME1 *in vitro.* MUS81-EME1 was shown to cleave a variety of substrates with a preference towards 3'-flaps, replication forks and nicked Holliday Junctions [154]. Z. Hasanova demonstrated that RECQ5 stimulated cleavage of these DNA substrates by MUS81-EME1 irrespective of the presence of ATP [153].

These data suggest that RECQ5 might promote cleavage of stalled replication forks by MUS81-EME1.

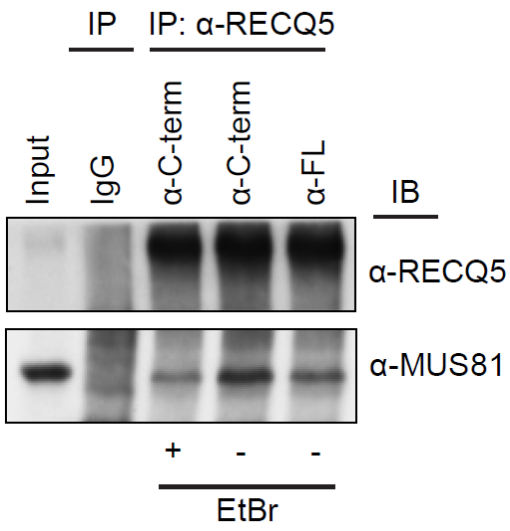

Figure 17. **Physical interaction between MUS81 and RECQ5.** Immunoprecipitation (IP) of RECQ5 from a total extract of U2OS cells was performed using rabbit polyclonal antibodies against a C-terminal (C-term) region of RECQ5 (411-991) or the full length (FL) RECQ5. IgG isolated from a preimmune serum was used in control. Immunoprecipitates were analyzed by immunoblotting (IB) using indicated antibodies. Where indicated, extracts were supplemented with ethidium bromide (EtBr) to disrupt DNA-protein interactions.

5.2 – RECQ5 is actively involved in expression of common fragile sites

MUS81-EME1 promotes CFS expression by cleaving replication intermediates at these loci in early mitosis, facilitating correct chromosome segregation. As we found that MUS81-EME1 interacts physically and functionally with RECQ5, we thought to test whether RECQ5 is required for expression of CFSs. CFS expression is assessed by quantification of chromatid breaks/gaps on metaphase chromosome spreads. Depletion of MUS81 from cells was shown to inhibit chromatid break formation induced by mild replication stress generated by exposure of cells to low doses of aphidicolin [138]. It has been estimated that aphidicolin promotes expression of 84 out of 89 common fragile sites [155]. We performed metaphase chromosome spread analysis of U2OS cells depleted of RECQ5, MUS81 or both. We found that RECQ5 depletion suppressed aphidicolin-induced chromatid breakage to the same

extent as MUS81 depletion. Simultaneous down-regulation of RECQ5 and MUS81 did not further decrease the frequency of CFS breakage, suggesting that the two proteins work in the same pathway (Figure 18).

The finding that RECQ5 is involved in CFS expression prompted us to examine whether it physically interacts with CFS regions. Chromatin immunoprecipitation (ChIP) is a powerful technique to study chromatin-protein interactions, even if the protein of interest is not directly bound to the DNA. Formaldehyde cross-linked chromatin fractions from U2OS cells treated or not with 0.2 µM aphidicolin were sonicated and immunoprecipitated with antibodies against RECQ5 or MUS81. The immunoprecipitates were subjected to quantitative real-time PCR (qPCR) analysis using primers specific to three different CFSs, namely FRA3B, FRA16D and FRA7H. Primers for GAPDH locus were used as control. We found that both RECQ5 and MUS81 were significantly enriched at all three CFSs as compared to GAPDH locus. Moreover, replication stress considerably enhanced the binding of RECQ5 and MUS81 to CFS loci, but not to the GAPDH locus (Figure 19).

To test whether MUS81 and RECQ5 associate with CFS chromatin in mitosis, we treated U2OS cells with a selective CDK1 inhibitor, RO-3306. CDK1/cyclin B complex regulates the G2/M transition, therefore, RO-3306 is commonly used to synchronize proliferating cells in late G2 phase [156]. After exposure of cells to RO-3306 in the absence (DMSO) or the presence of aphidicolin, we performed ChIP assay using antibodies against RECQ5 and MUS81. We again analyzed the immunoprecipitated material by qPCR for the presence of CFS regions (FRA3B, FRA16D and FRA7H). The results showed that if entry into mitosis was inhibited, MUS81 and RECQ5 were no longer recruited to CFSs. (Figure 19). We conclude that both MUS81 and RECQ5 start to associate with CFSs at an early step of mitosis.

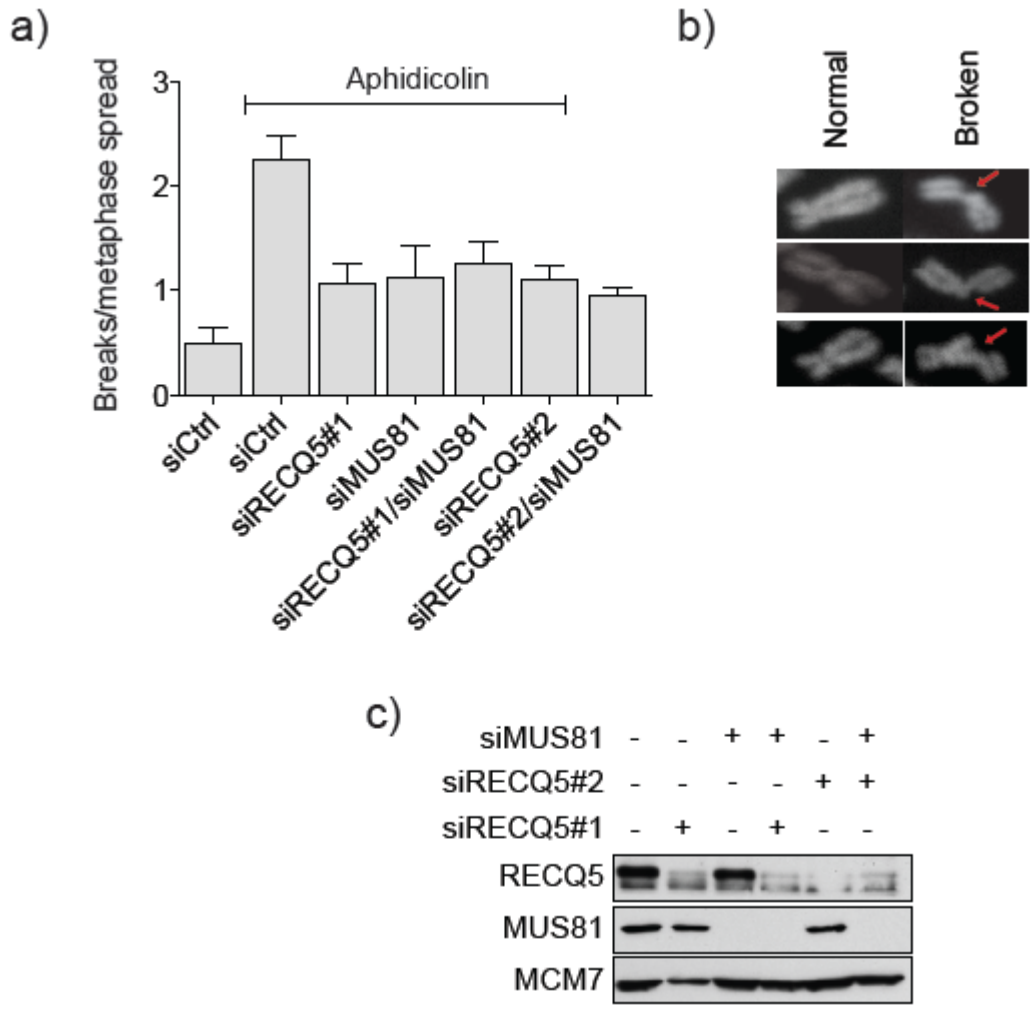

Figure 18. **RECQ5 promotes expression of common fragile sites. a)** U2OS cells were depleted of RECQ5 and/or MUS81 and then treated with 0.2 μM aphidicolin for 24 h. Nocodazole was added at a concentration of 200 ng/mL for the last 5 h in order to enrich mitotic population. Mitotic cells were harvested and swollen in hypotonic solution before methanol-acetic acid fixation. Metaphase cells were spread and visible chromatid breaks were counted. Two different siRNAs for RECQ5 depletion were used. At least 100 spreads were analyzed in three independent experiments. Error bars show S.D. **b)** Representative image of intact and broken chromatids. **c)** Western-blot analysis showing the efficiency of RECQ5 and MUS81 depletion.

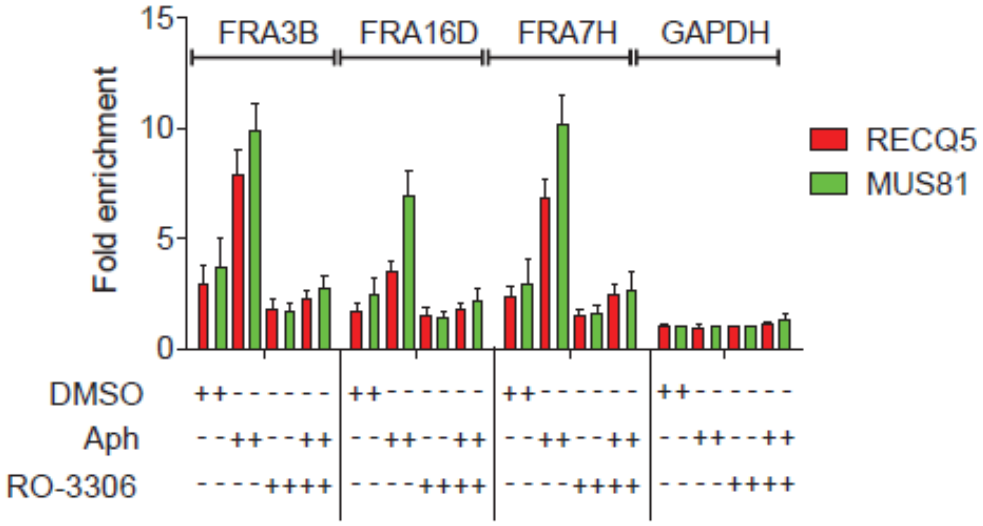

Figure 19. **RECQ5 and MUS81 bind to CFSs upon entry into mitosis.** Chromatin immunoprecipitation (ChIP) of RECQ5 or MUS81 was performed after treatment of cells with 0.2 µM aphidicolin or DMSO (control) for 24h. Were indicated, 9 µM RO-3306 was added together with aphidicolin/DMSO. Immuno-precipitated DNA was analyzed by qPCR, using primer pairs for three different CFSs (FRA3B, FRA16D, FRA7H) and GAPDH as control. Data are the mean of three independent experiments. Error bars show S.D.

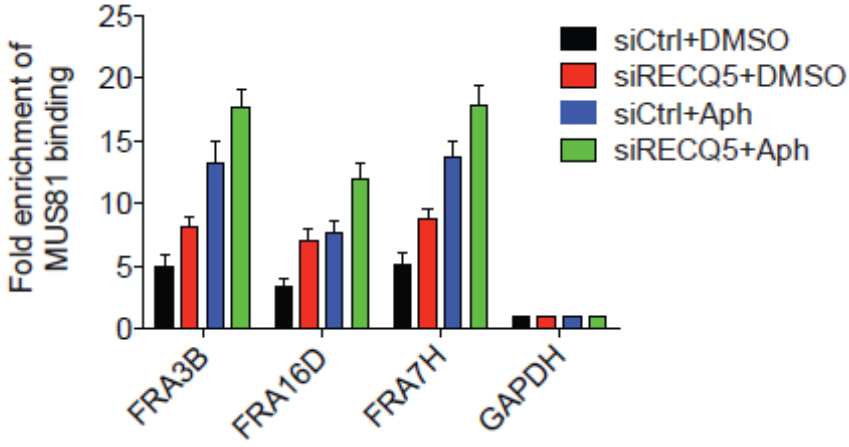

Figure 20. **Effect of RECQ5 depletion on MUS81 binding to CFSs.** Cross-linked chromatin of mock- or RECQ5-depleted U2OS cells treated or not (DMSO) with 0.2 µM aphidicolin for 24 h was subjected to immunoprecipitation with MUS81 antibody followed by qPCR analysis. FRA3B, FRA16D and FRA7H loci were used as representative regions for CFSs and GAPDH as a negative control. Data are the mean of three independent experiments. Error bars show S.D.

MUS81-EME1 was proposed to actively cleave fork-like structures persisting at CFSs during early mitosis [138]. Therefore, we reasoned that the binding of MUS81 and RECQ5 on CFSs revealed by ChIP (Figure 20) occurred at the G2/M transition or in prophase/pro-metaphase. Indeed, by immunofluorescence, it has been shown that MUS81 accumulates on CFSs (marked by FANCD2 foci) at the onset of mitosis until metaphase [138].

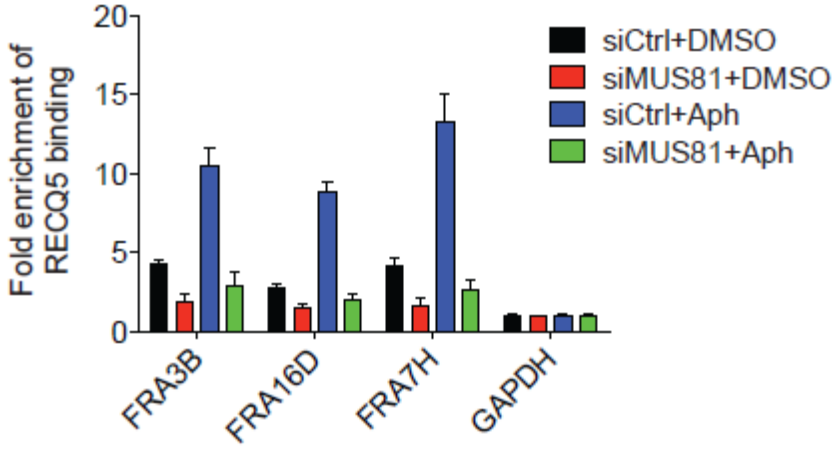

Figure 21. **MUS81 is required for RECQ5 recruitment on CFSs.** RECQ5 ChIP in MUS81-depleted U2OS cells in presence or absence of replication stress. Fold enrichment of RECQ5 binding on CFSs (FRA3B, FRA16D and FRA7H) and one control gene (GAPDH) was calculated by qPCR. Data represent the mean of 3 independent experiments. Error bars show S.D.

We next analyzed association of RECQ5 with CFSs in cells depleted of MUS81. Interestingly, we found that MUS81 depletion abrogated binding of RECQ5 to all three CFSs tested both in the absence and the presence of aphidicolin, suggesting that MUS81 might mediate RECQ5 recruitment to CFSs (Figure 21). On the contrary, depletion of RECQ5 caused a small enrichment of MUS81 on CFSs. This might reflect the defect in CFS breakage observed in RECQ5-deficient cells and implies that RECQ5 is not involved in MUS81 recruitment to CFSs.

Together, these data suggests that RECQ5 is actively involved in cleavage of CFSs by MUS81-EME1 in early mitosis.

5.3 – RECQ5 promotes correct chromosome segregation during anaphase

We further investigated whether RECQ5 acts in concert with MUS81 to promote correct sister chromatid disjunction by resolving replication intermediates persisting on CFSs. Unresolved replication intermediates that persist through mitosis are converted into DNA lesions and, in the next G1 phase of the cell cycle, daughter cells show accumulation of 53BP1 nuclear bodies that are thought to shield DNA lesions until repair mechanisms are available again in G1/S [134]. Depletion of MUS81 was shown to increase the frequency of 53BP1 nuclear bodies in G1 cells [138]. We therefore depleted RECQ5 or MUS81 (as positive control) from U2OS cells and analyzed 53BP1 nuclear body frequency in G1 cells by immunofluorescence. To distinguish G1 cells, we used a cyclin A antibody to stain replicating cells and counted the number of 53BP1 nuclear bodies in cyclinA-negative cells. Notably, RECQ5 depletion caused 53BP1 nuclear body accumulation in G1 cells (> 3 nuclear bodies of 53BP1), and double-depletion of RECQ5 and MUS81 brought about the same frequency of cyclinA-negative cells with 53BP1 nuclear bodies as single depletions (Figure 22).

Next, we wanted to determine whether depletion of RECQ5 caused accumulation of 53BP1 nuclear bodies at CFSs. To this end, we performed ChIP assay for 53BP1 using cells depleted of RECQ5, MUS81 or both. Cells were exposed to low doses of aphidicolin for 16 h or left untreated. As expected, aphidicolin induced 53BP1 accumulation on CFSs and not on the GAPDH gene. Depletion of RECQ5 or MUS81 caused enrichment of 53BP1 at CFSs both in non-treated and aphidicolin-treated cells.

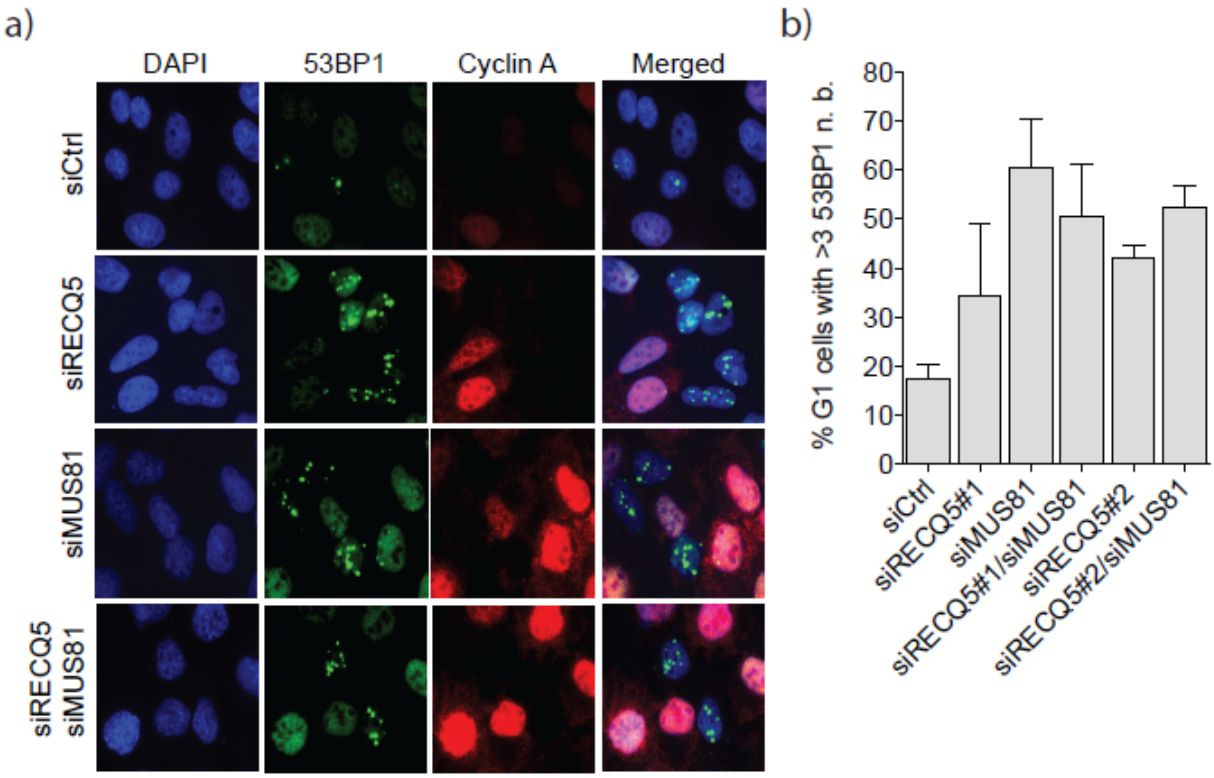

Figure 22. **Depletion of RECQ5 leads to accumulation of 53BP1 nuclear bodies in G1 cells. a)** Representative images of 53BP1 nuclear bodies in cyclinA-negative cells depleted for indicated proteins. Green staining is for 53BP1, red for cyclinA and blue DAPI. **b)** Quantification of the frequency of cyclinA-negative cells that have more than three nuclear bodies (n.b.). Two different siRNAs for RECQ5 depletion were used. The data represent the mean of 4 independent experiments. Error bars show S.D. At least 600 cyclin A-negative cells were scored for each condition.

Importantly, simultaneous knockdown of RECQ5 and MUS81 has no additive effect in comparison with knockdown of either protein, suggesting that RECQ5 and MUS81 act in the same pathway to promote chromosome segregation (Figure 23).

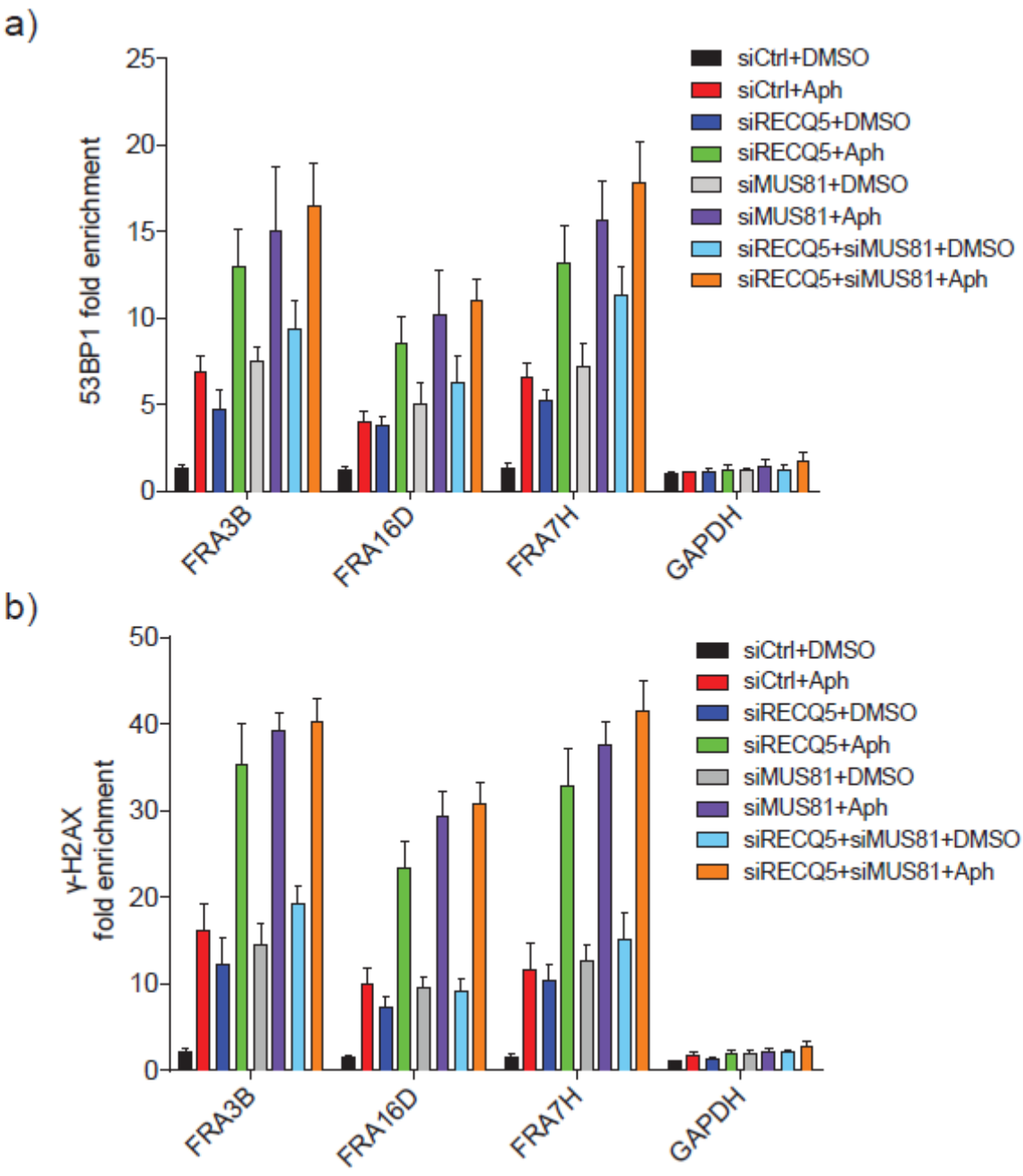

Figure 23. **RECQ5 depletion promotes 53BP1 and γ-H2AX accumulation on CFSs.** Mock-, RECQ5-, MUS81- and RECQ5/MUS81-depleted U2OS cells were grown with or without (DMSO) 0.2 μM aphidicolin for 24 h. Cross-linked chromatin of these cells was subjected to ChIP assay using 53BP1 (**a**) or γ-H2AX (**b**) antibodies. Immuno-precipitated DNA was analyzed by qPCR, using primer pairs for three different CFSs (FRA3B, FRA16D, FRA7H) and GAPDH as control . Data represent the mean of three independent experiments. Error bars show S.D.

In addition to 53BP1, we looked at another DNA damage marker, the phosphorylation of the histone variant H2A.X at Ser139 (γ-H2AX), which is also

known to be a marker for the presence of replication stress. By ChIP assay, we analyzed the levels of γ-H2AX on CFSs following the same conditions as those used in 53BP1 ChIP experiments. We observed that depletion of RECQ5 or MUS81 increased γ-H2AX levels at CFSs in both non-treated and aphidicolin-treated cells, and the combination of RECQ5 or MUS81 depletions did not have additive effect in comparison with depletion of either protein (Figure 23).

Unresolved replication intermediates generate well-characterized mitotic phenotypes that can be observed by standard immunofluorescence techniques. First, bulky DNA bridges can form during anaphase as a result of aberrant chromosome morphology or defects in the mitotic machinery [132]. Bulky anaphase bridges can be visualized by staining with DNA-intercalating dyes such as DAPI. MUS81 depletion increases bulky anaphase bridges as result of failure in resolution of replication intermediates [138]. Therefore, we asked whether RECQ5 depletion led to the same phenotype. We depleted RECQ5 in U2OS cells and scored the frequency of anaphase cells that showed one or more DAPI-positive bridges. We found that RECQ5 depletion increased anaphase bridge frequency to nearly 30% of the anaphase cells analyzed, whereas mock-depleted cells showed an anaphase bridge frequency of about 10%. MUS81 depletion increased anaphase bridge frequency to a level comparable with RECQ5 depletion. Importantly, simultaneous depletion of RECQ5 and MUS81 led to the same frequency of anaphase bridge formation as MUS81 or RECQ5 depletions, again confirming that the two proteins act in the same pathway for promotion of sister chromatid segregation (Figure 24).

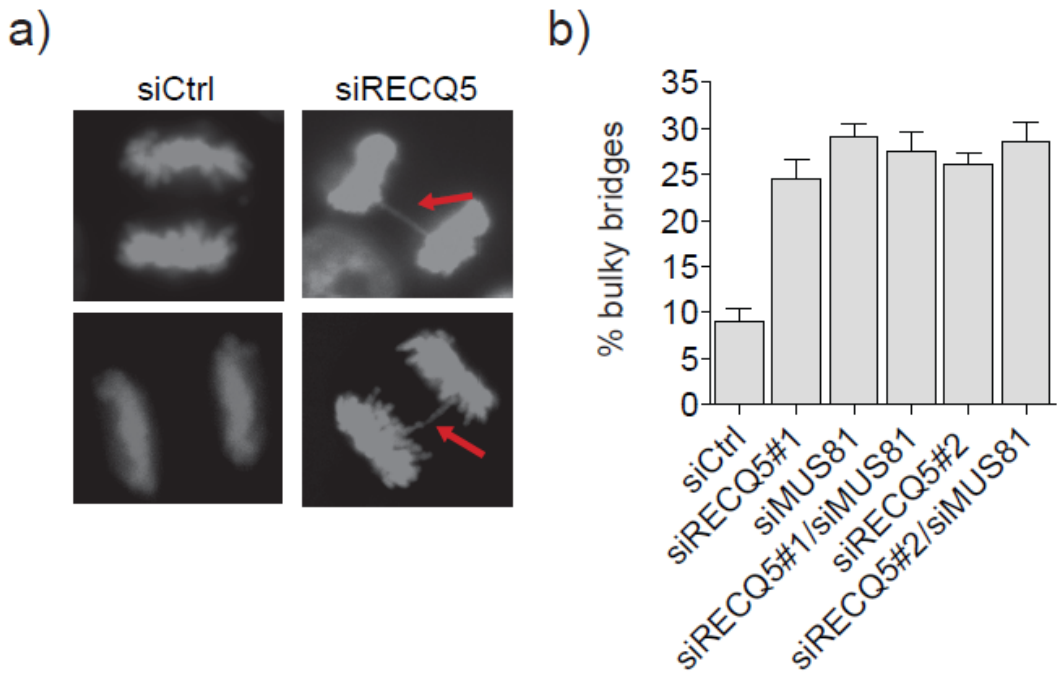

Figure 24. **RECQ5 depletion causes the formation of bulky anaphase DNA bridges. a)** Representative image of control anaphase cells and DAPI-positive DNA bridges in RECQ5-depleted cells. **b)** Quantitative analysis of the frequency of bulky anaphase bridges. RECQ5 or MUS81 were depleted of U2OS cells as indicated. After formaldehyde fixation, cells were stained with DAPI. Percentage of anaphase cells with DAPI-positive bridges was calculated for each condition. The data represent the mean of two independent experiments. Error bars show S.D. At least 150 anaphase cells were analyzed.

An additional, well characterized, category of anaphase bridges are the so-called ultrafine bridges (UFBs). This particular class of mitotic structures cannot be stained with classical DAPI dyes. Instead, UFBs could be visualized by immunofluorescence staining using BLM or PICH (Polo-like kinase 1 interacting checkpoint helicase) antibodies [157]. It has been shown that UFBs are formed naturally and are resolved by the BLM pathway [158]. The frequency of UFBs is dramatically increased upon treatment of cells with low doses of aphidicolin, and MUS81 depletion increases UFB formation at CFSs in aphidicolin-treated cells [138]. Therefore, we wanted to check whether down-regulation of RECQ5 had an effect on the frequency of UFB appearance. To this end, we depleted U2OS cells of RECQ5 or

MUS81, and determined the percentage of anaphase cells showing one or more PICH-positive bridges. Interestingly, we observed that the frequency of UFB bridges increased by about 2-fold if cells were depleted of RECQ5 or MUS81 (siCtrl: 8.4%, siRECQ5#1: 15.5%, siMUS81: 13.6%; Figure 25). Simultaneous depletion of RECQ5 and MUS81 did not lead to a further increase in UFB frequency as compared to depletion of either protein, indicating that RECQ5 and MUS81 act in the same pathway to suppress the formation of UFB bridges.

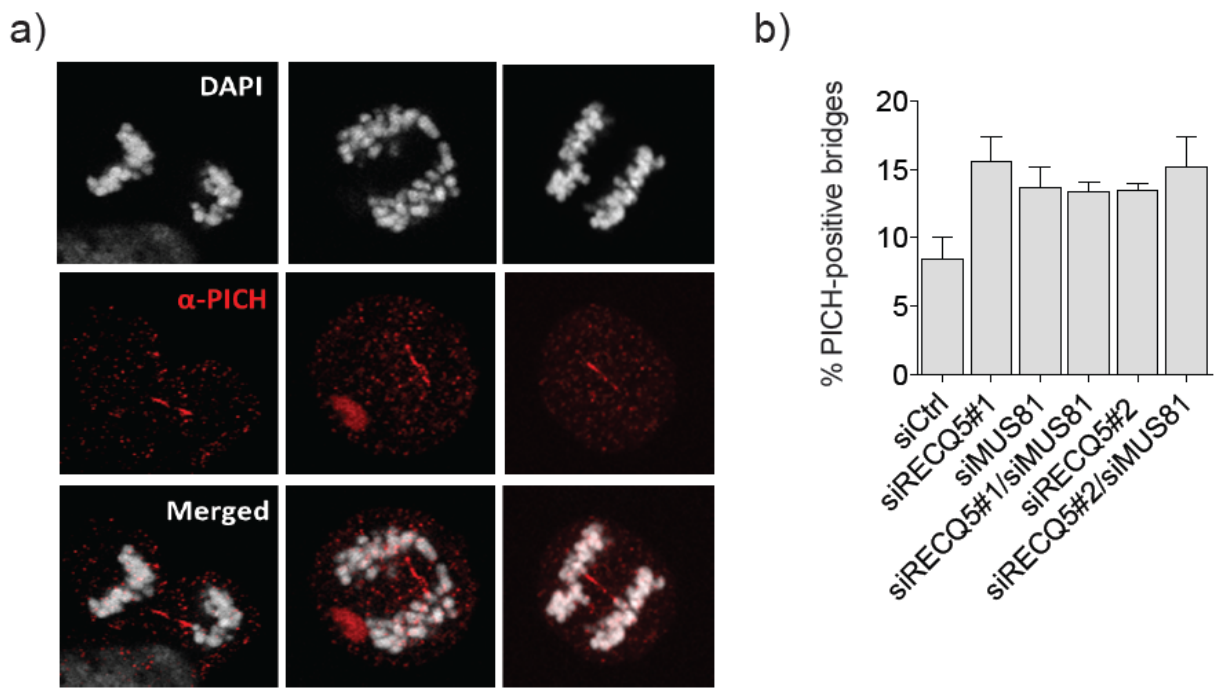

Figure 25. **Depletions of RECQ5 or MUS81 increase the frequency of PICH-positive UFBs.** U2OS cells were depleted of RECQ5 or MUS81 for 72 h, and RO-3306 was added for the last 16 h to block the cells at G2/M. Cells were then released from RO-3306 for 1.5 h and fixed/permeabilized in PTEM buffer for 15 min. **a)** Representative images of PICH-positive UFBs. An antibody against PICH was used in order to detect UFBs (red), and DAPI stained DNA (light grey). **b)** Quantitative analysis of UFB frequency in U2OS cells transfected with indicated siRNA. Data represent the mean of three independent experiments. Error bars show S.D. At least 120 anaphase cells were analyzed for each condition.

A third phenotype associated with incorrect chromosome disjunction is the formation of micronuclei. Micronuclei are small extranuclear bodies consisting of pieces of chromosomes/chromatids, and are considered as a symptom of genome

instability. They are formed upon treatment of cells with DNA-damaging chemicals or radiation, and are also observed in cancer cells [159, 160]. We determined the frequency of micronuclei in RECQ5- and MUS81-depleted U2OS cells. To this end, cells were blocked from entering cytokinesis by the addition of cytochalasin B and the percentage of binucleated cells having micronuclei was determined for each condition. We found that MUS81 depletion increased the frequency of micronuclei formation as previously reported [138]. An increased frequency of micronuclei was also observed in RECQ5-depleted cells. Simultaneous depletion of RECQ5 and MUS81 did not further increase the frequency of micronuclei appearance as compared to depletion of either protein (Figure 26).

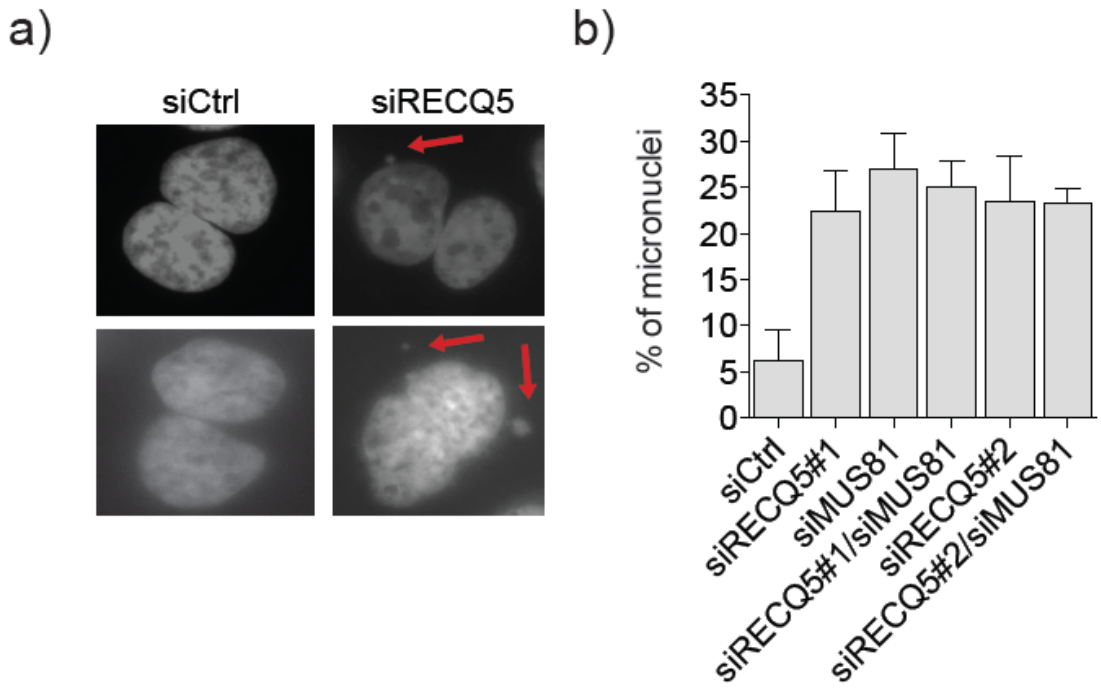

Figure 26. **Frequency of micronuclei formation increases upon RECQ5 depletion. a)** Representative image of mock- and RECQ5-depleted U2OS cells blocked in cytokinesis. RECQ5-depleted cells possess micronuclei (red arrows). **b)** Quantitative analysis of the formation of micronuclei in U2OS cells transfected with indicated siRNAs. Cells were incubated with 0.2 µM cytochalasin B for 16 h before fixation with formaldehyde and DAPI staining. Only cytokinesis-blocked cells were taken into consideration for micronuclei quantification. The data represent the mean of three independent experiments. Error bars show S.D. At least 500 binucleated cells were scored for each condition.

Taken together these data suggest a role for RECQ5 in promoting sister chromatid separation to avoid genome instability in daughter cells. Moreover, our data suggest that RECQ5 works in the same pathway as MUS81 and are consistent with our earlier findings suggesting that RECQ5 acts to promote MUS81-mediated cleavage of late replication intermediates at CFSs in early mitosis.

5.4 – Discovery of a novel RECQ5 phosphorylation site and its role in mitosis

A previous Master student in our laboratory, Jana Langhoff, observed that RECQ5 immunoprecipitated from cells synchronized in prometaphase by nocodazole treatment displayed a reduced electrophoretic mobility as compared to RECQ5 immunoprecipitated from non-synchronized cells. Treatment of immunoprecipitates with λ phosphatase abolished the RECQ5 band shift, suggesting a possible phosphorylation of RECQ5 in early mitosis. In collaboration with Stefano Ferrari lab, Jana Langhoff set up a kinase assay in which she incubated the full-length RECQ5 (1-991) or a RECQ5 truncated version spanning amino acids 1-725 with the CDK1/CycB1 complex and [γ-^{32}P]ATP. She observed that wild-type RECQ5 was extensively phosphorylated by CDK1/CycB1 under these conditions, while the truncated RECQ5 was not [161]. From the PhosphoSitePlus® (www.phosphosite.org) database, it is evident that two phosphorylation sites identified in human RECQ5 by mass spectrometry are part of the CDK consensus motif (S/T-P-X-R/K): Ser727 (SAHYGGP**s**PEKKAKS) and Thr845 (PEVQP**t**PAKDTWK, Figure 27). By site-directed mutagenesis, Jana Langhoff found that alanine substitutions at these two residues abolished RECQ5 phosphorylation by CDK1/CycB *in vitro* [161].

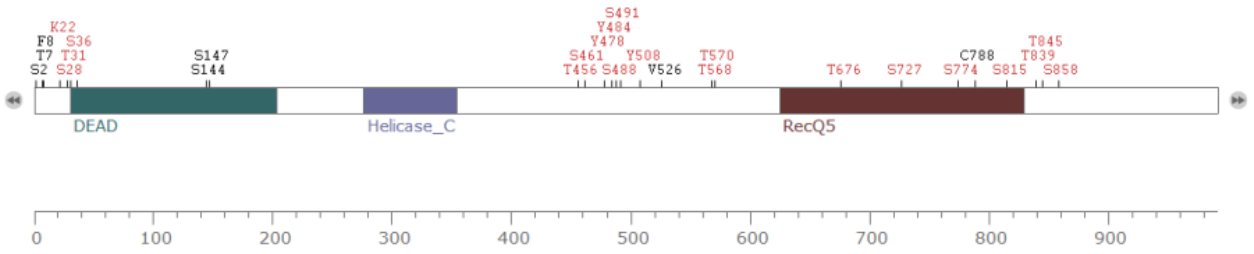

Figure 27. **Print screen from the PhosphoSitePlus database of the putative RECQ5 phosphorylation sites.** The scale bar represents the a.a. length of RECQ5.

To assess whether these residues are the targets of RECQ5 phosphorylation in mitosis, Jana Langhoff generated corresponding single and double-mutants mutants of Flag-tagged RECQ5 and tested whether these mutants, after transient expression in HeLa cells, display a shift in electrophoretic mobility if cells are subjected to nocodazole treatment. She found that RECQ5 shift was abolished by Ser727Ala mutation, suggesting that RECQ5 phosphorylation in early mitosis occurs at Ser727 [161].

These findings prompted us to investigate the biological role of RECQ5 phosphorylation at Ser727. First, we raised a rabbit polyclonal antibody against the phospho-Ser727 epitope. Using this antibody, we could confirm that RECQ5 phosphorylation at Ser727 was dramatically increased upon nocodazole treatment (Figure 27, lane 1 and 2). Moreover, we found that if cells were released from nocodazole block, the phosphorylated form of RECQ5 disappeared, suggesting that RECQ5 is dephosphorylated with the onset of anaphase (Figure 28, lane 3). From this experiment, we propose that RECQ5 phosphorylation occurs in early mitosis, between prophase and metaphase.

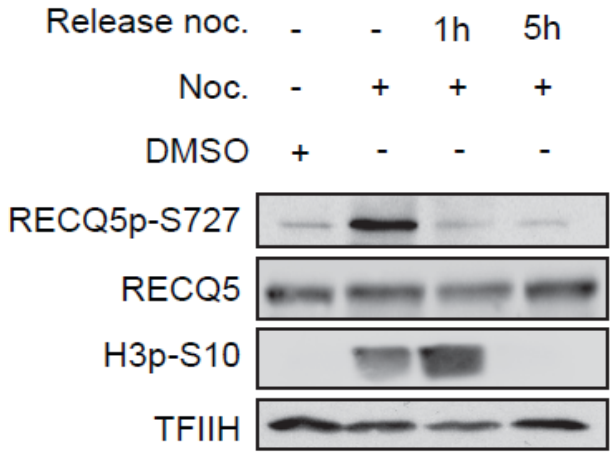

Figure 28. **RECQ5 is phosphorylated at Ser727 in early mitosis.** U2OS cells were treated with nocodazole for 16 h, and, eventually, released into fresh DMEM medium for 1 or 5 h. Total cell extracts were analyzed by western blotting. Blots were probed with antibody against the phospho-Ser727 epitope. TFIIH was used as loading control. Antibody raised against the full-length RECQ5 was used for monitoring RECQ5 protein levels. Mitosis was monitored by H3 phosphorylation at Ser10.

We prepared U2OS T-REx cell lines that express Flag-tagged versions of wild-type RECQ5 or its S727A mutant under control of a doxycyclin-regulated CMV promoter in the pAIO vector [162] (Figure 29). We took advantage of this inducible

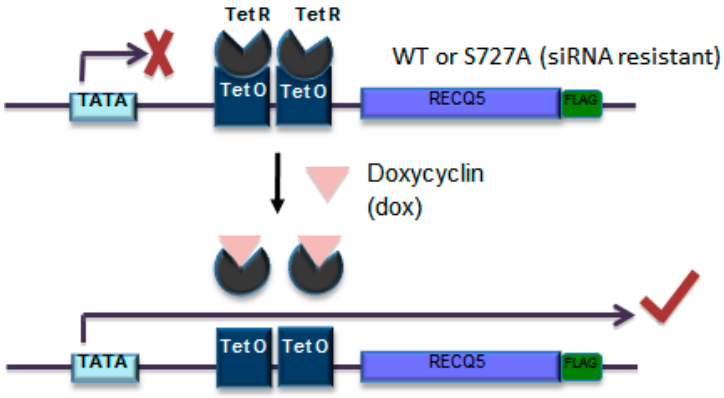

Figure 29. **Schematic of the inducible system for expression of wild-type and mutant forms of RECQ5-Flag fusion protein in U2OS-T-REx cells.** RECQ5 ORF is cloned under the control of a CMV promoter containing two copies of the tet operator (TetO2) sequence. Tet repressor, which is constitutively expressed in U2OS-T-REx cells, binds to the tet operator sequence and blocks expression of the RECQ5 transgene. Upon addition of doxycyclin, the expression of RECQ5 transgene is induced. RECQ5-Flag transcript is resistant to siRNA targeting the expression of endogenous RECQ5.

cellular system to explore the role of RECQ5 phosphorylation in the function of RECQ5 during mitosis, since we obtained evidence that RECQ5 is involved in CFS expression (see chapter 5.3). First, we wanted to test whether RECQ5 phosphorylation at Ser727 was required for the appearance of chromatid breaks/gaps on metaphase chromosomes upon replication stress. We depleted the endogenous RECQ5 with siRNA to which the ectopically expressed RECQ5 was resistant. To induce the expression of RECQ5 transgene in these cells lines, doxycyclin was added at 24 h after siRNA transfection and cells were cultures for additional 48 h. Western blot analysis of wild-type or S727A samples showed that under conditions used, endogenous RECQ5 and FLAG-tagged RECQ5 protein levels were nearly comparable (Figure 30; see RECQ5 blots, compare lanes 1 and 3).

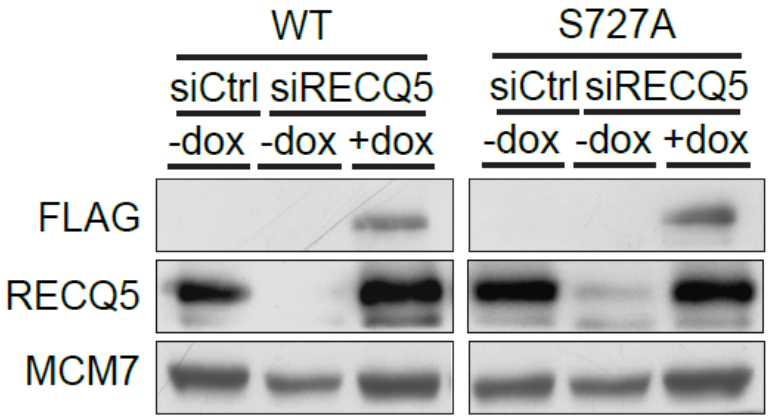

Figure 30. **Western blot analysis of expression of wild-type and S727A forms of RECQ5-Flag in** U2OS-T-REx cells. 24 h after siRNA transfection, doxycyclin (1 ng/mL or DMSO) was added with fresh medium for additional 48 h, and total cell extracts were analyzed by Western blot. Ectopic RECQ5 expression was monitored by anti-FLAG antibody. Blots were also probed with antibody raised against the full-length RECQ5. MCM7 was used as loading control.

In order to induce chromatid breakage at CFSs, cells were treated with low dose of aphidicolin for the last 24 h. As expected, aphidicolin treatment induced chromatid breakage, and RECQ5 depletion inhibited its formation in these cell lines. Ectopic expression of wild-type RECQ5 in substitution of the endogenous RECQ5, restored CFS expression. Importantly, when endogenous RECQ5 was replaced with the S727A mutant of RECQ5, chromatid breakage was impaired (Figure 31), suggesting that RECQ5 phosphorylation on S727 residue is important for CFS expression.

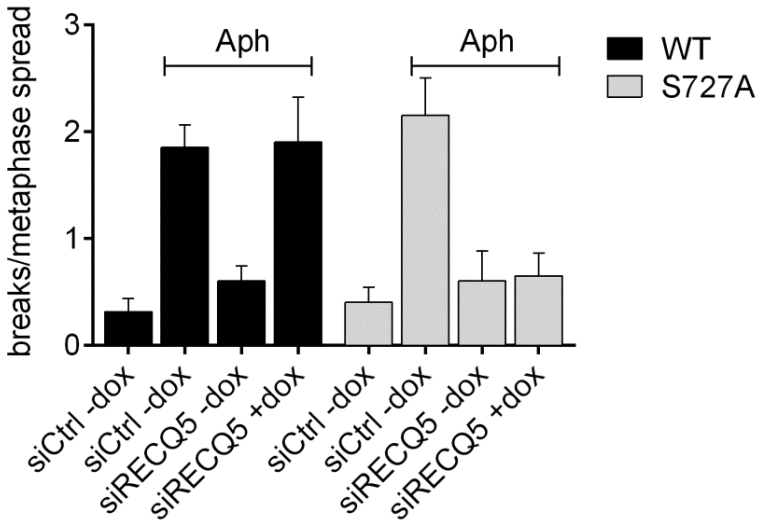

Figure 31. **RECQ5 phosphorylation on Ser727 is required for expression of CFSs.** Metaphase spread analysis of U2OS TREx cell lines expressing WT or S727A versions of RECQ5 upon doxycyclin treatment. After 24 h of siRNA transfection for down-regulation of endogenous RECQ5 depletion, doxycyclin was added to the medium for additional 48 h. 24 h before harvesting, cells were treated with 0.2 µM aphidicolin, and during the last 5 h, nocodazole was added to trap cells in metaphase. At least 100 metaphase spreads were analyzed for each condition in two independent experiments. The data represent the mean +/- S.D.

Next, we analyzed the frequencies of DAPI-positive anaphase bridges and micronuclei formation in U2OS T-REx cell lines expressing wild-type or S727A versions of RECQ5. Ectopic expression of wild-type RECQ5 on place of the endogenous RECQ5 appeared to rescue the phenotypes observed in RECQ5-

depleted cells. On the contrary, when S727A RECQ5 was expressed in absence of endogenous RECQ5, DAPI-positive anaphase bridges and micronuclei were elevated to levels observed in RECQ5-depleted cells (Figure 32, 33), suggesting that RECQ5 phosphorylation at Ser727 is necessary for proper sister chromatid separation.

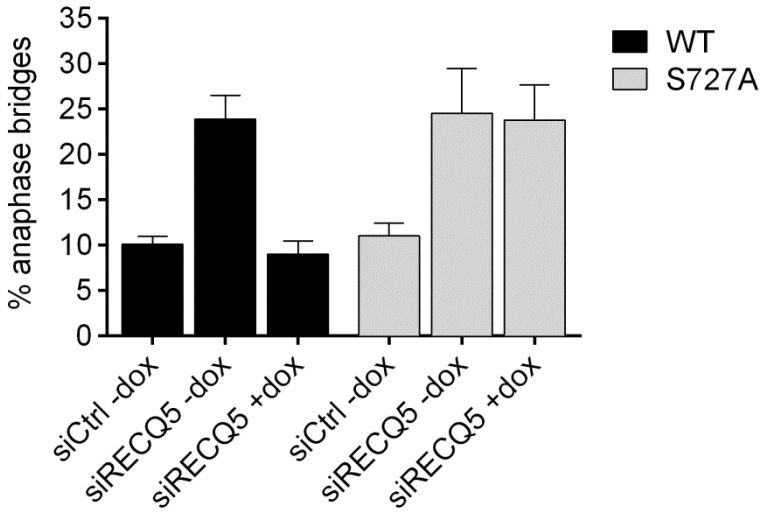

Figure 32. **Suppression of bulky anaphase bridge formation depends on RECQ5 phosphorylation at Ser727.** The frequency of bulky anaphase bridges in U2OS TREx cell lines expressing WT or S727A versions of RECQ5 was measured. After 24 h of siRECQ5 transfection, doxycylin (or DMSO) was added to the medium for additional 48 h, before cell fixation with formaldehyde and DAPI staining. At least 100 anaphase cells were scored in two independent experiments. The data represent the mean +/- S.D.

We conclude that RECQ5 phosphorylation at Ser727 is fundamental for maintenance of genomic stability during chromosome segregation.

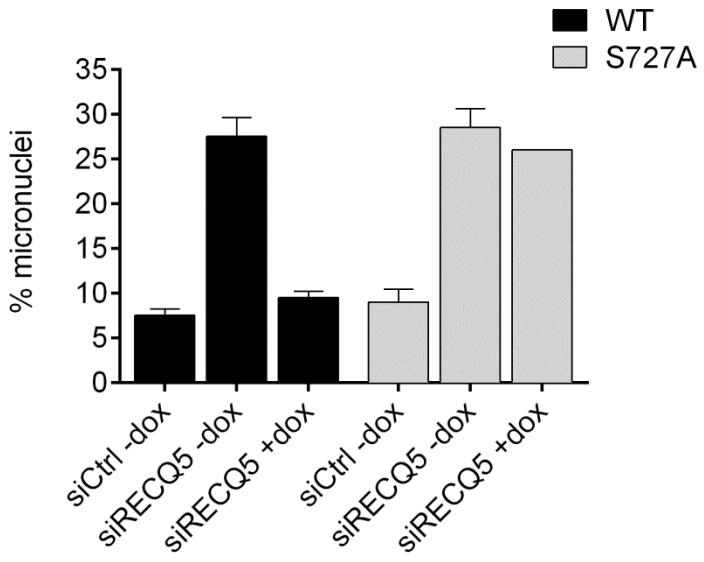

Figure 33. **Phosphorylation of RECQ5 at Ser727 is required to suppress formation of micronuclei.** The formation of micronuclei in U2OS TREx cell lines expressing WT or S727A versions of RECQ5 was analyzed. The condition used were the same as in Figure 32, except that cyctochalasin B was added to the cell culture for the last 16 h to block cytokinesis. At least 300 binucleated cells were analyzed in two independent experiments. The data represent the mean +/- S.D.

5.5 – Molecular mechanism underlying the action of RECQ5 on CFSs during early mitosis

One of the characteristic features of RECQ5 helicase is its ability to disrupt RAD51-ssDNA filaments. Stalled forks and, in general, replication intermediates contain stretches of ssDNA that, theoretically, can be a suitable substrate for RAD51 filament formation. Interestingly, recent studies have revealed that RAD51 filaments assemble on stalled replication forks to protect nascent DNA strands from MRE11-dependent degradation [163]. This could also be the case for CFSs, where stalled replication forks tend to accumulate, especially in the presence of replication stress. We therefore reasoned that RECQ5 could disrupt RAD51 filaments on persistent replication intermediates at CFSs, allowing MUS81-EME1 cleavage. To address this hypothesis, we sought to evaluate the effect of RECQ5 depletion on RAD51

occupancy on CFSs in the absence and the presence of replication stress generated by 0.2 µM aphidicolin. By ChIP assay, we found that aphidicolin treatment caused increased binding of RAD51 to CFSs, but not to the GAPDH gene. Importantly, depletion of RECQ5 caused a significant enrichment of RAD51 at CFSs both in non-treated and aphidicolin-treated cells as compared to mock-depleted cells (Figure 34).

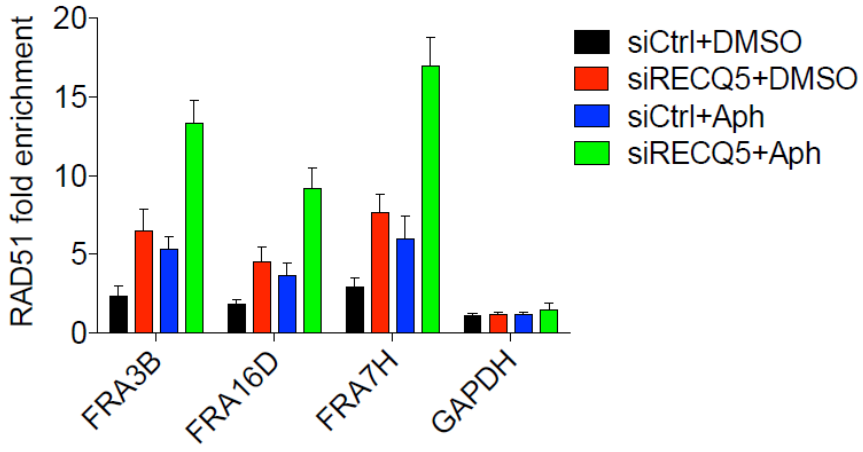

Figure 34. **RECQ5 depletion promotes RAD51 accumulation on CFSs.** Cross-linked chromatin of mock- or RECQ5 depleted cells treated cultured in the presence of 0.2 µM aphidicolin (or DMSO) for 24 h was immunoprecipitated with anti-RAD51 antibody. Immunoprecipitated DNA samples were analyzed by qPCR using primer pairs for three different CFSs (FRA3B, FRA16D, FRA7H) and GAPDH as control. Data represent the mean of three independent experiments. Error bars show S.D.

RECQ5 disrupts RAD51 filaments in a reaction dependent on its helicase activity and binding to RAD51 [90]. We therefore investigated the role of these activities of RECQ5 in its regulatory effect on RAD51 binding to CFSs. For this, we had already available U2OS T-REx cell lines inducibly expressing RECQ5 mutants defective in helicase activity (K58R substitution in Walker A motif) and interaction with RAD51 (F666A substitution in RAD51-binding domain), respectively [152]. We found that replacement of endogenous RECQ5 with either of these mutants, but not with wild-type RECQ5, significantly increased RAD51 occupancy at CFSs, providing strong support for our hypothesis that RECQ5 eliminates RAD51 filaments formed

on late replication intermediates at CFSs (Figure 35 and Figure 36a). Increased RAD51 binding to CFSs was also observed in cells expressing RECQ5 S727A mutant, suggesting that RECQ5 processes these RAD51 filaments during early mitosis in a manner dependent on its phosphorylation by CDK1 (Figure 36b).

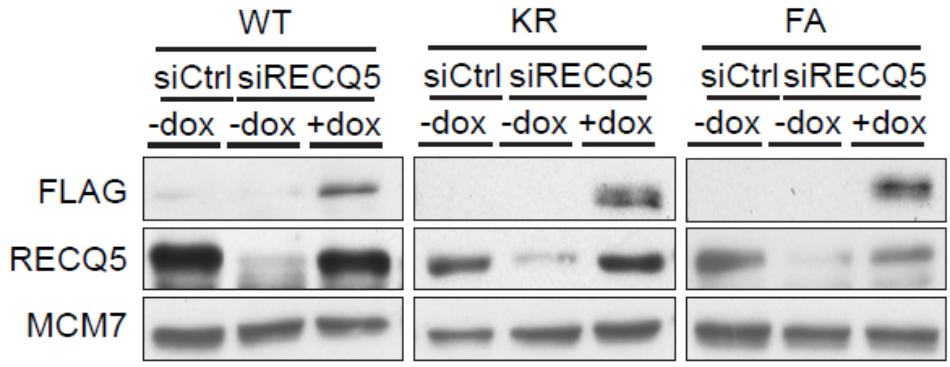

Figure 35. **Western blot analysis of expression of WT, K58R and F666A variants of RECQ5-Flag protein in U2OS T-REx cells.** 24 h after siRNA transfection, doxycyclin (1 ng/mL or DMSO) was added with fresh medium for additional 48 h, and total cell extracts were analyzed by Western blot. Ectopic RECQ5 expression was monitored by anti-FLAG antibody, while endogenous RECQ5 down-regulation was monitor by anti-RECQ5 antibody. MCM7 was used as loading control.

To gain further support for the above hypothesis, we asked whether helicase and RAD51-binding activities of RECQ5 are needed for expression of CFSs. We found that if the K58R or F666A mutants of RECQ5 were expressed in U2OS T-REx cells on place of endogenous RECQ5, aphidicolin-induced chromatid breakage was inhibited (Figure 37), suggesting a functional role for RECQ5 helicase activity and its binding to RAD51 in CFS expression.

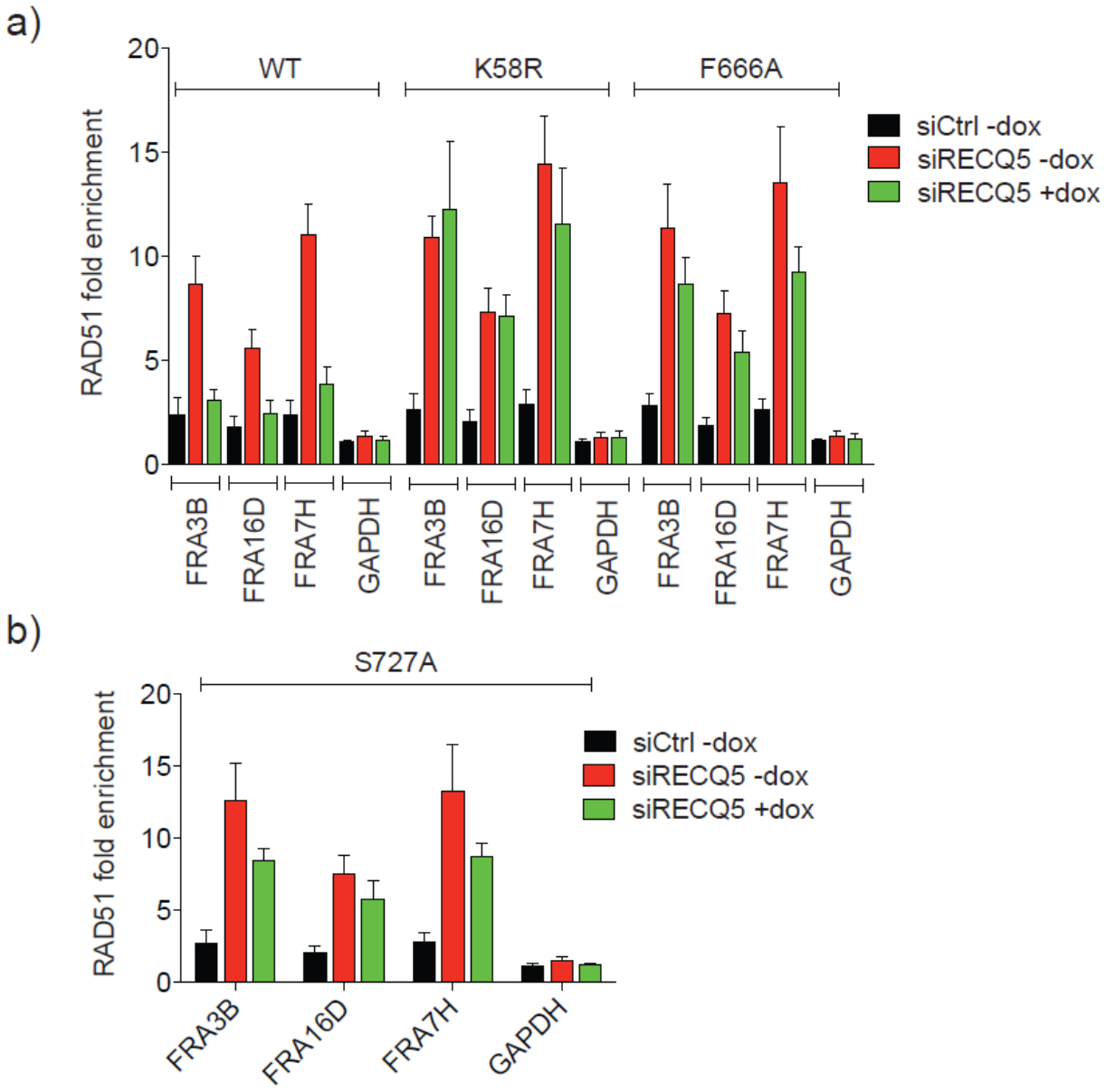

Figure 36. **RAD51 occupancy at CFSs in U2OS T-Rex cell expressing RECQ5 mutants.** After endogenous RECQ5 down-regulation and doxycyclin treatment for RECQ5 mutant expression, cells were cross-linked, lysed and sonicated for ChIP. Fragmented chromatin was immunoprecipitated by a specific antibody against RAD51, and the isolated DNA was used for qPCR analysis using specific primers for FRA3B, FRA16D, FRA7H and GAPDH (negative control). The data represent the mean of three independent experiments. Error bars show S.D.

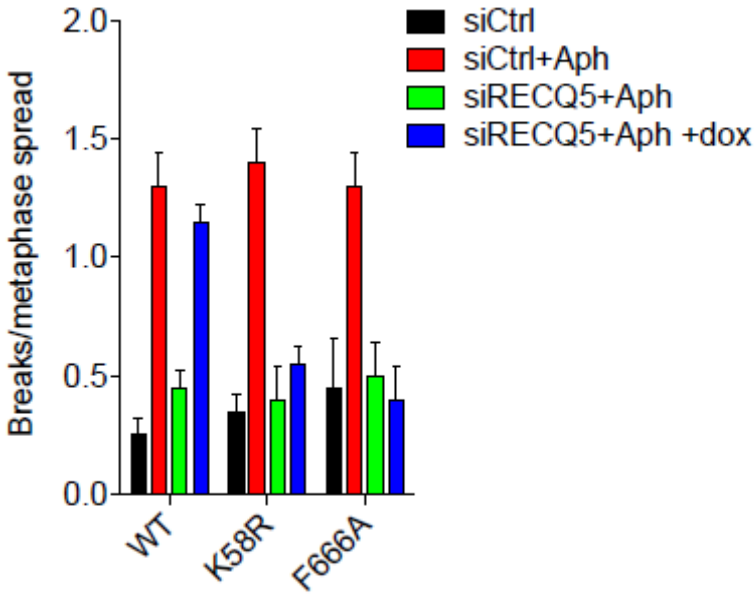

Figure 37. **RECQ5 helicase activity and its RAD51-binding domain are necessary for CFS expression.** Metaphase spread analyses of U2OS T-REx cells expressing WT, K58R and F666A versions of RECQ5-Flag, respectively. Cell culture conditions were the same as in Figure 31. At least 100 metaphase spreads were analyzed for each condition in two independent experiments. The data represent the mean +/- S.D.

Finally, we investigated whether the helicase activity of RECQ5 and its ability to interact with RAD51 are needed for proper chromosome separation in mitosis. For this, we measured the frequency of DAPI-stained bulky anaphase bridges and micronuclei in U2OS T-REx cell lines expressing the K58R and F666A mutants of RECQ5, respectively. We found that if either of these mutants was expressed on place of endogenous RECQ5, the frequency of these aberrant mitotic phenotypes was significantly increased as compared to cells expressing wild-type RECQ5 (Figure 38, 39).

In conclusion, our data provide evidence that RECQ5 acts during early mitosis to eliminate RAD51 filaments from stalled replication forks at CFSs and hence facilitates sister chromatid disjunction by MUS81-EME1.

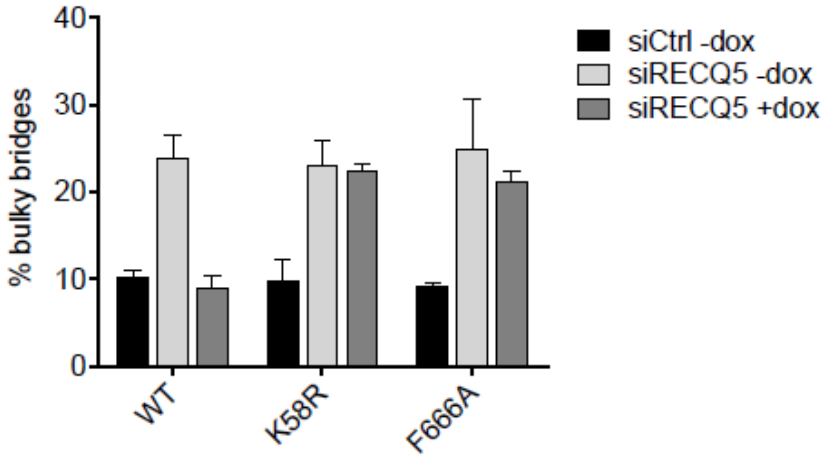

Figure 38. **Elevated frequency of bulky anaphase bridges in U2OS T-REx cells expressing K58R or F666A mutants of RECQ5.** Cell culturing and analysis of DAPI-stained anaphase bridges were performed as in Figure 32. At least 100 anaphase cells were analyzed in two independent experiments. The data represent the mean +/- S.D.

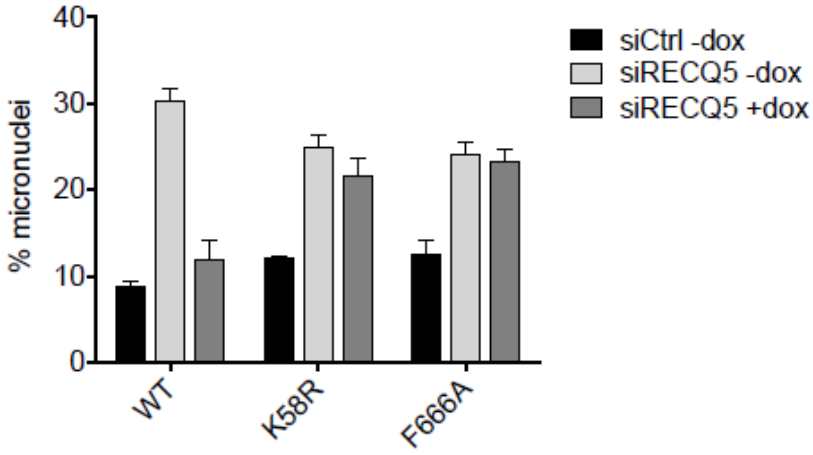

Figure 39. **RECQ5 helicase activity and its binding to RAD51 are required for suppression of micronuclei formation.** Cell culturing conditions were the same as in Figure 33. At least 400 binucleated cells were analyzed in two independent experiments. Error bars show S.D.

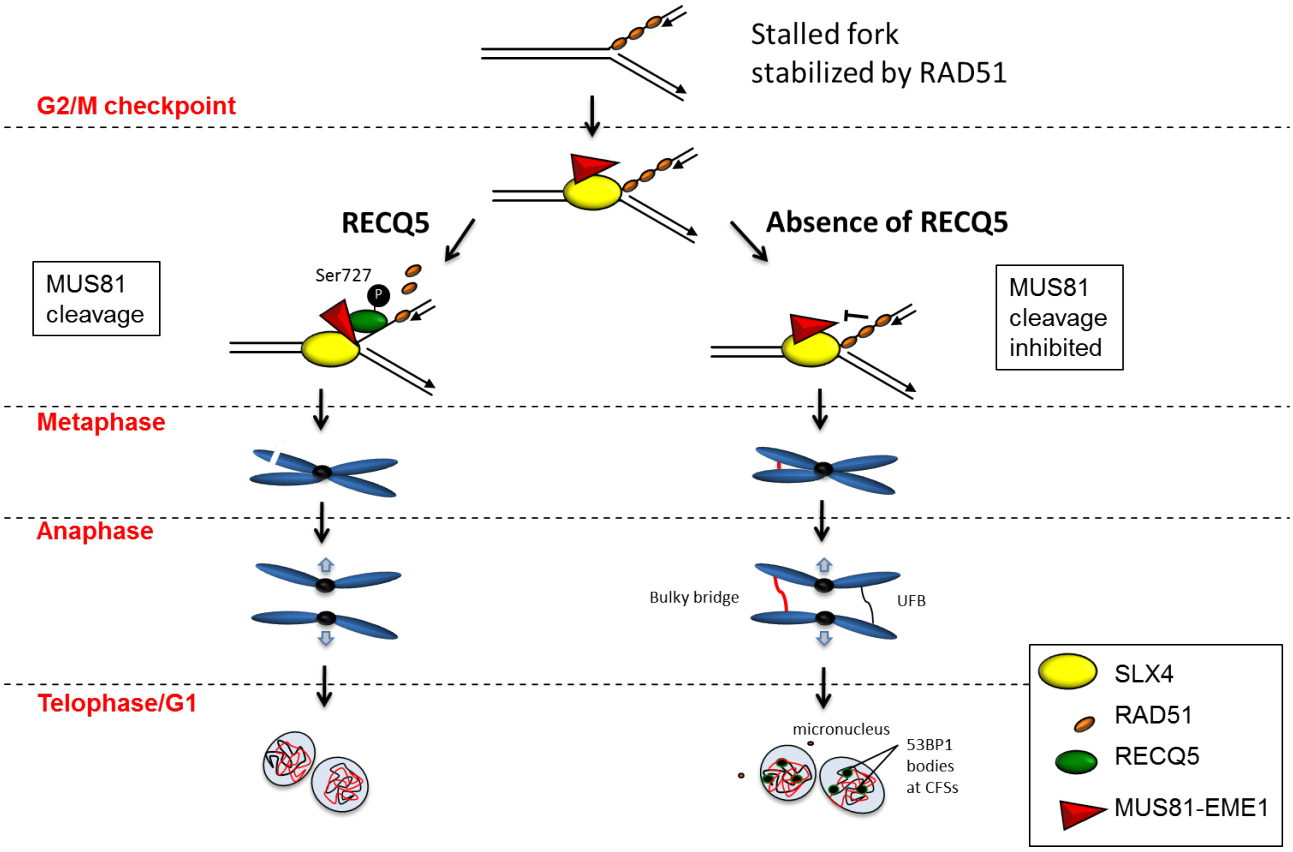

Figure 40. **Model for the role of RECQ5 in MUS81-mediated resolution of stalled replication forks in early mitosis.** For detailed description see the last paragraph of chapter 7. Discussion.

6. Additional results

6.1 – Mechanism of the formation of DNA DSBs after CHK1 inhibition

When replication forks stall, DNA damage checkpoint kinases activate a signaling cascade, spreading the signal to numerous effector proteins that regulate cell physiology. Replication stress generates extended ssDNA tracks at replication forks, and these serve as a signal to trigger replication checkpoint activation [164, 165]. ATR kinase is the major player of the replication stress response, and it is involved in fork stabilization, repair and restart. At the same time, ATR phosphorylates and activates CHK1, which promotes cell cycle arrest and inhibits additional origin firing [166]. Previous studies have shown that CHK1 inhibition promotes MUS81-dependent DSB formation [167]. CHK1 inhibition also promotes premature entry into mitosis, excessive origin firing and massive ssDNA generation [168]. For this reason, we were interested to study whether RECQ5 could have a role in DSB formation upon CHK1 inhibition along with the MUS81 endonuclease. To inhibit CHK1 activity *in vivo*, we used the small molecule UCN-01. When we treated HeLa cells with UCN-01 for 7 h, we could not observe DSB formation by pulsed-field gel electrophoresis (PFGE; Figure 1S lane 3). We therefore synchronized HeLa cells at G1/S transition by HU treatment for 16 h, and at 1 h after HU release, UCN-01 was added for additional 7 h. Under these conditions, we could observe DSB accumulation by PFGE (Figure S1 lane 4).

Figure S1. **UCN-01 induces DSB formation only in S-phase synchronized cells.** HeLa cells were treated with 300 nM UCN-01 for 7 h prior to and after synchronization in S-phase by 2 mM HU (16 h) as indicated. HU synchronized cells were released for 1 h in fresh medium to allow replication restart. Genomic DNA was isolated and analyzed by pulsed field electrophoresis. 16 h HU treatment did not induce DSB formation. The bands in the wells correspond to intact genomic DNA. The lower band and the smear correspond to fragmented DNA.

Next, we used U2OS cell line to monitor DSB formation after UCN-01 treatment. We treated asynchronous or HU-synchronized U2OS cells by UCN-01 for 7 h. Interestingly, we observed that HU synchronization was not required for UCN-01 to induced DSB formation in U2OS, although it increased the amount of DSBs as compared to asynchronous cells (Figure S2). We speculate that the differences observed between HeLa and U2OS cells could arise from the fraction of the S phase population; U2OS cell population has a higher percentage of S-phase cells than HeLa (Figure S2 lane 3).

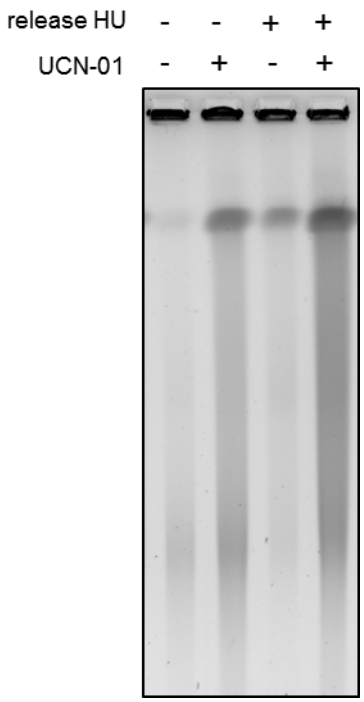

Figure S2. **UCN-01 promotes DSB formation without HU synchronization in U2OS cells.** U2OS cells were treated with 300 nM UCN-01 for 7 h prior to and after synchronization by HU treatment (see Figure S1). DSB formation was monitored by pulsed field electrophoresis.

Since DSB formation upon CHK1 inhibition required the cells to be in S phase, we wanted to determine whether these breaks were dependent on replication fork movement. To this end, we treated U2OS with UCN-01 in the presence of a high dose of aphidicolin, known to completely inhibit replicative DNA polymerases. By PFGE, we observed that aphidicolin completely inhibited DSB formation upon CHK1 inhibition (Figure S3), confirming that breakage depends on replication.

Figure 3S. **DSB formation induced by CHK1 inhibition depends on DNA replication.** U2OS cells were treated with 300 nM UCN-01 for 10 h in the absence or the presence of 5µM aphidicolin. Genomic DNA was isolated and analyzed by pulsed field electrophoresis.

Our previous results showed that RECQ5 and MUS81 bind to CFSs where replication intermediates accumulate, and where RECQ5 facilitates MUS81-mediated cleavage of stalled replication forks in early mitosis. Therefore, we wanted to investigate whether DSBs formed upon UCN-01 treatment depended on RECQ5 and MUS81. We down-regulated RECQ5 and MUS81 in U2OS cells and then treated them with UCN-01 for 10 h. We found that both MUS81 and RECQ5 were required for DNA breakage induced by CHK1 inhibition (Figure 4S). Double-depletion of these proteins did not further decreased DSB levels, confirming that RECQ5 and MUS81 work in the same pathway for DSB formation. The same results were obtained in HeLa cells (data not shown).

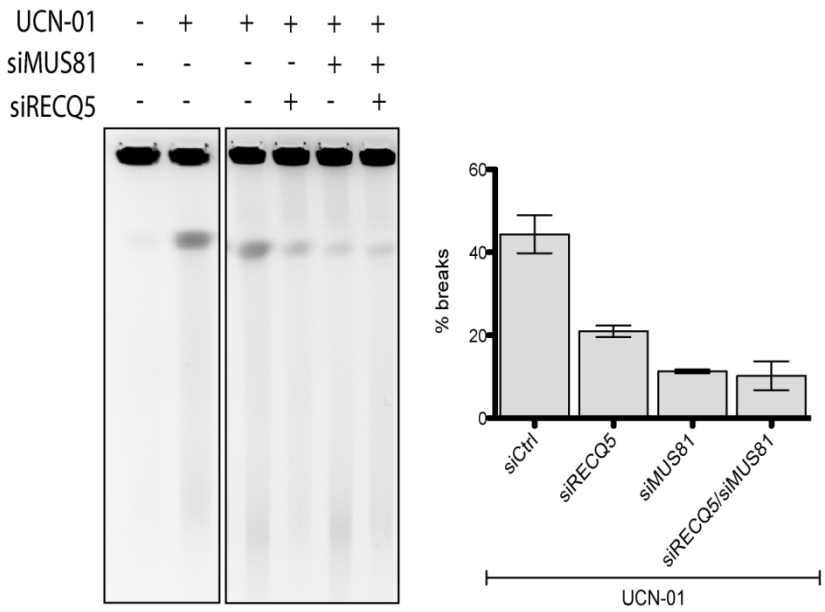

Figure 4S. **UCN-01-induced DSBs depend on both RECQ5 and MUS81. a)** RECQ5 or MUS81 were depleted in U2OS cells, and the last 10 h, UCN-01 (300 nM) was added. DSB formation was monitored by PFGE. **b)** Quantification of the gel shown in (a). The data represent the mean of three independent experiments. Error bars show S.D.

According to our results, RECQ5 and MUS81 are recruited on CFSs during an early step of mitosis, and RO-3306 treatment prevented RECQ5 and MUS81 binding to those regions. We therefore wanted to investigate whether UCN-01-induced chromosome breakage is dependent upon entry of cells into mitosis. To this end, UCN-01 was combined with nocodazole or RO-3306 treatment in U2OS cells, and DSB formation under these conditions was analyzed by PFGE. Interestingly, blockage of cells in prometaphase by nocodazole did not prevent DNA breakage. On the contrary, blockage of cell at G2/M transition by RO-3306 treatment, inhibited DSB formation (Figure 5S), suggesting that in order to break, stalled replication forks and other replication intermediates need to enter in mitosis where probably RECQ5 and MUS81 are activated to resolve these structures.

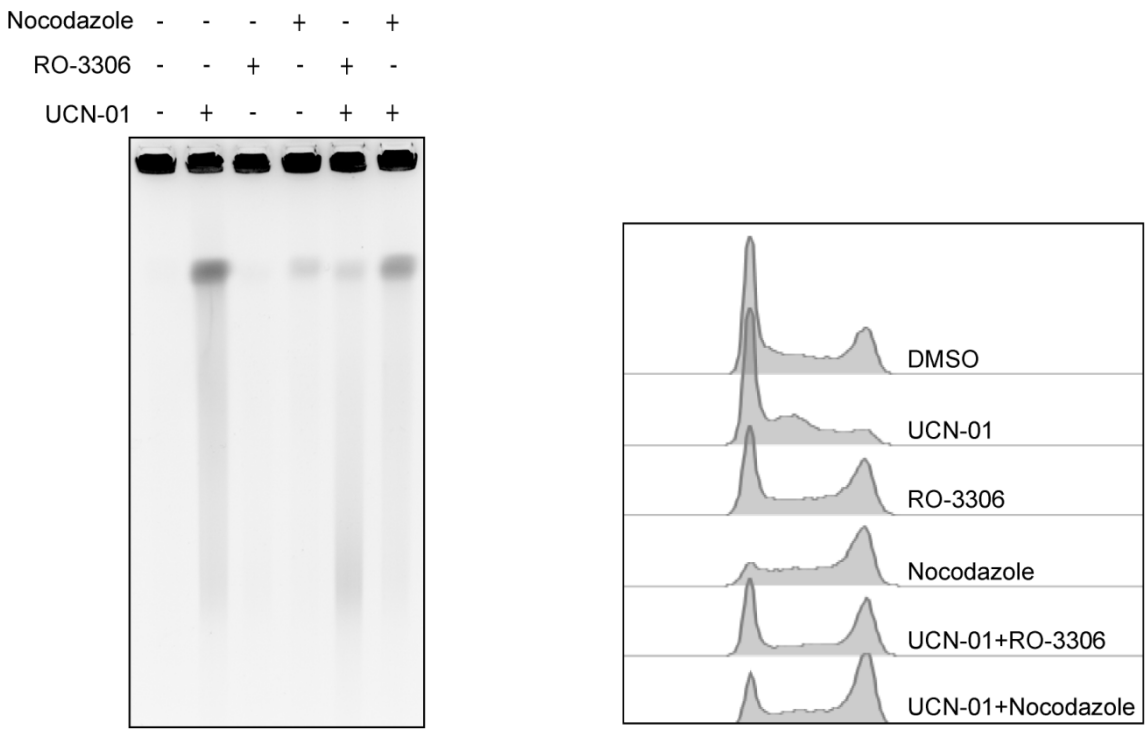

Figure 5S. **DSB formation induced by CHK1 inhibition occurs upon entry into mitosis. a)** U2OS cells were treated for 10 h with 300 nM UCN-01, 9µM RO-3306 and 200ng/mL] as indicated. Genomic DNA was analyzed by PFGE. **b)** FACS analysis of U2OS cell treated with indicated drugs. Condition for treatments were the same as in (a).

7. Discussion

DNA replication allows faithful duplication of the genetic material and its segregation to daughter cells. However, replication forks encounter numerous roadblocks during DNA synthesis, such as unrepaired DNA lesions, active transcription complexes or secondary DNA structures, which can halt their progression. Structure-specific endonucleases play an important role in resolving stalled replication forks and other aberrant structures arising in response to replication perturbation. In recent years, a number of studies have shown that chromosome segregation is heavily affected by unresolved replication intermediates, generating the basis for genome instability and tumorigenesis [169].

The MUS81-EME1 endonuclease was shown to actively resolve toxic replication intermediates at late replicating common fragile sites (CFSs) during early mitosis [138, 139]. Under conditions of replication stress, CFSs are usually under-replicated and escape the G2/M checkpoint and, if not expressed, they can give rise to anaphase DNA bridges and micronuclei, leading to loss of heterozygosity (LOH) or aneuploidy. Earlier studies conducted by our collaborator Prof. Lumir Krejci, and also by our laboratory, have shown that the MUS81-EME1 complex interacts with RECQ5 DNA helicase both *in vitro* and *in vivo*. Moreover, biochemical experiments revealed that RECQ5 could stimulate MUS81-EME1-mediated cleavage of 3'-flap DNA structures [153]. Therefore, our work focused on the biological function of RECQ5-MUS81 interaction in response to replication stress. We have shown that the absence of RECQ5 in the cell impairs CFS expression that, in turn, causes anaphase bridging, micronucleus formation and 53BP1 accumulation in the following G1 phase of the cell cycle. Moreover, we have found that RECQ5 depletion leads to RAD51 accumulation on CFSs. Expression of RECQ5 mutants with impaired helicase activity (K58R) or impaired binding to RAD51 (F666A) caused increased binding of RAD51 to

CFSs, inhibited CFS expression and promoted aberrant sister chromatid separation leading to genomic instability. Based on these findings, we propose that RECQ5 has a dual role in CFS expression: (i) it removes RAD51 from aberrant replication intermediates, a prerequisite for MUS81-EME1 cleavage; and (ii) it stimulates the nuclease activity of MUS81-EME1. This model is reminiscent of the model recently proposed for the yeast Srs2 DNA helicases that, like RECQ5, possess the ability to dismantle Rad51 nucleoprotein filaments [170, 171]. It has been shown that Srs2 interacts with the Mus81-Mms4 endonuclease, promoting its nuclease activity on different DNA substrates and stripping RAD51 filament from ssDNA, thus generating a suitable substrate for Mus81-Mms4 [170].

Consistent with our findings, it has been shown that the fission yeast RecQ homolog, Rqh1, promotes correct chromosome segregation at rDNA array, and Rqh1 mutant cells show delayed anaphase progression and lagging chromosomes [172]. Moreover, another publication demonstrated that the absence of Rqh1 impairs Mus81-Eme1-mediated cleavage of stalled forks after HU treatment [110]. Interestingly, it has been also shown that loss of RECQ5 in *Drosophila melanogaster* embryos leads to an increase in the frequency of anaphase bridge formation [173]. Thus, it appears that the cooperation between a RecQ-type DNA helicase and the Mus81 endonuclease in the resolution of replication intermediates during mitosis is evolutionary conserved.

We have shown that RECQ5 depletion leads to the formation of bulky DNA bridges and PICH-positive UFBs, where the latter are considered to originate from CFSs if they also contain FANCD2 foci. Therefore, it would be interesting to distinguish those UFBs arising from centromeric regions and those from CFSs.

A previous study demonstrated that depletion of TopBP1/Dpb11 in budding yeast and chicken cells, increases DAPI-positive bridges and BLM-positive UFBs [174], and another publication showed that TopBP1 absence from the cell promotes

53BP1 nuclear body accumulation and inhibits SLX4 foci formation in mitosis [175]. Since SLX4 acts as a scaffold for SLX1, XPF-ERCC1 and MUS81-EME1, and all these endonucleases have been demonstrated to prevent chromosome segregation defects, it is plausible to propose that RECQ5 also associates with the TopBP1/SLX4 scaffold. One can speculate that depletion of TopBP1 can disrupt the entire SLX4-MUS81-RECQ5 complex, therefore placing RECQ5 in the pathway for resolution interlinked chromosomes in mitosis. It is possible that RECQ5 can stimulate other endonucleases present in this complex.

Work in Prof. Lumir Krejci's laboratory has revealed that RAD51 inhibits MUS81-EME1-mediated cleavage of 3'-flaps *in vitro* [153], and we have shown that the helicase and RAD51-binding activities of RECQ5 are required to promote correct chromosome segregation and to prevent RAD51 binding to CFSs. Interestingly, studies conducted in budding yeast and mammalian cells have shown that RAD51 over-expression induces anaphase bridge formation [174] and promotes aneuploidy and chromosomal rearrangements [176]. Thus, it would be interesting to study the effect of RAD51 over-expression on aphidicolin-induced breakage of CFSs, and also to study micronucleus and anaphase bridge formation in this setting. Since our study showed that RECQ5 evicts RAD51 from replication intermediates on CFSs, we could expect that RAD51 over-expression would counteract MUS81-EME1 cleavage activity on replication intermediates at CFS, leading to impairment of chromosome segregation. It would be also interesting to test whether the observed defect in chromosome segregation of RECQ5-depleted cells is dependent on the presence of RAD51.

We have found that RECQ5 is phosphorylated by CDK1 on Ser727 in early mitosis, and this phosphorylation is required for CFS expression and proper chromosome segregation. Mus81-Mms4 has been shown to be hyper-phosphorylated in meiosis and early mitosis to generate crossover events essential

for chromosome segregation in yeast [177]. Although the function of RECQ5 phosphorylation is elusive, we provided evidence that it is involved in RAD51 displacement from CFSs, since expression of RECQ5 S727A mutant lead to RAD51 accumulation on these regions. Interestingly, Ser727 is located in close proximity to the RAD51 binding domain, therefore its phosphorylation could positively affect RECQ5-RAD51 interaction that is required for the recruitment of RECQ5 on RAD51 filaments and their disruption by RECQ5.

Based on our findings, we propose a model wherein RECQ5 counteracts an inhibitory effect of RAD51 on MUS81-EME1-mediated cleavage of replication intermediates in mitosis (Figure 40). Studies have shown that RAD51 filaments assemble on stalled replication forks to prevent degradation of the nascent DNA strands by the MRE11 complex [163]. These structures could escape the G2/M checkpoint and enter into mitosis where they would hamper sister chromatid segregation by inhibiting MUS81-EME1 cleavage. We propose that in early mitosis, MUS81 endonuclease is recruited to stalled replication forks by SLX4 and in turn recruits RECQ5 as we found that the association of RECQ5 with CFSs is dependent on MUS81. Upon recruitment, RECQ5 removes RAD51 filament formed on the leading strand arm of the fork and stimulates fork cleavage by the MUS81-EME1 complex. RECQ5 recruitment and/or its RAD51 filament disruption activity are driven by CDK1-dependent phosphorylation of RECQ5 at Ser727. If RECQ5 is absent in the cell, MUS81-EME1 cannot cleave replication intermediates because of the presence of RAD51. RAD51 persistency on replication intermediates does not impede chromosome segregation, however, the cell will inevitably go through to an aberrant anaphase separation, leading to genomic instability.

9. Material and Methods

Cell culture

U2OS and HeLa cells were maintained in Dulbecco Modified Eagle's Medium (DMEM; Invitrogen) supplemented with 10% fetal calf serum (FCS; Life Technologies) and streptomycin/penicillin (100 U/mL) at 37°C in a humidified incubator containing 5% CO_2. U2OS T-REx cell lines expressing pAll-In-One (pAIO) vector (WT, K58R, F666A and S727A RECQ5 variants), were cultivated in DMEM supplemented with 10% FBS (Tet-free approved), streptomycin/penicillin (100 U/mL), 1 µg/mL puromycin and 50µg/mL hygromycin B.

Small-interfering RNA (siRNA) transfection

U2OS, HeLa or U2OS T-REx cells were seeded in DMEM complete medium (for U2OS T-Rex cells the medium was supplemented with puromycin and hygromycin) to reach a cell confluency of 30-40% at the day of transfection. For transfection on a 10-cm plate, 15 µL of Lipofectamine RNAiMAX (Invitrogen) was mixed in 250 µL of OptiMEM medium (antibiotic free) in a 1.5-mL Eppendorf tube. In a separated 1.5-mL Eppendorf tube, the siRNA was mixed with 250 µL of OptiMEM medium to obtain a final siRNA concentration of 40 nM. After briefly vortexing and spinning-down, the siRNA mix was added to the RNAiMAX-OptiMEM tube. After 15-min incubation, the siRNA complexes were added dropwise to the plate containing 5 mL of complete medium to get a final volume of 5.5 mL, and gently swirled before returning plates to the incubator. After 24 h the medium was exchanged with fresh DMEM medium. 48 or 72 h after transfection, cells were used for following treatments or used for experiments.

Lyophilized siRNA oligonucleotides purchased from Microsynth were dissolved in distilled water.

For RECQ5 expression in U2OS TREx cell lines, endogenous RECQ5 was depleted for a total time of 72 h. After 24 h of transfection, 1 ng/mL doxycyclin was added to induce expression of WT, F666A, S727A, or K58R RECQ5 variants for additional 48 h.

Sequences of siRNA oligonucleotides used in this study:

Gene target	**Abbreviation used**	**Oligonucleotide sequence**
Luciferase	siCtrl	CGUACGCGGAAUACUUCGAdTdT
RECQ5	siRECQ5#1	GGAGAGUGCGACCAUGGCUdTdT
RECQ5	siRECQ5#2	CAGGUUUGUCGCCCAUUGGAAdTdT
MUS81	siMUS81	CAGCCCUGGUGGAUCGAUAdTdT

Immunofluorescence

Cells grown on cover slips, transfected or treated with drugs, were fixed with 4% formaldehyde. After several washes with PBS, cells were permeabilized in cold methanol (-20°C) or in 50:50 methanol/acetone mix (-20°C) for 15 min at -20°C. Cells were then washed with PBS and blocked in 5% BSA/PBS solution for 45 min. Cover slips were then incubated with the appropriate primary antibody, diluted in 5% BSA, at 4°C O.N. The following day, cover slips were washed several times with PBS and incubated with the secondary antibody for 45 min at RT. After washing with PBS, cover slips were mounted with Vectashield medium containing DAPI. The mounted slides were left to dry at RT for 30 min and then sealed with nail polish. Slides were analyzed with a Leica DM2700 upright fluorescent microscope.

For anaphase bridge analysis, cells were synchronized with 9 µM RO-3306 for 16h before releasing the cells first in 1X PBS for 5 min at RT and eventually in DMEM medium for a total time of 1.5 h at 37°C. After RO-3306 release, cells were simultaneously crosslinked and permeabilized in a PTEM buffer (20 mM PIPES pH 6.8, 10 mM EGTA, 0.2% Triton X-100, 1 mM $MgCl_2$) containing 4% formaldehyde. Washing steps were performed in PBS containing 0.2 % Triton-X.

List of antibodies and dilutions used in this study:

Antibody	**Company**	**Catalog number**	**Dilution**
53BP1 rabbit polyclonal	Santa Cruz	sc-22760	1:200
Cyclin A mouse monoclonal	Santa Cruz	sc-271682	1:50
PICH mouse monoclonal	Millipore	04-1540	1:50

Metaphase chromosome analysis

U2OS cells were seeded in 10-cm dishes and transfected with siRNA or treated as indicated in Figure legends. 5h before harvesting, 200 ng/mL nocodazole was added to the medium. Cells were harvested by mitotic shake-off and collected in a 15-mL tube. After centrifugation for 5 min at 4°C (2000 x g), the supernatant was removed and the pellet resuspended in 1 mL of DMEM. 8 mL of a 75 mM KCl solution was added to the cells and afterwards they were incubated at 37°C for 15 min. In the meantime, Carnoy's buffer was prepared (75% methanol, 25% glacial acetic acid) and 5 mL added to the KCl solution for 15 min at RT. The fixing steps with Carnoy's buffer were repeated 3 times with 8 mL of Carnoy’s buffer for each incubation. Cells were then spread on slides drop-wise and let dry O.N. at RT. The following day, dried slides were mounted with mounting media and DAPI (Vectashield). Chromosome spreads were analyzed on a Leica DM2700 upright fluorescent microscope and visible gaps/breaks were quantified for each spread.

Micronuclei assay

Cells were grown on cover slips in 6-well plates. 16 h before fixation, cell culture medium was supplemented with 2 µg/mL cytochalasin B to block cells in cytokinesis. Cells were fixed with 4% formaldehyde for 10 min and mounted with Vectashield mounting media containing DAPI. For quantification, only DAPI-stained binucleated cells were counted, and distinct micronuclei were considered as positive.

Western-blot analysis

Cell were suspended in a 50 mM Tris-HCl buffer (pH 7.5) containing 120 mM NaCl, 20 mM NaF, 1 mM EDTA, 6 mM EGTA, 15 mM Na-Pyrophosphate and 0.5% NP-40, and sonicated for 5 min with a Diagenode sonicator. Cellular debris was isolated from soluble fraction by centrifugation at 18000 x g for 30 min at 4°C. Samples were subjected to SDS PAGE. Separated proteins were transferred to a Hybond-P PVDF membrane (GE Healthcare) in a semi-dry apparatus (Sigma) for approx. 100 min at 0.8 mA/cm2. The membrane was blocked with 5% non-fat dry milk in TBS-T (20 mM Tris-HCl pH 7.4, 150 mM NaCl, 0.1% (v/v) Tween-20) for 1 h. Afterwards, the membrane was incubated with the respective primary antibody in 5% milk/TBS-T at 4°C O.N. The membrane was then washed three times in TBS-T and incubated with anti-mouse or anti-rabbit horseradish peroxidase-coupled (HRP) secondary antibody (1:10000 and 1:5000 dilution, respectively) for 45 min at RT. Afterwards, the membrane was washed three times with TBS-T and bands were detected by luminol-based reaction using a chemiluminescence reagent (Pierce).

Antibody	Company	Catalog number	Dilution
FLAG mouse monoclonal	Sigma	F1804	1:500
MCM7 mouse monoclonal	Sigma	M7931	1:2000
MUS81 mouse monoclonal	Sigma	M1445	1:2000
RECQ5 pSer727 rabbit polyclonal	Janscak Lab		1:2000
H3 pSer10 rabbit polyclonal	Millipore	06-570	1:1000
RECQ5 rabbit polyclonal	Janscak Lab		1:2000
TFIIH rabbit polyclonal	Santa Cruz	sc-293	1:2000

Chromatin-Immunoprecipitation (ChIP) assay

ChIP experiments were done with the ChIP-IT® Express kit (Active Motif) as described previously with minor modifications [144]. Briefly, U2OS cells were seeded in a 10-cm plate and transfections of indicated siRNAs were performed twice at 24 h and 48 h post seeding. Where indicated, aphidicolin (0.4 μM) and/or RO-3306 (9 μM) were added to cells after 2 days of first siRNA transfection. Cells were crosslinked 24 h later with 1X formaldehyde solution [1.1% formaldehyde, 10 mM NaCl, 0.1 mM EDTA (pH 8.0), 5 mM HEPES (pH 7.9)] at room temperature for exactly 15 min, followed by addition of glycine solution (125 mM, let sit at room temperature for 5 min) to quench the crosslinking reaction. Cells were harvested and collected by centrifugation at 1200 rpm in a refrigerated centrifuge for 10 min. Cells were then washed twice with PBS containing 0.5% Igepal. Chromatin fragments used in immunoprecipitation reactions were prepared by shearing of crosslinked chromatin using a bioruptor sonication device (Diagenode). Ten percent of the sonicated chromatin were stored at -80°C for use as an input sample. For each ChIP reaction, sonicated chromatin (7.5 μg) was immunoprecipitated O.N. at 4°C with either indicated antibody or a control IgG (4 - 5 μg each). After washing, immunocomplexes were eluted from the beads and de-crosslinked according to the manufacturer's instructions (Active Motif). ChIP and input samples were purified with the QIAquick PCR Purification Kit (Qiagen) and DNA was

eluted with 50 μl of sterile water. At least three independent experiments were performed for each ChIP. In each case, eluted DNA sample (2 – 3 μl) was used in quantitative real-time PCR (q-PCR) analysis in triplicate on a Roche LightCycler 480 Real-time PCR system with the use of Roche LightCycler 480 DNA SYBR Green I master for each primer pair. Data were analysed using the Pfaffl's method as described previously [144]. Fold enrichment of each target region was calculated as ratio of the amount of immunoprecipitated DNA estimated for the specific versus control IgG antibody.

Antibodies used for ChIP in this study:

Antibody	**Company**	**Catalog number**
γ-H2AX Ser139 mouse monoclonal	Millipore	JBW301
53BP1 rabbit polyclonal	Novus Biological	NB100-304
MUS81 mouse monoclonal	Abcam	ab14387
RAD51 rabbit polyclonal	Santa Cruz	sc-8349
RECQ5 rabbit polyclonal	Janscak Lab	

Primers used for qPCR in this study:

Primer Name	**Sequence 5'-3'**
FRA3B	*CACTTCCTAACAGGCCCAAA* *CCTCCACTTCTCCTCCCTCT*
FRA16D	*TCCTGTGGAAGGGATATTTA* *CCCCTCATATTCTGCTTCTA*

FRA7H	*TAATGCGTCCCCTTGTGACT* *GGCAGATTTTAGTCCCTCAGC*
GAPDH	*CCCTCTGGTGGTGGCCCCTT* *GGCGCCCAGACACCCAATCC*

FACS analysis

For cell cycle analysis, cells were detached from the plate with trypsin. Afterwards, the number of cells was counted to have a density of $1.0*10^6$ per sample. After washing with PBS, cells were fixed with 1 mL of 70% cold ethanol added drop-wise. After 30 min of incubation in ethanol (the sample can be stored in ethanol at 4°C up to 3 weeks), cells were washed with PBS and resuspended in 500 µL of PBS. Cells were then treated with 100 µg/mL RNase A at 37°C for 30 min. Finally, cell suspension was incubated with 20 µg/mL propidium iodide (PI) for 30 min in the dark, followed by FACS analysis with a CyAn ADP Analyzer flow cytometer.

Pulsed-field gel electrophoresis (PFGE)

For plug preparation, 1.5% LMT (low melting temperature) agarose (SeaPlaque GTG agarose, Lonza) was dissolved in PBS in the microwave, and incubated in 50°C water bath until the use. Cells were trypsinized, collected in a Falcon tube (including the PBS supernatant) and washed with cold PBS. Afterwards, cells were counted and resuspended in PBS to have a $1*10^6$/100 µL concentration. Cells were equilibrated at 50°C, followed by the addition of 100 µL agarose, and finally, the mixture was transfered into PFGE plugs. Plugs were let dry for at least 15 min. The plugs were then incubated in lysis buffer (100 mM EDTA, pH 8.0, 0.02% sodium deoxycholate,

1% sodium lauryl sarcosine) supplemented with 20 µg/mL proteinase K (Roche). Plugs were incubated for 36-72 h at 37°C, and then washed 3 times with washing buffer (20 mM Tris-HCl, 50 mM EDTA, pH 8.0) for 30 min/wash. At this step, plugs were stored at 4°C or immediately used for electrophoresis analysis. For PFGE gel, 0.9% pulse field certified agarose (Pulse Field Certified Agarose, Bio-Rad) were dissolved in 0.5X TBE in microwave, and incubated at 50°C in water bath for at least 15 min before casting.

Setting for the PFGE chamber (Bio-Rad):

BLOCK	I	II	III
TIME (h)	9	6	6
INCLUDED ANGLE	120	117	112
V/cm	5.5	4.5	4.0
SWITCH (s)	30-18	18-9	9-5

Gel electrophoresis was let run O.N. using the settings listed in the previous table. The gel was stained with EtBr solution for 30 min and analyzed with an Alpha Innotech AlphaImager Gel Documentation Station. The ImageJ Software was used for band quantification.

10. References

1. Loeb, K.R. and L.A. Loeb, *Genetic instability and the mutator phenotype. Studies in ulcerative colitis.* Am J Pathol, 1999. **154**(6): p. 1621-6.
2. Negrini, S., V.G. Gorgoulis, and T.D. Halazonetis, *Genomic instability--an evolving hallmark of cancer.* Nat Rev Mol Cell Biol, 2010. **11**(3): p. 220-8.
3. Hanahan, D. and R.A. Weinberg, *Hallmarks of cancer: the next generation.* Cell, 2011. **144**(5): p. 646-74.
4. Hanahan, D. and R.A. Weinberg, *The hallmarks of cancer.* Cell, 2000. **100**(1): p. 57-70.
5. Hoeijmakers, J.H., *Genome maintenance mechanisms for preventing cancer.* Nature, 2001. **411**(6835): p. 366-74.
6. Lindahl, T., *Genetic instability in cancer. Introduction.* Cancer Surv, 1996. **28**: p. 1-2.
7. Lander, E.S., et al., *Initial sequencing and analysis of the human genome.* Nature, 2001. **409**(6822): p. 860-921.
8. Christmann, M., et al., *Mechanisms of human DNA repair: an update.* Toxicology, 2003. **193**(1-2): p. 3-34.
9. McKinnon, P.J., *DNA repair deficiency and neurological disease.* Nat Rev Neurosci, 2009. **10**(2): p. 100-12.
10. Khalil, H.S., et al., *Pharmacological inhibition of ATM by KU55933 stimulates ATM transcription.* Exp Biol Med (Maywood), 2012. **237**(6): p. 622-34.
11. Watson, J.D. and F.H. Crick, *A structure for deoxyribose nucleic acid. 1953.* Nature, 2003. **421**(6921): p. 397-8; discussion 396.
12. McCulloch, S.D. and T.A. Kunkel, *The fidelity of DNA synthesis by eukaryotic replicative and translesion synthesis polymerases.* Cell Res, 2008. **18**(1): p. 148-61.
13. Leman, A.R. and E. Noguchi, *The replication fork: understanding the eukaryotic replication machinery and the challenges to genome duplication.* Genes (Basel), 2013. **4**(1): p. 1-32.
14. Okazaki, R., et al., *Mechanism of DNA chain growth. I. Possible discontinuity and unusual secondary structure of newly synthesized chains.* Proc Natl Acad Sci U S A, 1968. **59**(2): p. 598-605.
15. Alani, E., et al., *Characterization of DNA-binding and strand-exchange stimulation properties of y-RPA, a yeast single-strand-DNA-binding protein.* J Mol Biol, 1992. **227**(1): p. 54-71.
16. Siegal, G., et al., *A 5' to 3' exonuclease functionally interacts with calf DNA polymerase epsilon.* Proc Natl Acad Sci U S A, 1992. **89**(20): p. 9377-81.
17. Waga, S., G. Bauer, and B. Stillman, *Reconstitution of complete SV40 DNA replication with purified replication factors.* J Biol Chem, 1994. **269**(14): p. 10923-34.
18. Budd, M. and J.L. Campbell, *Temperature-sensitive mutations in the yeast DNA polymerase I gene.* Proc Natl Acad Sci U S A, 1987. **84**(9): p. 2838-42.
19. Sitney, K.C., M.E. Budd, and J.L. Campbell, *DNA polymerase III, a second essential DNA polymerase, is encoded by the S. cerevisiae CDC2 gene.* Cell, 1989. **56**(4): p. 599-605.
20. Fisher, P.A., T.S. Wang, and D. Korn, *Enzymological characterization of DNA polymerase alpha. Basic catalytic properties processivity, and gap utilization of the homogeneous enzyme from human KB cells.* J Biol Chem, 1979. **254**(13): p. 6128-37.
21. Nethanel, T., T. Zlotkin, and G. Kaufmann, *Assembly of simian virus 40 Okazaki pieces from DNA primers is reversibly arrested by ATP depletion.* J Virol, 1992. **66**(11): p. 6634-40.
22. Neuwald, A.F., et al., *AAA+: A class of chaperone-like ATPases associated with the assembly, operation, and disassembly of protein complexes.* Genome Res, 1999. **9**(1): p. 27-43.
23. Labib, K., J.A. Tercero, and J.F. Diffley, *Uninterrupted MCM2-7 function required for DNA replication fork progression.* Science, 2000. **288**(5471): p. 1643-7.
24. Pacek, M. and J.C. Walter, *A requirement for MCM7 and Cdc45 in chromosome unwinding during eukaryotic DNA replication.* EMBO J, 2004. **23**(18): p. 3667-76.

25. Aparicio, O.M., D.M. Weinstein, and S.P. Bell, *Components and dynamics of DNA replication complexes in S. cerevisiae: redistribution of MCM proteins and Cdc45p during S phase.* Cell, 1997. **91**(1): p. 59-69.
26. Nishitani, H. and Z. Lygerou, *Control of DNA replication licensing in a cell cycle.* Genes Cells, 2002. **7**(6): p. 523-34.
27. Coleman, T.R., P.B. Carpenter, and W.G. Dunphy, *The Xenopus Cdc6 protein is essential for the initiation of a single round of DNA replication in cell-free extracts.* Cell, 1996. **87**(1): p. 53-63.
28. Remus, D., et al., *Concerted loading of Mcm2-7 double hexamers around DNA during DNA replication origin licensing.* Cell, 2009. **139**(4): p. 719-30.
29. Dahmann, C., J.F. Diffley, and K.A. Nasmyth, *S-phase-promoting cyclin-dependent kinases prevent re-replication by inhibiting the transition of replication origins to a pre-replicative state.* Curr Biol, 1995. **5**(11): p. 1257-69.
30. Hartwell, L.H. and T.A. Weinert, *Checkpoints: controls that ensure the order of cell cycle events.* Science, 1989. **246**(4930): p. 629-34.
31. Weinert, T. and L. Hartwell, *Control of G2 delay by the rad9 gene of Saccharomyces cerevisiae.* J Cell Sci Suppl, 1989. **12**: p. 145-8.
32. Harper, J.W. and S.J. Elledge, *The DNA damage response: ten years after.* Mol Cell, 2007. **28**(5): p. 739-45.
33. Zeman, M.K. and K.A. Cimprich, *Causes and consequences of replication stress.* Nat Cell Biol, 2014. **16**(1): p. 2-9.
34. Abraham, R.T., *Cell cycle checkpoint signaling through the ATM and ATR kinases.* Genes Dev, 2001. **15**(17): p. 2177-96.
35. Willis, N. and N. Rhind, *Regulation of DNA replication by the S-phase DNA damage checkpoint.* Cell Div, 2009. **4**: p. 13.
36. Larner, J.M., H. Lee, and J.L. Hamlin, *Radiation effects on DNA synthesis in a defined chromosomal replicon.* Mol Cell Biol, 1994. **14**(3): p. 1901-8.
37. Tercero, J.A., M.P. Longhese, and J.F. Diffley, *A central role for DNA replication forks in checkpoint activation and response.* Mol Cell, 2003. **11**(5): p. 1323-36.
38. Sogo, J.M., M. Lopes, and M. Foiani, *Fork reversal and ssDNA accumulation at stalled replication forks owing to checkpoint defects.* Science, 2002. **297**(5581): p. 599-602.
39. Noguchi, E., et al., *Swi1 prevents replication fork collapse and controls checkpoint kinase Cds1.* Mol Cell Biol, 2003. **23**(21): p. 7861-74.
40. Sale, J.E., A.R. Lehmann, and R. Woodgate, *Y-family DNA polymerases and their role in tolerance of cellular DNA damage.* Nat Rev Mol Cell Biol, 2012. **13**(3): p. 141-52.
41. Branzei, D., *Ubiquitin family modifications and template switching.* FEBS Lett, 2011. **585**(18): p. 2810-7.
42. Luo, J., N.L. Solimini, and S.J. Elledge, *Principles of cancer therapy: oncogene and non-oncogene addiction.* Cell, 2009. **136**(5): p. 823-37.
43. Halazonetis, T.D., V.G. Gorgoulis, and J. Bartek, *An oncogene-induced DNA damage model for cancer development.* Science, 2008. **319**(5868): p. 1352-5.
44. Gorgoulis, V.G., et al., *Activation of the DNA damage checkpoint and genomic instability in human precancerous lesions.* Nature, 2005. **434**(7035): p. 907-13.
45. Bartkova, J., et al., *Oncogene-induced senescence is part of the tumorigenesis barrier imposed by DNA damage checkpoints.* Nature, 2006. **444**(7119): p. 633-7.
46. d'Adda di Fagagna, F., *Living on a break: cellular senescence as a DNA-damage response.* Nat Rev Cancer, 2008. **8**(7): p. 512-22.
47. Bartek, J., M. Mistrik, and J. Bartkova, *Thresholds of replication stress signaling in cancer development and treatment.* Nat Struct Mol Biol, 2012. **19**(1): p. 5-7.
48. Lambert, S. and A.M. Carr, *Checkpoint responses to replication fork barriers.* Biochimie, 2005. **87**(7): p. 591-602.
49. Byun, T.S., et al., *Functional uncoupling of MCM helicase and DNA polymerase activities activates the ATR-dependent checkpoint.* Genes Dev, 2005. **19**(9): p. 1040-52.

50. Hustedt, N., S.M. Gasser, and K. Shimada, *Replication checkpoint: tuning and coordination of replication forks in s phase.* Genes (Basel), 2013. **4**(3): p. 388-434.
51. Eklund, H., et al., *Structure and function of the radical enzyme ribonucleotide reductase.* Prog Biophys Mol Biol, 2001. **77**(3): p. 177-268.
52. Poli, J., et al., *dNTP pools determine fork progression and origin usage under replication stress.* EMBO J, 2012. **31**(4): p. 883-94.
53. Ikegami, S., et al., *Aphidicolin prevents mitotic cell division by interfering with the activity of DNA polymerase-alpha.* Nature, 1978. **275**(5679): p. 458-60.
54. MacDougall, C.A., et al., *The structural determinants of checkpoint activation.* Genes Dev, 2007. **21**(8): p. 898-903.
55. Lambert, S., et al., *Schizosaccharomyces pombe checkpoint response to DNA interstrand cross-links.* Mol Cell Biol, 2003. **23**(13): p. 4728-37.
56. Raschle, M., et al., *Mechanism of replication-coupled DNA interstrand crosslink repair.* Cell, 2008. **134**(6): p. 969-80.
57. Povirk, L.F., *DNA damage and mutagenesis by radiomimetic DNA-cleaving agents: bleomycin, neocarzinostatin and other enediynes.* Mutat Res, 1996. **355**(1-2): p. 71-89.
58. Huang, J.C., et al., *Human nucleotide excision nuclease removes thymine dimers from DNA by incising the 22nd phosphodiester bond 5' and the 6th phosphodiester bond 3' to the photodimer.* Proc Natl Acad Sci U S A, 1992. **89**(8): p. 3664-8.
59. Hsiang, Y.H., et al., *Camptothecin induces protein-linked DNA breaks via mammalian DNA topoisomerase I.* J Biol Chem, 1985. **260**(27): p. 14873-8.
60. Strumberg, D., et al., *Conversion of topoisomerase I cleavage complexes on the leading strand of ribosomal DNA into 5'-phosphorylated DNA double-strand breaks by replication runoff.* Mol Cell Biol, 2000. **20**(11): p. 3977-87.
61. Regairaz, M., et al., *Mus81-mediated DNA cleavage resolves replication forks stalled by topoisomerase I-DNA complexes.* J Cell Biol, 2011. **195**(5): p. 739-49.
62. Singleton, M.R., M.S. Dillingham, and D.B. Wigley, *Structure and mechanism of helicases and nucleic acid translocases.* Annu Rev Biochem, 2007. **76**: p. 23-50.
63. Kusano, K., M.E. Berres, and W.R. Engels, *Evolution of the RECQ family of helicases: A drosophila homolog, Dmblm, is similar to the human bloom syndrome gene.* Genetics, 1999. **151**(3): p. 1027-39.
64. Chakraverty, R.K. and I.D. Hickson, *Defending genome integrity during DNA replication: a proposed role for RecQ family helicases.* Bioessays, 1999. **21**(4): p. 286-94.
65. Bernstein, D.A. and J.L. Keck, *Domain mapping of Escherichia coli RecQ defines the roles of conserved N- and C-terminal regions in the RecQ family.* Nucleic Acids Res, 2003. **31**(11): p. 2778-85.
66. Kitano, K., S.Y. Kim, and T. Hakoshima, *Structural basis for DNA strand separation by the unconventional winged-helix domain of RecQ helicase WRN.* Structure, 2010. **18**(2): p. 177-87.
67. Pike, A.C., et al., *Structure of the human RECQ1 helicase reveals a putative strand-separation pin.* Proc Natl Acad Sci U S A, 2009. **106**(4): p. 1039-44.
68. Lucic, B., et al., *A prominent beta-hairpin structure in the winged-helix domain of RECQ1 is required for DNA unwinding and oligomer formation.* Nucleic Acids Res, 2011. **39**(5): p. 1703-17.
69. Wu, L., *Role of the BLM helicase in replication fork management.* DNA Repair (Amst), 2007. **6**(7): p. 936-44.
70. Karmakar, P., et al., *BLM is an early responder to DNA double-strand breaks.* Biochem Biophys Res Commun, 2006. **348**(1): p. 62-9.
71. Samanta, S. and P. Karmakar, *Recruitment of HRDC domain of WRN and BLM to the sites of DNA damage induced by mitomycin C and methyl methanesulfonate.* Cell Biol Int, 2012. **36**(10): p. 873-81.
72. Karow, J.K., L. Wu, and I.D. Hickson, *RecQ family helicases: roles in cancer and aging.* Curr Opin Genet Dev, 2000. **10**(1): p. 32-8.
73. Brosh, R.M., Jr., *DNA helicases involved in DNA repair and their roles in cancer.* Nat Rev Cancer, 2013. **13**(8): p. 542-58.

74. Berti, M., et al., *Human RECQ1 promotes restart of replication forks reversed by DNA topoisomerase I inhibition.* Nat Struct Mol Biol, 2013. **20**(3): p. 347-54.
75. Pike, A.C., et al., *Human RECQ1 helicase-driven DNA unwinding, annealing, and branch migration: insights from DNA complex structures.* Proc Natl Acad Sci U S A, 2015. **112**(14): p. 4286-91.
76. Ozgenc, A. and L.A. Loeb, *Current advances in unraveling the function of the Werner syndrome protein.* Mutat Res, 2005. **577**(1-2): p. 237-51.
77. Muftuoglu, M., et al., *The clinical characteristics of Werner syndrome: molecular and biochemical diagnosis.* Hum Genet, 2008. **124**(4): p. 369-77.
78. Liu, Y., *Rothmund-Thomson syndrome helicase, RECQ4: on the crossroad between DNA replication and repair.* DNA Repair (Amst), 2010. **9**(3): p. 325-30.
79. Bloom, D., *Congenital telangiectatic erythema resembling lupus erythematosus in dwarfs; probably a syndrome entity.* AMA Am J Dis Child, 1954. **88**(6): p. 754-8.
80. Chaganti, R.S., S. Schonberg, and J. German, *A manyfold increase in sister chromatid exchanges in Bloom's syndrome lymphocytes.* Proc Natl Acad Sci U S A, 1974. **71**(11): p. 4508-12.
81. Wu, L. and I.D. Hickson, *RecQ helicases and cellular responses to DNA damage.* Mutat Res, 2002. **509**(1-2): p. 35-47.
82. Ira, G., et al., *Srs2 and Sgs1-Top3 suppress crossovers during double-strand break repair in yeast.* Cell, 2003. **115**(4): p. 401-11.
83. Kee, Y. and A.D. D'Andrea, *Molecular pathogenesis and clinical management of Fanconi anemia.* J Clin Invest, 2012. **122**(11): p. 3799-806.
84. Adamo, A., et al., *Preventing nonhomologous end joining suppresses DNA repair defects of Fanconi anemia.* Mol Cell, 2010. **39**(1): p. 25-35.
85. Meetei, A.R., et al., *A multiprotein nuclear complex connects Fanconi anemia and Bloom syndrome.* Mol Cell Biol, 2003. **23**(10): p. 3417-26.
86. Suhasini, A.N., et al., *Interaction between the helicases genetically linked to Fanconi anemia group J and Bloom's syndrome.* EMBO J, 2011. **30**(4): p. 692-705.
87. Suhasini, A.N., et al., *Fanconi anemia group J helicase and MRE11 nuclease interact to facilitate the DNA damage response.* Mol Cell Biol, 2013. **33**(11): p. 2212-27.
88. Chan, K.L., et al., *Replication stress induces sister-chromatid bridging at fragile site loci in mitosis.* Nat Cell Biol, 2009. **11**(6): p. 753-60.
89. Naim, V. and F. Rosselli, *The FANC pathway and BLM collaborate during mitosis to prevent micro-nucleation and chromosome abnormalities.* Nat Cell Biol, 2009. **11**(6): p. 761-8.
90. Hu, Y., et al., *RECQL5/Recql5 helicase regulates homologous recombination and suppresses tumor formation via disruption of Rad51 presynaptic filaments.* Genes Dev, 2007. **21**(23): p. 3073-84.
91. Wang, W., et al., *Functional relation among RecQ family helicases RecQL1, RecQL5, and BLM in cell growth and sister chromatid exchange formation.* Mol Cell Biol, 2003. **23**(10): p. 3527-35.
92. Jeong, Y.S., et al., *Deficiency of Caenorhabditis elegans RecQ5 homologue reduces life span and increases sensitivity to ionizing radiation.* DNA Repair (Amst), 2003. **2**(12): p. 1309-19.
93. Shimamoto, A., et al., *Human RecQ5beta, a large isomer of RecQ5 DNA helicase, localizes in the nucleoplasm and interacts with topoisomerases 3alpha and 3beta.* Nucleic Acids Res, 2000. **28**(7): p. 1647-55.
94. Garcia, P.L., et al., *Human RECQ5beta, a protein with DNA helicase and strand-annealing activities in a single polypeptide.* EMBO J, 2004. **23**(14): p. 2882-91.
95. Aygun, O., J. Svejstrup, and Y. Liu, *A RECQ5-RNA polymerase II association identified by targeted proteomic analysis of human chromatin.* Proc Natl Acad Sci U S A, 2008. **105**(25): p. 8580-4.
96. Kanagaraj, R., et al., *RECQ5 helicase associates with the C-terminal repeat domain of RNA polymerase II during productive elongation phase of transcription.* Nucleic Acids Res, 2010. **38**(22): p. 8131-40.
97. Saponaro, M., et al., *RECQL5 controls transcript elongation and suppresses genome instability associated with transcription stress.* Cell, 2014. **157**(5): p. 1037-49.
98. Aguilera, A. and B. Gomez-Gonzalez, *Genome instability: a mechanistic view of its causes and consequences.* Nat Rev Genet, 2008. **9**(3): p. 204-17.

99. Alvino, G.M., et al., *Replication in hydroxyurea: it's a matter of time.* Mol Cell Biol, 2007. **27**(18): p. 6396-406.
100. Rass, U., *Resolving branched DNA intermediates with structure-specific nucleases during replication in eukaryotes.* Chromosoma, 2013. **122**(6): p. 499-515.
101. Errico, A. and V. Costanzo, *Mechanisms of replication fork protection: a safeguard for genome stability.* Crit Rev Biochem Mol Biol, 2012. **47**(3): p. 222-35.
102. Petermann, E. and T. Helleday, *Pathways of mammalian replication fork restart.* Nat Rev Mol Cell Biol, 2010. **11**(10): p. 683-7.
103. Schwartz, E.K. and W.D. Heyer, *Processing of joint molecule intermediates by structure-selective endonucleases during homologous recombination in eukaryotes.* Chromosoma, 2011. **120**(2): p. 109-27.
104. Interthal, H. and W.D. Heyer, *MUS81 encodes a novel helix-hairpin-helix protein involved in the response to UV- and methylation-induced DNA damage in Saccharomyces cerevisiae.* Mol Gen Genet, 2000. **263**(5): p. 812-27.
105. Mullen, J.R., et al., *Requirement for three novel protein complexes in the absence of the Sgs1 DNA helicase in Saccharomyces cerevisiae.* Genetics, 2001. **157**(1): p. 103-18.
106. Zhang, C., et al., *Suppression of genomic instability by SLX5 and SLX8 in Saccharomyces cerevisiae.* DNA Repair (Amst), 2006. **5**(3): p. 336-46.
107. Heyer, W.D., *Biochemistry of eukaryotic homologous recombination.* Top Curr Genet, 2007. **17**: p. 95-133.
108. Whitby, M.C., *Making crossovers during meiosis.* Biochem Soc Trans, 2005. **33**(Pt 6): p. 1451-5.
109. Boddy, M.N., et al., *Damage tolerance protein Mus81 associates with the FHA1 domain of checkpoint kinase Cds1.* Mol Cell Biol, 2000. **20**(23): p. 8758-66.
110. Froget, B., et al., *Cleavage of stalled forks by fission yeast Mus81/Eme1 in absence of DNA replication checkpoint.* Mol Biol Cell, 2008. **19**(2): p. 445-56.
111. Boddy, M.N., et al., *Mus81-Eme1 are essential components of a Holliday junction resolvase.* Cell, 2001. **107**(4): p. 537-48.
112. Constantinou, A., et al., *Holliday junction resolution in human cells: two junction endonucleases with distinct substrate specificities.* EMBO J, 2002. **21**(20): p. 5577-85.
113. Ehmsen, K.T. and W.D. Heyer, *Saccharomyces cerevisiae Mus81-Mms4 is a catalytic, DNA structure-selective endonuclease.* Nucleic Acids Res, 2008. **36**(7): p. 2182-95.
114. Ehmsen, K.T. and W.D. Heyer, *A junction branch point adjacent to a DNA backbone nick directs substrate cleavage by Saccharomyces cerevisiae Mus81-Mms4.* Nucleic Acids Res, 2009. **37**(6): p. 2026-36.
115. Ciccia, A., N. McDonald, and S.C. West, *Structural and functional relationships of the XPF/MUS81 family of proteins.* Annu Rev Biochem, 2008. **77**: p. 259-87.
116. Amangyeld, T., et al., *Human MUS81-EME2 can cleave a variety of DNA structures including intact Holliday junction and nicked duplex.* Nucleic Acids Res, 2014. **42**(9): p. 5846-62.
117. Pepe, A. and S.C. West, *MUS81-EME2 promotes replication fork restart.* Cell Rep, 2014. **7**(4): p. 1048-55.
118. Furukawa, T., et al., *OsSEND-1: a new RAD2 nuclease family member in higher plants.* Plant Mol Biol, 2003. **51**(1): p. 59-70.
119. Rass, U., et al., *Mechanism of Holliday junction resolution by the human GEN1 protein.* Genes Dev, 2010. **24**(14): p. 1559-69.
120. Blanco, M.G., et al., *Functional overlap between the structure-specific nucleases Yen1 and Mus81-Mms4 for DNA-damage repair in S. cerevisiae.* DNA Repair (Amst), 2010. **9**(4): p. 394-402.
121. Dunin-Horkawicz, S., M. Feder, and J.M. Bujnicki, *Phylogenomic analysis of the GIY-YIG nuclease superfamily.* BMC Genomics, 2006. **7**: p. 98.
122. Fricke, W.M. and S.J. Brill, *Slx1-Slx4 is a second structure-specific endonuclease functionally redundant with Sgs1-Top3.* Genes Dev, 2003. **17**(14): p. 1768-78.
123. Munoz, I.M., et al., *Coordination of structure-specific nucleases by human SLX4/BTBD12 is required for DNA repair.* Mol Cell, 2009. **35**(1): p. 116-27.

124. Paques, F. and J.E. Haber, *Multiple pathways of recombination induced by double-strand breaks in Saccharomyces cerevisiae.* Microbiol Mol Biol Rev, 1999. **63**(2): p. 349-404.
125. Bzymek, M., et al., *Double Holliday junctions are intermediates of DNA break repair.* Nature, 2010. **464**(7290): p. 937-41.
126. Sarbajna, S. and S.C. West, *Holliday junction processing enzymes as guardians of genome stability.* Trends Biochem Sci, 2014. **39**(9): p. 409-19.
127. Hoadley, K.A., et al., *Structure and cellular roles of the RMI core complex from the bloom syndrome dissolvasome.* Structure, 2010. **18**(9): p. 1149-58.
128. Wu, L. and I.D. Hickson, *The Bloom's syndrome helicase suppresses crossing over during homologous recombination.* Nature, 2003. **426**(6968): p. 870-4.
129. Rouzeau, S., et al., *Bloom's syndrome and PICH helicases cooperate with topoisomerase IIalpha in centromere disjunction before anaphase.* PLoS One, 2012. **7**(4): p. e33905.
130. Wyatt, H.D., et al., *Coordinated actions of SLX1-SLX4 and MUS81-EME1 for Holliday junction resolution in human cells.* Mol Cell, 2013. **52**(2): p. 234-47.
131. Minocherhomji, S. and I.D. Hickson, *Structure-specific endonucleases: guardians of fragile site stability.* Trends Cell Biol, 2014. **24**(5): p. 321-7.
132. Mankouri, H.W., D. Huttner, and I.D. Hickson, *How unfinished business from S-phase affects mitosis and beyond.* EMBO J, 2013. **32**(20): p. 2661-71.
133. Mirkin, E.V. and S.M. Mirkin, *Replication fork stalling at natural impediments.* Microbiol Mol Biol Rev, 2007. **71**(1): p. 13-35.
134. Lukas, C., et al., *53BP1 nuclear bodies form around DNA lesions generated by mitotic transmission of chromosomes under replication stress.* Nat Cell Biol, 2011. **13**(3): p. 243-53.
135. Debatisse, M., et al., *Common fragile sites: mechanisms of instability revisited.* Trends Genet, 2012. **28**(1): p. 22-32.
136. Magenis, R.E., F. Hecht, and E.W. Lovrien, *Heritable fragile site on chromosome 16: probable localization of haptoglobin locus in man.* Science, 1970. **170**(3953): p. 85-7.
137. Harvey, J., C. Judge, and S. Wiener, *Familial X-linked mental retardation with an X chromosome abnormality.* J Med Genet, 1977. **14**(1): p. 46-50.
138. Ying, S., et al., *MUS81 promotes common fragile site expression.* Nat Cell Biol, 2013. **15**(8): p. 1001-7.
139. Naim, V., et al., *ERCC1 and MUS81-EME1 promote sister chromatid separation by processing late replication intermediates at common fragile sites during mitosis.* Nat Cell Biol, 2013. **15**(8): p. 1008-15.
140. Westhorpe, F.G. and A.F. Straight, *Functions of the centromere and kinetochore in chromosome segregation.* Curr Opin Cell Biol, 2013. **25**(3): p. 334-40.
141. McFarlane, R.J. and T.C. Humphrey, *A role for recombination in centromere function.* Trends Genet, 2010. **26**(5): p. 209-13.
142. Greenfeder, S.A. and C.S. Newlon, *Replication forks pause at yeast centromeres.* Mol Cell Biol, 1992. **12**(9): p. 4056-66.
143. Simi, S., et al., *Fragile sites at the centromere of Chinese hamster chromosomes: a possible mechanism of chromosome loss.* Mutat Res, 1998. **397**(2): p. 239-46.
144. Sundin, O. and A. Varshavsky, *Arrest of segregation leads to accumulation of highly intertwined catenated dimers: dissection of the final stages of SV40 DNA replication.* Cell, 1981. **25**(3): p. 659-69.
145. Porter, A.C. and C.J. Farr, *Topoisomerase II: untangling its contribution at the centromere.* Chromosome Res, 2004. **12**(6): p. 569-83.
146. Spence, J.M., et al., *Depletion of topoisomerase IIalpha leads to shortening of the metaphase interkinetochore distance and abnormal persistence of PICH-coated anaphase threads.* J Cell Sci, 2007. **120**(Pt 22): p. 3952-64.
147. Ishikawa, F., *Portrait of replication stress viewed from telomeres.* Cancer Sci, 2013. **104**(7): p. 790-4.
148. Palm, W. and T. de Lange, *How shelterin protects mammalian telomeres.* Annu Rev Genet, 2008. **42**: p. 301-34.

149. Verdun, R.E. and J. Karlseder, *Replication and protection of telomeres.* Nature, 2007. **447**(7147): p. 924-31.
150. Sfeir, A., et al., *Mammalian telomeres resemble fragile sites and require TRF1 for efficient replication.* Cell, 2009. **138**(1): p. 90-103.
151. Fumagalli, M., et al., *Telomeric DNA damage is irreparable and causes persistent DNA-damage-response activation.* Nat Cell Biol, 2012. **14**(4): p. 355-65.
152. Hühn, D., *Functional characterization of the human RECQ5 helicase*, in *IMCR*. 2010.
153. Hasanova, Z., *PhD thesis*, in *National Centre for Biomolecular Research*. 2016.
154. Pepe, A. and S.C. West, *Substrate specificity of the MUS81-EME2 structure selective endonuclease.* Nucleic Acids Res, 2014. **42**(6): p. 3833-45.
155. Morelli, C., et al., *Cloning and characterization of the common fragile site FRA6F harboring a replicative senescence gene and frequently deleted in human tumors.* Oncogene, 2002. **21**(47): p. 7266-76.
156. Vassilev, L.T., et al., *Selective small-molecule inhibitor reveals critical mitotic functions of human CDK1.* Proc Natl Acad Sci U S A, 2006. **103**(28): p. 10660-5.
157. Liu, Y., et al., *The origins and processing of ultra fine anaphase DNA bridges.* Curr Opin Genet Dev, 2014. **26**: p. 1-5.
158. Chan, K.L. and I.D. Hickson, *New insights into the formation and resolution of ultra-fine anaphase bridges.* Semin Cell Dev Biol, 2011. **22**(8): p. 906-12.
159. Fenech, M., et al., *Molecular mechanisms of micronucleus, nucleoplasmic bridge and nuclear bud formation in mammalian and human cells.* Mutagenesis, 2011. **26**(1): p. 125-32.
160. Terradas, M., et al., *DNA lesions sequestered in micronuclei induce a local defective-damage response.* DNA Repair (Amst), 2009. **8**(10): p. 1225-34.
161. Langhoff, J., *Analysis of posttranslational modification of RECQ5 DNA helicase*, in *IMCR*. 2012.
162. Ghodgaonkar, M.M., et al., *Phenotypic characterization of missense polymerase-delta mutations using an inducible protein-replacement system.* Nat Commun, 2014. **5**: p. 4990.
163. Schlacher, K., H. Wu, and M. Jasin, *A distinct replication fork protection pathway connects Fanconi anemia tumor suppressors to RAD51-BRCA1/2.* Cancer Cell, 2012. **22**(1): p. 106-16.
164. You, Z., L. Kong, and J. Newport, *The role of single-stranded DNA and polymerase alpha in establishing the ATR, Hus1 DNA replication checkpoint.* J Biol Chem, 2002. **277**(30): p. 27088-93.
165. Zou, L. and S.J. Elledge, *Sensing DNA damage through ATRIP recognition of RPA-ssDNA complexes.* Science, 2003. **300**(5625): p. 1542-8.
166. Petermann, E., M. Woodcock, and T. Helleday, *Chk1 promotes replication fork progression by controlling replication initiation.* Proc Natl Acad Sci U S A, 2010. **107**(37): p. 16090-5.
167. Forment, J.V., et al., *Structure-specific DNA endonuclease Mus81/Eme1 generates DNA damage caused by Chk1 inactivation.* PLoS One, 2011. **6**(8): p. e23517.
168. Syljuasen, R.G., et al., *Inhibition of human Chk1 causes increased initiation of DNA replication, phosphorylation of ATR targets, and DNA breakage.* Mol Cell Biol, 2005. **25**(9): p. 3553-62.
169. Gaillard, H., T. Garcia-Muse, and A. Aguilera, *Replication stress and cancer.* Nat Rev Cancer, 2015. **15**(5): p. 276-89.
170. Chavdarova, M., et al., *Srs2 promotes Mus81-Mms4-mediated resolution of recombination intermediates.* Nucleic Acids Res, 2015. **43**(7): p. 3626-42.
171. Krejci, L., et al., *DNA helicase Srs2 disrupts the Rad51 presynaptic filament.* Nature, 2003. **423**(6937): p. 305-9.
172. Win, T.Z., et al., *A role for the fission yeast Rqh1 helicase in chromosome segregation.* J Cell Sci, 2005. **118**(Pt 24): p. 5777-84.
173. Sakurai, H., et al., *Anaphase DNA bridges induced by lack of RecQ5 in Drosophila syncytial embryos.* FEBS Lett, 2011. **585**(12): p. 1923-8.
174. Germann, S.M., et al., *TopBP1/Dpb11 binds DNA anaphase bridges to prevent genome instability.* J Cell Biol, 2014. **204**(1): p. 45-59.
175. Pedersen, R.T., et al., *TopBP1 is required at mitosis to reduce transmission of DNA damage to G1 daughter cells.* J Cell Biol, 2015. **210**(4): p. 565-82.

176. Richardson, C., et al., *Rad51 overexpression promotes alternative double-strand break repair pathways and genome instability.* Oncogene, 2004. **23**(2): p. 546-53.
177. Matos, J., et al., *Regulatory control of the resolution of DNA recombination intermediates during meiosis and mitosis.* Cell, 2011. **147**(1): p. 158-72.

11. Acknowledgements

First I would like to thank Dr. Pavel Janscak for the opportunity to let me come back to his laboratory and to do my PhD. I am very grateful for his advice, support and patience he provided me.

I would also like to thank Prof. Massimo Lopes for being my doctor father, Prof. Petr Cejka and Dr. Pietro Pichierri, that together provided support and useful suggestions and scientific advise throughout my PhD years.

My gratitude goes also towards the past (Amlan, Shreya, Adisa) and present (Andreas, Naga Raja, Shruti, Domino) members of Pavel's lab.

I would like to extend my sincerest gratitude to Prof. Josef Jiricny and the IMCR staff for supporting and maintaining the institute perfectly running every day.

I especially thank Shruti for becoming a good friend and for her moral support in difficult periods, and Domino for her suggestions for my covers, putting a lot of creativeness in making them.

Finally, I acknowledge my parents for their support and care.

12. Curriculum Vitae

PERSONAL INFORMATION

Stefano Di Marco

Frohburgstrasse 85, 8006 Zurich, Switzerland
+41 (0)79 890 48 39
dimarco@imcr.uzh.ch

Swiss C permit

Marital status Single | Date of birth 05.03.1987 | Nationality Italian

WORK EXPERIENCE

2013-2016 PhD in Cancer Biology

Institute of Molecular Cancer Research (IMCR) – University of Zurich

- DNA repair mechanisms in human cells treated with chemotherapy drugs
- Clinical cancer research
- Molecular and cell biology of cancer

2011-2012 Research Assistant

Institute of Oncology Research (IOR) – IOSI Bellinzona, Ticino, Switzerland

- Independent research project on DNA damage and ncRNAs in prostate cancer
- Experimental therapeutics

EDUCATION AND TRAINING

2009-2010 Master in Cellular and Molecular Biology

Institute of Molecular Cancer Research (IMCR) – University of Zurich

- DNA damage and repair

2006-2009 Bachelor in Industrial and Environmental Biotechnology

University of Milan – Milan, Italy

- Curriculum in bioinformatics

PERSONAL SKILLS

Mother tongue	Italian
Business language	English
Others	German (basic)

Job-related skills	Project Management for advanced stage researchers ▪ Intensive course at EUrelations in Zurich
Computer skills	▪ excellent command of Microsoft Office tools ▪ advanced knowledge of Adobe Illustrator and Adobe Photoshop ▪ Macintosh and Windows O.S. ▪ GraphPad for statistical analysis
Other skills	▪ piano (diploma), guitar ▪ painting ▪ novel writing
Driving licence	▪ B

ADDITIONAL INFORMATION

Publications

In progress for submission:

RECQ5 DNA helicases removes RAD51 from late replication intermediates at common fragile sites to promote their resolution by MUS81 endonuclease in early mitosis, **Di Marco S**, Hasanova Z et al. *manuscript in preparation*.

Published:

RNAi-mediated silencing of Myc transcription inhibits stem-like cell maintenance and tumorigenicity in prostate cancer, Civenni G, Malek A, Albino D, Garcia-Escudero R, Napoli S, **Di Marco S** et al., Cancer Res. 2013 Nov 15;73(22):6816-27